SITE-SPECIFIC CARBON STOCK ASSESSMENTS OF SHELTERBELT TREES IN SASKATCHEWAN

A Thesis Submitted to the
College of Graduate and Postdoctoral Studies
In Partial Fulfillment of the Requirements
For the Degree of Doctor of Philosophy
In the School of Environment and Sustainability
University of Saskatchewan
Saskatoon

By

RAFAELLA CARVALHO MAYRINCK

PERMISION TO USE

In presenting this thesis/dissertation in partial fulfillment of the requirements for a Postgraduate degree from the University of Saskatchewan, I agree that the Libraries of this University may make it freely available for inspection. I further agree that permission for copying of this thesis/dissertation in any manner, in whole or in part, for scholarly purposes may be granted by the professor or professors who supervised my thesis/dissertation work or, in their absence, by the Head of the Department or the Dean of the College in which my thesis work was done. It is understood that any copying or publication or use of this thesis/dissertation or parts thereof for financial gain shall not be allowed without my written permission. It is also understood that due recognition shall be given to me and to the University of Saskatchewan in any scholarly use which may be made of any material in my thesis/dissertation.

Requests for permission to copy or to make other uses of materials in this thesis/dissertation in whole or part should be addressed to:

School of Environment and Sustainability

University of Saskatchewan

Room 323 Kirk Hall, 117 Science Place

Saskatoon, Saskatchewan, S7N 5C8, Canada

OR

Dean

College of Graduate and Postdoctoral Studies

University of Saskatchewan

116 Thorvaldson Building, 110 Science Place

Saskatoon, Saskatchewan, S7N 5C9, Canada

ABSTRACT

Climate change is threatening the entire planet, so collective efforts to mitigate it are crucial to our future. Planting trees is one of the easiest alternatives known to help sequester the carbon causing problem, yet this procedure is underutilized, especially in agricultural areas. This dissertation is an attempt to link the theoretical and practical issues regarding carbon stock assessments on a farm-level basis that could underpin policies aimed at mitigating climate change in rural areas. The goal of this study was to establish a method to retrieve past tree growth using increment cores, and to test if this information is reliable as input data to model carbon stocks on a farm-level basis. To do so, data was collected from shelterbelt grown trees of varying ages, species, and management conditions in farms across Saskatchewan, Canada, during the summers of 2018 and 2019. This dissertation presents many of the theoretical and historical aspects of shelterbelts in the early chapters, and then works towards finding practical solutions to some of the carbon modeling issues from shelterbelts in the later chapters.

The first manuscript I developed discusses early shelterbelt history in Canada, and the environmental benefits that they have provided over the last century. I focus on the carbon sequestration potential from both above- and below-ground accrual, by examining the historical changes in the publication records on the subject through time. Contrasting shelterbelt effects on crops is also illustrated by comparing many studies from around the world, and how these effects change for different crops grown adjacent to shelterbelts. The many facets of carbon sequestration potential of shelterbelts were assessed by examining agroforestry studies from around the world. Conclusions drawn from this process are that shelterbelts represent a great potential for carbon sequestration and global warming mitigation. I argue that shelterbelts should therefore be more heavily applied to the existing agricultural land base, and discuss some potential policy changes that would assist in motivating more planting of trees to be implemented. Without a major change in policy, I argue that the full potential of carbon sequestration from shelterbelt systems will not occur.

The goal of my second manuscript was to derive a precise and practical method to retrieve past tree growth using increment cores, and to better understand the associated error that came with such derivations. If accomplished, then shelterbelt carbon stock assessments could be improved, by allowing for a quicker and easier method of assessment. Factors such as the number of increment cores used, if a core reached the pith or the center of the tree, as well as

species, age, and tree shape were assessed. Fifty-six combinations of these factors as well as their associated errors were processed, and the conclusion was that the more increment cores used reaching the pith, the better. The study also concludes that dendrochronologically derived increment core data, although not currently used for allometric purposes, is reliable as a mechanism to retrieve growth data (e.g., diameter at breast height, or basal area), which is commonly only measured in forestry operations from repeated visits and repeated measurements.

In my last manuscript, the goal was to use data retrieved using the method described in my second manuscript, as input variables in the 3-PG model. This common forestry model was used to assess accuracy and how geographically specific fitting needs to be for the most precise estimates of past growth. It was found that using increment-core derived growth data yields a strong fitting, and that tree-level and site-specific fittings are more precise than the regional methods currently described in the literature. Both these results support that better carbon stock models could be made with this knowledge for two reasons. First, a greater database, i.e., *ex-situ* radial-growth data from tree-ring databanks, or *in-situ* obtained tree data, can be now considered for modeling purposes. Second, precise site-specific modeling can be used to calculate a farm-specific carbon footprint, which can ultimately be used as a tool to implement carbon incentivizing policies.

The implications of being able to make a farm-based carbon stock model, is that it can support farm-specific carbon footprint calculations. This was the only theoretical-based factor remaining, a factor that precluded incentivization policies from being implemented by federal or provincial governments. Such policies could support a carbon market among farmers or/and a policy rewarding the carbon that many farmers are already sequestering. These policy/market changes would motivate shelterbelt tree planting, which would help the landowners, the agricultural sector, and most importantly, everyone, by assisting in the mitigation of global warming concerns.

ACKNOWLEDGEMENTS

I thank the existence for the opportunity to be alive, to learn from my mistakes, from my achievements, and learn that sometimes I cannot learn yet, but I will someday. I appreciate having the opportunity for taking this PhD, which has taught me so much, and changed me. I'm grateful for having the chance to be in another country, learning about a new culture, a new language, and learning about myself.

I thank my supervisor Dr. Colin Laroque for being an amazing supervisor, who helped me in all circumstances to find a better path, better way to think, and for making things less difficult than I thought they would be. Thanks for being kind and for cheering me up when I needed it. Thanks for the hard field work we have done, and for teaching me the "chainsaw mama" works! I thank my committee members for all of their guidance and support: Murray Bentham, Eric Lamb, Ken van Rees, and Dave Schneider. Thanks to Beyhan Amichev for being so helpful during this study. I am grateful for AGGP for providing project funding and the University of Saskatchewan for providing me many other funding opportunities. I also thank all of the landowners and farmers in Saskatchewan who provided me with their trees.

I thank the MAD Labbers for all the help and fun days: Jay Maillet, Magali Nehemy, Scott Wood, Gary Beckhusen, Sheri Andrews-Key, Beckett Stark, Megan Horachek, Brooke Howat, Teagan Lubiniecki, Tiara Jackle, Annette Bellinger, Bryan Mood, Chloe Canning, and Ben Nykiforuk. A special thanks to Bryan Mood for all of the hard fieldwork we have done together. I also thank Chukwudi, Kim, Mark and Michael for their free welcoming smiles.

I thank my husband Vinicius for always being with me and ignoring the many kilometres between us. I thank my mom, dad, siblings, and grandma for being my rock, and my nephew for being this little happy buddy. I thank my friends back home for all the online laughs and cozy support: Giovana Resca, Paula Scolforo, Tereza Gabriela, Hortencia Botelho, Ariela Thomas, Isabela Mayrinck, Manoel Neto, Bruna Lima, and Ximena Oliveira. I thank Magali Nehemy again, who was the essential link between me, and my PhD, she allowed all this adventure to begin.

TABLE OF CONTENTS

TABLE OF TABLES

TABLE OF FIGURES

LIST OF ABBREVIATIONS

3-PG	Principles Predicting Growth
BA	Basal Area
C	Carbon
CBM	Canadian Budget Model
CG	Caragana
CH_4	Methane
cm	Centimetre
CO_2	Carbon Dioxide
C stock	Carbon Stock
DBH	Diameter at Breast Height
DSS	Decision Supporting System
FCA	Full Canopy Age
GA	Green Ash
GDP	Gross Domestic Product
GHG	Greenhouse Gases
GPP	Gross Primary Production
H	Shelterbelt Tree Height
ha	Hectares
HP	Hybrid Poplar
ITRDB	International Tree Ring Databank
Kg	Kilograms
m	Metre
MAE	Mean Absolute Error
MAD Lab	Mistik Askiwin Dendrochronology Laboratory
MM	Manitoba Maple
NPP	Net Primary Production
N_2O	Nitrogen Dioxide
PFRA	Prairie Farm Rehabilitation Administration
PSFP	Prairie States Forestry Project
PSP	Prairie shelterbelt Program

RMSE	Root Mean square Error
R^2	Coefficient of Determination
SP	Scots pine
WS	White spruce
yr	Year

CHAPTER 1

INTRODUCTION

1.1 General introduction

Landowners have planted long rows of trees, called shelterbelts, in the Prairie Provinces since they began to be settled by European immigrants in the early 1900s. They planted these trees for two main reasons: to improve field conditions for agriculture, and to make their farms more aesthetically pleasing (Anstey, 1986; Dunlop, 2000; Richardson et al., 2007; Marchildon, 2014). Since 1901 the Federal government supported shelterbelt planting by offering technical support, and free seedlings to farmers. The program was stopped in 2013, but not before over 600 million shelterbelt trees were planted in Saskatchewan (Amadi et al., 2016). This backing by the Federal government program was crucial to assist in sheltering crops from drought and wind erosion that have hit the Province through various times in the past 100 plus years of the initiative (Anstey, 1986; Dunlop, 2000; Marchildon, 2014).

Through the intervening years of the Federal program, other techniques began to be introduced to offset the use of shelterbelts to protect crops from drought and wind erosion, such as optimized irrigation, and no-till systems. As the new techniques for farming were introduced, some landowners started to feel that they did not need shelterbelts anymore, and a switch from planting shelterbelts to removing shelterbelts in the 2010s became common. The ongoing trend of removing shelterbelts in the Prairies continues to this day (Rempel et al., 2014, 2017; Ha et al., 2018; Amichev et al., 2020b). In some of the worst hit areas from 2008 to 2016 (e.g., Outlook, SK), 29.8% of the farmers removed their shelterbelts within a 1400 km^2 region (Ha et al., 2018).

Despite this apparent shelterbelt obsolescence, they have always provided many precious environmental services that have been under-accounted for by landowners (Kulshreshtha & Kort, 2009; Rempel et al., 2014; Amichev et al., 2016). By removing their shelterbelts, landowners suddenly halt all of the greater environmental benefits that the shelterbelts were providing, including the annual accrual of carbon into the trees themselves, as well as into the surrounding soil.

Some scholars have tried to focus on a means to motivate landowners to keep their trees sequestering carbon to assist in efforts to reduce carbon dioxide in the atmosphere. They

point out that a key factor would be increasing the awareness of the benefits of shelterbelts by communicating what landowners lose when they remove them (Rempel et al., 2014, 2017; Amichev et al., 2020b). Or to provide an annual subsidy to help compensate farmers for the work that their shelterbelts are doing for the greater good of our society (Helmers & Brandle, 2005; Amichev et al., 2020a). To do so, a mechanism to calculate a farm-based carbon footprint including all activities resulting in carbon emission and sequestration is needed (Franks & Hadingham, 2012; Amichev et al., 2020b). Each farm's balance could be tradable in a market to benefit those farmers with a positive balance sequestered (Amichev et al., 2020a). Carbon sequestered would therefore bring reliable financial benefits that would make growing trees an asset in the overall farm production system, just like growing crops or raising cattle would be seen as a benefit.

Rewarding a landowner for long-term carbon sequestration in agricultural areas would benefit many local economies around the word, but it could provide a revolutionary shift in locations like Saskatchewan by offsetting seasonal food production, that releases much of the per capita carbon emissions for the Province (Izaurraude et al. 2004; Liu et al. 2019). Quantifying carbon sequestration in shelterbelt trees and estimating how they will grow in the future would be part of a farm management toolbox. All landowners would need is a mechanism to calculate their carbon stocks, by collecting data on the annual growth of their trees. Since no landowners currently measure these data, a simple, easy, and cheap method to retrieve this growth information is required to move forward.

1.2 Main goal and objectives of the research

The main goal of this study is to develop a method that allows for the retrieval of tree growth information from increment cores, and to use this information as an input for allometric models for a specific species of tree at a location. This would allow an assessment of carbon stock accrual to be made for the past, and would assist in the prediction of tree growth at individual farms into the future. The specific objectives of this study were to:

i) Conduct a literature review assessing the main aspects of above- and below-ground carbon sequestration of shelterbelts in Canada;
ii) Create a method to retrieve radial growth in diameter at breast height (DBH) and basal area (BA) by using increment cores;
iii) Provide the error in DBH and BA yielded from this method;

iv) Assess if the 3-PG model can be used to estimate shelterbelt tree growth using data retrieved according to the method proposed in i);

v) Assess if 3-PG model building needs to be tree-specific, site-specific or if it can be assessed from a wide geographic region;

vi) Assess how precise 3-PG models can estimate growth over the years of a tree's life.

1.3 Organization of the dissertation

This dissertation is composed of seven chapters. The first Chapter offers a quick introduction, a general rationale for the study topic, and lists the main objectives of this dissertation. The second Chapter is a literature review explaining the main topics necessary to understand the underpinnings of the dissertation. Chapter 3 is the first of three manuscript-styled Chapters entitled "Above- and Below-Ground Carbon Sequestration in Shelterbelt Trees in Canada: A Review" published in *Forests* in 2019. It specifically is a review about the shelterbelt carbon sequestration potential focused on the above- and below-ground carbon pools. Chapter 4 is entitled "Estimating DBH through time using a varying number of increment cores and methods". In this paper, DBH was calculated testing several methods and the error from each method is reported. Chapter 5 is entitled "Exploring the alpha parameter for modeling future growth using 3-PG in shelterbelts in Saskatchewan". In this paper, the effects of fitting the "alpha tree" parameter under various spatial scales are assessed, along with evaluating the fitting precision of the 3-PG models over the tree life. Chapter 6 is a concluding Chapter that draws the results from the three main manuscripts together and summarizes my study more holistically. Next are the Appendix Chapter, where some details and analysis of this wider study are explained further.

CHAPTER 2

LITERATURE REVIEW

2.1 Climate change for Western Canada agriculture

Recent climatic changes have been shown to be heating the planet, causing glaciers and sea ice to melt, sea levels to rise, linked to increased acidification of the oceans, more frequent extreme weather events, heat waves, increases in infectious disease and insect outbreaks, and many other deleterious effects globally (Das & Horton, 2018; Kompas et al., 2018; Aggarwal et al., 2019; Schnitter & Berry, 2019). In a global context, average temperature is raising faster in Canada than in most of the rest of the planet, and this trend is projected to remain, moving into the immediate future (He et al., 2018; Qian et al., 2019). Central and Western Canada are projected to become dryer (Schindler & Donahue, 2006; Bush & Lemmen, 2019), while more moisture is projected at fall in Northeastern Canada (Wang et al., 2014; Bush & Lemmen, 2019), although this increase in precipitation will be offset by projected higher evapotranspiration rates (Wang et al., 2014). It is thought that these changing weather patterns will lead to more severe and more frequent fires within the Canadian plains, especially in Saskatchewan and Alberta (Wang et al., 2014).

Specifically in the Canadian Prairies, a water crisis, in terms of water quantity and water quality, is predicted to take place by 2100 (Schindler & Donahue, 2006). The main causes of the crisis are the increasing local temperatures (a rise of 1 to 4°C), increasing evapotranspiration (by approximately 55%), and a higher water demand (due to increasing population and crop irrigation practices), added to a decrease in precipitation levels. These factors will result in a 20 to 84% decrease in summer river flow rates compared to 20th century flows (Schindler & Donahue, 2006). A warmer and dryer climate in the Prairies will impact Canadian and global food security (He et al., 2018; Schnitter & Berry, 2019), since a significant portion of Canadian agriculture takes place in the Prairie provinces which produce about 70% of the food in the country (Schindler & Donahue, 2006; Qian et al., 2019). All the more important since Canada is the fifth largest global food exporter, and much of the Canadian Prairie crops are bound for the export market (Qian et al., 2019).

Water availability and its linked food security are crucial issues in the coming years since global populations are projected to reach 9.7 billion people by 2050 (UN, 2019), which will

necessitate an increased demand for food production of 1.5% / yr by 2030, and 0.9% / yr by 2050 (Conforti 2011). Increasing food production is not a new issue, as since 1970, agricultural production has doubled (Bennetzen et al., 2016). However, meeting this increasing food demand will also likely contribute to more extreme climatic changes, because under current conventional methods, tonnes of greenhouse gases are released by agricultural production (Bennetzen et al., 2016; Carlson et al., 2017). Even though food production is rising more than carbon released which is attributed to more optimized agriculture techniques and to less land use changes, total agricultural energy-based emissions have tripled, which is caused by fossil fuel use and especially by fertilizers (Bennetzen et al., 2016).

Fertilizers are perhaps the biggest issue in the rise of greenhouse gases release within the agricultural environment, emitting not just CO_2, but CH_4, N_2 and N_2O, all very powerful greenhouse gases (Franks & Hadingham, 2012; Tubiello et al., 2013; Bennetzen et al., 2016; Carlson et al., 2017). Unfortunately, to increase the needed food production, even more fertilizer will likely be required, which in turn will increase greenhouse gas release from fertilizers even more. Nitrogen leaching is also predicted to increase up to 317 % by 2080 (Patil et al., 2012; He et al., 2018), and to replace the loss of this essential nutrient to plant growth, an increase in the use of even more fertilizers is warranted (He et al., 2018).

Other large releasers of greenhouse gases from agricultural practices are rice production (Bennetzen et al., 2016; Carlson et al., 2017), peatland cultivation (Carlson et al., 2017), enteric fermentation, and manure management (O'Mara, 2011). Animal agriculture alone, is responsible for 10.8% of the global annual emissions of greenhouse gases, which is mainly related to CH_4 and N_2O emission from enteric and manure fermentation (O'Mara, 2011). In all, agriculture is responsible for a quarter (Bennetzen et al., 2016) to a third (Carlson et al., 2017) of the global agricultural releases, which is rising 1% every year (Lamb et al., 2016). The more greenhouse gasses released, and the longer it takes to have these gasses sequestered, the more they build up in the atmosphere, and exacerbate the climatic changes that will occur in the future. Future climate change will impact every production chain, but it will especially affect food production, since this chain relies directly on climate conditions to grow plants.

Climate change will affect crops differently based on their species-specific adaptations and on the specific land locations where they are planted. For example, cereals, nuts and oilseeds availability will tend to decrease globally (Nelson et al., 2018). For most parts of Canada, the

growing season is projected to lengthen with the rise in average temperatures, increasing both in the spring and autumn seasons. For some crops, such as maize, the yield is projected to increase as the temperature rises up to a further 2.5°C, but then it will decrease yield after any further average temperature warming (He et al., 2018). Canola's yield is projected to drop overall because of the predicted dryer environments (He et al., 2018). Even with minor increases in yields for some crops, the overall impact of climate change will be negative for most countries. For Canada specifically, estimates assert that if the average temperature increase is kept under 2°C, the loss in Gross Domestic Product (GDP) of the country will be 5.2 US$ Billion/Year. If the temperature rises 3°C or 4°C, the annual GPD loss will reach 11.4 and 45.29 US$ billion by 2100, respectively (Kompas et al., 2018).

These losses can be minimized by introducing adaptations to climate change (He et al., 2018; Bizikova et al., 2019; Qian et al., 2019), which is especially important for the agricultural sector which is particularly vulnerable to natural climate conditions. Adaptations within the agricultural environment can be better made if farmers, policy makers, and academics work together (He et al., 2018; Bizikova et al., 2019; Qian et al., 2019). For example, since weather will be dryer in the Prairies, farmers will have to improve irrigation facilities (He et al., 2018; Qian et al., 2019), which can be done easier if the government offers some sort of subsidy for the changes needed, and if academia improves the hydrologic models needed to assess future needs, and to optimize irrigation systems in general.

Adaptations to climate change in the agricultural sector have been focused on production systems, crops, yields, infrastructure, financial performance, farmers' livelihoods, and food security (Bizikova et al., 2019). However, adaptation also can also be made by implementing new policies. By incentivizing adding trees to agricultural land systems to optimize carbon sequestration, the trees would add other environmental benefits for the good of society, and in doing so, positive steps can be taken overall for the agricultural sector. Many famers already see climate change as a threat, and many are also willing to take some actions to fight it. A study in the United Kingdom illustrated that 47% of farmers are willing to take some action to reduce climate change (Franks & Hadingham, 2012). Agroforestry may be an inexpensive and relatively simple way to start adapting farms to the upcoming challenges, and to build a greener food chain for the next generation.

2.2 Agroforestry and Shelterbelts

Agroforestry can be defined as a broad science employed on any land-use combining woody perennial plants with animal and or agricultural crops in spatial or temporal arrangements (Raintree, 1987). Agroforestry can be used as a key tool to optimize carbon sequestration in rural areas, offsetting at least some portion of the greenhouse gases released by agriculture (Perry et al., 2009; Amadi et al., 2016; Amichev et al., 2016; Amadi, et al., 2017; Schnitter & Berry, 2019). Despite this carbon sequestration potential (Beach et al., 2008; Carlson et al., 2017), agroforestry has not been used to its full potential. Schoeneberger (2009) and Perry et al., (2009) state that the reason for this underutilization is that it is a relatively new science, bridging forestry and agriculture. Since it is not an established practice in either agriculture or in forestry, each discipline seldom applies it. When decreasing greenhouse gases release is discussed in agricultural literature, it has regularly been advised by many studies to avoid food waist (O'Mara, 2011; Franks & Hadingham, 2012), to eliminate peatland cultivation (Carlson et al., 2017), to enhance animal breeding (O'Mara, 2011; Franks & Hadingham, 2012), to improve farm management (O'Mara, 2011; Franks & Hadingham, 2012) and even to be a global volunteer to change dietary habits by eating less meat and replacing beef for chicken, pork for fish (Franks & Hadingham, 2012; Bennetzen et al., 2016). However, agroforestry use is rarely discussed, and if it is being advised at all, it occurs only in agroforestry-related studies not in general management, assessment, and policy-related studies. There are several kinds of agroforestry styles providing many benefits, and the ones with the greatest carbon sequestration potential are seen as riparian forest buffers, and windbreaks, also known as shelterbelts (Batish et al., 1976; Schoeneberger, 2009).

Shelterbelts are lines of trees planted adjacent to cropped fields or farm yards, providing many public and private environmental services (Kulshreshtha & Kort, 2009; Schoeneberger, 2009). Examples include enhancing habitat for biodiversity by functioning as travel corridors (Gámez-Virués et al., 2007; Mize et al., 2008); increasing pollinators, and fungi activity (Kujawa & Kujawa 2008); working as biological pest control for crops (Strange & Brandle, 2006; Gámez-Virués et al., 2007; Mize et al., 2008); reducing odor spread from livestock systems (Tyndall & Colletti 2007); increasing soil water infiltration (Carroll et al., 2004); improving soil proprieties in terms of fertility and structure (Zhou et al., 2005; Liu et al., 2015); reducing pollen dispersal contaminating crops (Meyer et al., 2017); improving crop yield (Batish et al., 1976; Kort &

Turnock, 1999; Gosme et al., 2016); protecting oases and stabilizing dunes in desert locations (Zhou, 2005; Liu et al., 2015); protecting crops from wind (Kort & Turnock, 1999; Agriculture and Agri-Food Canada, 2008; Mize et al. , 2008; Amichev et al., 2020b); and sequestering carbon (Kort & Turnock, 1999; Sauer et al., 2007; Amichev et al., 2015; Amichev et al., 2016; Amadi et al., 2017). In some cases, shelterbelts can also be seen to be creating a negative disturbance to the environment by the reduction of native habitat and thereby offsetting species associated with the natural territory. For example, bobolinks (*Dolichonyx oryzivorus*), savannah sparrows (*Passerculus sandwichensis*), and sedge wrens (*Cistothorus stellaris*) occupancy decreases in the presence of shelterbelts in grasslands in North America when shelterbelts are introduced into their native habitats (Tack et al. 2017). However, shelterbelts are also generally introduced between cropped fields, which are seen as exotic species as well, so the positive effects of the shelterbelts for other species may surpass the negative aspects for the few. In spite of all of these environmental services shelterbelts provide, they only occupy a small amount of land. This limited competition for land with food production and environmental damage minimizes any contribution to a rise in food prices (Perry et al., 2009; Schoeneberger, 2009; Kreidenweis et al., 2016; Aggarwal et al., 2019).

Shelterbelt affects can also be considered a type of adaptation for crops under climate change, by making crops less vulnerable to extreme temperatures, drought, and harsh winds that are projected to come under various climate change scenarios (He et al., 2018). Winds and their drying capacity already affect crops even before harsher climatic changes become more noticeable (Dunlop, 2000). This natural drying effect is due to the Rocky Mountain's rain shadow effect, which prevents moist air currents from the Pacific Ocean reaching the prairies (Crossley, 1935). Shelterbelt were crucial in dealing with this issue during the Great Depression of the 1930s, because they protected soil from wind erosion and drought (Kulshreshtha & Kort, 2009; Rempel et al., 2014). Now that climatic changes are starting to add more evapotranspiration and higher wind regimes to the area (Schindler & Donahue, 2006; Bush & Lemmen, 2019), shelterbelts should be seen as even more necessary.

Over the last few years fewer shelterbelts have been planted in the Prairies then have been removed (Rempel et al., 2017; Ha et al., 2019; Amichev et al., 2020a). Three main reasons for this have been proposed: 1) new farming techniques, such as minimal and no-till systems that are seen by farmers to protect soil from wind erosion; 2) the cost to farmers to maintain their existing

shelterbelts (e.g. fertilizer, weed, and pests control); and 3) lines of shelterbelt trees within existing field complexes can make it more difficult to maneuver the new larger farming equipment.

Even though the benefits of shelterbelts for the whole of society are known, it is still hard to quantify these benefits farm-specifically, and consequently, shelterbelt value is underestimated by many farmers on a local scale (Rempel et al., 2014, 2017; Ha et al., 2019; Amichev et al., 2020a). Shelterbelts have been considered by policy makers as a tool to assist farmers, earlier in the 1900's to fight the change from native prairie to cropped fields, during the "Dirty 30s" to combat the droughts on the Prairies, and currently, to combat global warming concerns. In fact, some of same reasons used to establish the creation of the Prairie Farm Rehabilitation Administration in 1901, were again used to establish the Agricultural Greenhouse Gasses Program in 2013.

2.3 The evolution of shelterbelt research in Western Canada

Early federal action to help agriculture development in Canada was seen by the creation of the Central Experimental Farm, in Ontario, in 1887 (Dunlop, 2000). There, a series of experiments were conducted including some early trials with shelterbelts (Dunlop, 2000), to assist farmers in the best way to use shelterbelts as a tool to increase crop yield (Dunlop, 2000). At first, the interest in shelterbelts was related to these agriculture improvements, as well to make Canada more similar to the treed European environment where most early farmers were more familiar with (Rees, 1988 in Dunlop, 2000). By 1890, there were more experimental stations in the country, including two in Western Canada (Indian Head, SK, and Brandon, MB), all which provided technical information, free seedlings, and free seeds for the public (Anstey, 1986).

These experimental stations in the Prairie Provinces provided important support to fight the dry conditions in the area. In fact many droughts hit the Prairies from the 1880s to 1980s (Dunlop, 2000; Marchildon, 2014), with the worst being the prolonged drought of the 1930s. During this time, the Prairie region faced prolonged drought, insect infestation, and dropping commodities prices on global markets because of the Great Depression (Marchildon, 2014). To remedy the situation and aid farmers in better establishing agriculture, the experimental station in Indian Head had its tree nursery expanded under the Department of Interior, which would later become the Prairie Farm Rehabilitation Administration (PFRA) in 1963 (Dunlop, 2000; Richardson et al., 2007; Marchildon, 2014). Since its inauguration, until its shut down in 2013,

the Indian Head tree nursery provided over 600 million trees (Agriculture and Agri-Food Canada, 2008; Amadi et al., 2016), resulting in a current total shelterbelt length of 60,633 km just within the province of Saskatchewan (Amichev et al., 2015). In the USA., a similar movement was taking place at that time, the Prairie States Forestry Project, delivering about 217 million trees in North Dakota, South Dakota, Nebraska, Kansas, Oklahoma, and Texas (Sauer et al., 2007; Perry et al., 2009).

Years after the creation of the PFRA, human induced climate change started to become an environmental concern in the Prairies, along with most regions of the world. To mitigate these changes, Canada signed onto the Copenhagen Accord in 2009, which aimed to reduce greenhouse gas emissions by 17% by 2020, based on 2005 levels. To reach this goal, the Federal government launched a one-billion-dollar project called the Agricultural Greenhouse Gases Program (AGGP), aiming to help farmers to mitigate greenhouse gases emissions through new technologies, conservation practices, and by changing agricultural processes (Agriculture and Agri-Food Canada, 2017). The program focused on four priority areas, agroforestry, livestock, cropping, and agricultural water use efficiency systems. The AGGP aimed to motivate landowners to keep trees on their farms, encourage soil conservation practices, such as the no-till systems, and reduce CH_4, N_2O releases by optimizing manure and fertilizer management.

One of the agroforestry projects financed during the first phase of the AGGP was led by researchers at the University of Saskatchewan (Principal Investigator = van Rees). In the second phase of AGGP funding, another agroforestry project at the U of S was funded (Principal Investigator = Laroque). Phase I started in 2011, and the phase II started in 2017. At first, a preliminary study considered studying nine shelterbelt species (*Salix acutifolia* (Acute willow), *Caragana arborescens* (caragana), *Picea pungens* (Colorado spruce), *Fraxinus pennsylvanica* (green ash), *Populus* sp. (hybrid poplar), *Acer negundo* (Manitoba maple), *Pinus sylvestris* (Scots pine), *Ulmus pumila* (Siberian elm) and *Picea glauca* (white spruce)) (Davis, Laroque, and van Rees, 2013); however, as it was deemed to be too many species to study in a time- and budget-limited project, only six species were ultimately selected (caragana, green ash, hybrid poplar, Manitoba maple, Scots pine, and white spruce). Phase I focused on mapping shelterbelt across the southern half of the province, and understanding the growth regime within the different soil zones in Saskatchewan (Kulshreshtha & Kort, 2009; Davis et al., 2013; Rempel et al., 2014; Amichev et

al., 2015, 2016; Dhillon, 2016; Amadi et al., 2016, 2017; Dhillon and Rees, 2017; Maillet et al., 2017; Rempel et al., 2017).

Phase II is nearing completion and ends in early 2021. It is focused on predicting growth and carbon sequestration based on climate in a more site-specific approach. All of the past information gained in both phases of the projects are being incorporated into a decision supporting system (DSS) to help farmers to manage their shelterbelts based on local conditions. At the end of phase II, the DSS will be available for the public in a new computer application housed at *shelterbelt-sk.ca* that includes a wide range of shelterbelt information on maintenance, carbon sequestration, shelterbelt design, and planting recommendations for shelterbelt species in southern Saskatchewan based on the goal of each landowner. Phase II has also resulted in a wide array of new literature on the subject of shelterbelts (Ha et al., 2019; Mayrinck et al., 2019; Amichev et al., 2020a, 2020b; Howat, 2020; Rudd, 2020).

2.4 Policies against climate change

The next federal action taken to combat global warming was developing the Pan-Canadian Framework on Clean Growth and Climate Change, which proposed a series of policy changes. The framework was the Canadian answer to reach the commitments it made by signing onto the Paris Agreement in 2016. Canada aimed to reduce its emissions, while making the economy more resilient and diversified. The main resolution of the Pan-Canadian Framework was to implement a carbon pricing system across all provinces, and to let the provinces use the revenue to fix environmental, social, and economic damages caused by climate change in any way that they decided (Environment and Climate Change Canada, 2016).

A debate over a carbon pricing system is not a new discussion for Saskatchewan. In 1997, the federal government proposed a cooperative provincial effort to reach Kyoto's Protocol targets, but Saskatchewan opted out (Olive, 2019). Despite this, in 2000, the government of Saskatchewan launched an ambitious plan aiming to drop 32% and 80% of its releases by 2020 and 2050, respectively, by volunteer industry adherence where emissions were still not charged (Olive, 2019). However, an election and a switch in premiers discredited the plan, and instead of dropping, emissions rose again. In 2015, the federal commitment to the Paris agreement, and the creation of the Pan-Canadian Framework, once again created issues in Saskatchewan. By 2015 it was harder for Saskatchewan to catch up with so many years of neglecting global warming initiatives, so the province did not sign onto the framework. Instead, the province challenged the

federal government in the Supreme Court (Olive, 2019; SaskPower, 2019). Despite this challenge, the federal government levy on carbon pricing took place anyway in April 2019 (Olive, 2019; SaskPower, 2019). Saskpower for example passed the carbon tax on to its customers, which was equal to $22 per year more on the electricity bill for each average residence (SaskPower, 2019).

There remains a big debate on how to make carbon pricing fair to all provinces and avoid job loss in specific sectors hardest hit by the change in policy. Different sectors release different amounts of greenhouse gases and each province's economy relies on activities with different emission rates. The province of Saskatchewan, for example, does not welcoming any carbon pricing system, and continues to work towards eliminating the system thrust upon them. Since the province's main energy sources are coal and oil, and the economy is heavily based on activities such as mineral extraction and agriculture, all sectors are heavily penalized in all carbon pricing systems (Liu et al., 2018; Olive, 2019). Unfortunately, due to Saskatchewan's main reliance on its energy sources, its per capita emissions are much higher than the national average (Olive, 2019). Given this, the province has acted in other ways to try to create a more sustainable agriculture sector. Examples are the Indian Head Agricultural Research Foundation (IHARF) and the Saskatchewan Soil Conservation Association (SSCA), both focused on making agricultural innovations, that bring to the forefront more sustainable agriculture practices.

Although the ongoing debate on carbon pricing remains in Saskatchewan, other Canadian provinces have been embracing carbon pricing systems for a while. The first province implementing a pricing system was British Columbia in 2008. As of 2013, the province had decreased its releases by 12.9%, while the rest of the country reduced emissions by only 3.7% (Komanoff & Gordon 2015). Carbon pricing has been used as a tool to try to keep carbon emissions under certain thresholds, but scholars have pointed out that carbon pricing alone is not enough to drop emissions (Boyce, 2018; Klenert et al., 2018; Tvinnereim & Mehling, 2018). Several authors indicate that a promising approach to offset carbon emissions would be to implement incentivized policies that reward land-owners for carbon sequestered (Kooten et al., 1995; Fitzsimmons et al., 2004; Sobool et al., 2004; Mize et al., 2008; Kulshreshtha & Kort, 2009; Cortus et al., 2011; Neuman & Belcher, 2011; Amichev et al., 2020b), or create a carbon market to trade credits among farmers (Schoeneberger, 2009; Amichev et al., 2020b). Such systems would be a good solution for Saskatchewan's agricultural sector's reluctance to implement carbon pricing. It also would motivate farmers to keep their shelterbelts and reverse

the trend of removing them (Rempel et al., 2014, 2017; Ha et al., 2019; Amichev et al., 2020a). Planting trees would assist Saskatchewan landowners to sequester carbon annually through time, and if incentivized, would eventually become part of the basic economics of a farm. Saskatchewan farmers could specially benefit from such a policy, especially if a process that many are already doing (i.e., growing trees), was incorporated into its provincial carbon pricing system. Since there are approximately 60,633 km of trees already growing in the province that has already sequestrated 10.8 Tg C since 1990 (Amichev et al., 2015, 2017), shelterbelts could provide an even bigger environmental service for farmers, the province, and especially the planet.

CHAPTER 3

This chapter was originally written as one part of my written comprehensive exams, and after feedback on the piece from my committee, it was turned into a journal article. The chapter was published in the journal *Forests*, in a collaboration with three more authors, Dr. Colin P. Laroque, Dr. Beyhan Y. Amichev, and Dr. Ken Van Rees (Mayrinck et al. 2019). Contributions of each additional author to the paper following my original conceptualization was: C.P.L., B.Y.A., and K.V.R., editing and suggestions for rewriting, and suggestions of the addition of Tables and Figures to round out the original draft.

ABOVE- AND BELOW-GROUND CARBON SEQUESTRATION IN SHELTERBELT TREES IN CANADA: A REVIEW

3.1 Abstract

Shelterbelts have been planted around the world for many reasons. Recently, due to increasing awareness of climate change risks, shelterbelt agroforestry systems have received special attention because of the environmental services they provide, including their greenhouse gas (GHG) mitigation potential. This paper aims to discuss shelterbelt history in Canada, and the environmental benefits they provide, focusing on carbon sequestration potential, above- and below-ground. Shelterbelt establishment in Canada dates back to more than a century ago, when their main use was protecting the soil, farm infrastructure and livestock from the elements. As minimal-and no-till systems have become more prevalent among agricultural producers, soil has been less exposed and less vulnerable to wind erosion, so the practice of planting and maintaining shelterbelts has declined in recent decades. In addition, as farm equipment has grown in size to meet the demands of larger landowners, shelterbelts are being removed to increase efficiency and machine maneuverability in the field. This trend of shelterbelt removal prevents shelterbelt's climate change mitigation potential to be fully achieved. For example, in the last century, shelterbelts have sequestered 4.85 Tg C in Saskatchewan. To increase our understanding of carbon sequestration by shelterbelts, in 2013, the Government of Canada launched the Agricultural Greenhouse Gases Program (AGGP). In five years, 27 million dollars were spent supporting technologies and practices to mitigate GHG release on agricultural land, including understanding shelterbelt carbon sequestration and to encourage planting on farms. All these topics are further

explained in this paper as an attempt to inform and promote shelterbelts as a climate change mitigation tool on agricultural lands.

3.2 Overview: Shelterbelt Qualities and Their Role around the World

Shelterbelts, also known as windbreaks, are agroforestry systems that can be defined as barriers of trees, or trees combined with shrubs, that are planted to reduce wind speed (Price, 1993; Brandle et al., 2004; Zhu, 2008). Hedges are a similar feature, defined as a narrow row of a low and dense shrub species used to separate fields (Price, 1993). Sometimes shelterbelt and hedge concepts can be interchangeable, because shelterbelts are also used to separate fields and hedges end up reducing wind speed. However, in this paper, we will be focusing on the aspects of shelterbelts only.

Shelterbelts have been established all over the world to protect soil, crops, homes, farm infrastructure, livestock, and pastures. In Britain, shelterbelts were largely planted in the mid-18th century for crop protection and to keep farm pollution away from busy roads (Heath et al., 1999). In the United States (U.S.), a shelterbelt-incentive program was carried out by the Prairie States Forestry Project (PSFP), which resulted in nearly 30,000 km of shelterbelts planted from 1935 to 1942 across six Great Plains states (Dunlop, 2000). In China, shelterbelts have been used to isolate the coastal zone from sea and land disturbances (Wu et al., 2017), to protect agricultural systems from dry winds and sandstorms (Xiao & Huang, 2016), and to stabilize sand dunes (Zhou et al., 2007). In 1950, an extensive shelterbelt planting took place, aimed at defeating agricultural lands from erosion (Zhou et al., 2005). Later, the "Three-North Shelterbelt Project" started, and has increased treed land area from 5%, in 1978, to 10%, in 2008 (Zhou et al., 2007). In New Zealand, landowners have planted shelterbelts since 1850, when the settlers arrived, totaling more than 300,000 km in length (Hawke & Tombleson, 1993). In Australia, shelterbelts were planted on treeless areas such as the western plains of Victoria (Burke, 1998). In Argentina, there are more than 1500 km of windbreaks planted to protect crops, cattle and homes from wind (Peri & Bloomberg, 2002).

Shelterbelts can be composed of perennial and or annual trees and shrubs (Zhu, 2008; Brandle et al., 2004). The species chosen should be adapted to local climate, topography, and soil (Wight, 1988). To make it sustainable through time, it is recommended to alternate rows of fast and slow-growing species (FAO, 2019), creating a forest-like dynamic. Fast-growing species start protecting the area earlier allowing the slow-growing species to reach maturity when the fast-

growing species are in decline, thus always maintaining an effective shelter. This system enriches biodiversity, while producing wood that can be harvested periodically for fencing, furniture and housing, as well as increasing carbon residence time in the system. Combining species within the overall design makes the shelterbelt system sustainable through time, as well as making the system more resistant to pests and disease, diversifying shelterbelt structure and assisting to mitigate any of its vulnerabilities (Wight, 1988; Zhou et al., 2007).

Ideal shelterbelt structure and design depend on its function (Brandle et al., 2004). For example, for wind protection, it should have multiple rows (usually 2–3) of trees to achieve high shelterbelt density, located at 2–5 times the shelterbelt height (H) from the edge of the field, to increase the amount of land protected and amplify economic returns (Wight, 1988; Strange & Brandle, 2006). For snow management, normally, the ideal design is planting one single row with a tall deciduous tree species using wide spacing (5 to 7 meters between trees to achieve a medium shelterbelt density), perpendicular to the prevailing winds (Strange & Brandle, 2006). In many cases, there are other directions that winds can put crops in danger, rather than the prevailing winds, so it is beneficial to have two right-angle oriented shelterbelt rows (Wight, 1988). For severe winters, as in the Canadian Prairies, five to seven rows may provide the ideal protection from weather events (Wight, 1988). For livestock systems, shelterbelt rows should be dense, planted at narrow spacing (2–3 meters between trees), so that the animals are protected from associated wind chill (Strange & Brandle, 2006). Normally, one windbreak is not enough to protect a whole field, so more rows need to be added, within a distance of 10–20 times the shelterbelt height, depending on the level of protection desired, size of equipment used, and degree of crop tolerance to wind (Strange & Brandle, 2006; Helmers & Brandle, 2016). For example, Helmers & Brandle (2016) recommended to add a shelterbelt every 13 H for corn and soybean production in a 70-year planning horizon.

An important factor on establishing shelterbelts is row spacing indicated by the distance between planted trees within a shelterbelt row. If narrow spacing is adopted, the trees will shade the soil beneath much sooner, which can reduce the costs of weed control; however, the disadvantage is that trees will be competing earlier for resources, and if not managed properly, could lead to reducing their health and growth (Wight, 1988). Wider spacing also has disadvantages, since the trees will take longer to shade the soil to avoid weed competition, so the landowner will have to combat weeds; the trees will develop larger crowns, demanding more

water; greater tree and soil exposure to the sun and wind between the rows will also increase evapotranspiration. Between shrubs, conifers and deciduous trees the minimal recommended spacing is 0.3–1, 2.0–2.5 and 3 meters, respectively (Agriculture and Agi-Food Canada 2015).

Shelterbelt maintenance is similar to forest maintenance. At their establishment, weeding and pest control should be conducted, to help seedlings get established. If the shelterbelt is planted in a pasture or an area with wild animals, building a fence should be considered to protect the seedlings from animal injuries (FAO, 2016; Helmers & Brandle, 2016). Later, branch pruning and thinning of densely planted rows may be required in some cases, to boost height and diameter growth, respectively (FAO, 2016).

The efficiency of a shelterbelt as a wind barrier is determined by its external and internal structure. Its external structure is related to its height, length, orientation, continuity, width, and cross-sectional shape; its internal structure is related to the amount and structure of open and solid spaces in the tree crowns, plant shape, and surface area (Brandle et al., 2004; Zhou et al., 2005). Shelterbelt height and length determine the extent of windbreak protection (Strange & Brandle, 2006; Zhou et al., 2007). Shelterbelt length should be 10 (Zhou et al., 2005; Strange & Brandle, 2006) to 20 (Cleugh, 1998) times its height, to reduce wind flow around the ends of the shelterbelt (Strange & Brandle, 2006; Zhou et al., 2007).

As shelterbelt use and importance become more popular around the world, more research on the topic has been published. Figure 3.1a) illustrates the percentage of existing literature published per year, available on the Web of Science, on the topic of shelterbelts and the respective percentages of published papers per year on the topics of agriculture and forestry. It was expected that agriculture and forestry publication rates would surpass shelterbelt publication rates for three main reasons. First, agriculture and forestry are crucial to feed the increasing demand of the growing global population. Second, shelterbelts are normally not established with the intention of producing material goods as they are for agriculture and forestry. Third, the environmental benefits provided by shelterbelts are only mostly experienced in the long run and are difficult to be translated into monetary values, unlike the products from agriculture and forestry. However, shelterbelt publications were increasing at a pace similar to agriculture and forestry rates, rising sharply after the 90s (Figure 3.1a). This may be attributed to the increasing access to computers, making it easy to process studies and publish more, or perhaps to the increasing awareness on climate change and environmental issues. In either case, awareness on the importance of

shelterbelts and their environmental services was increasing, regardless of their smaller role on providing material goods. Similar searches were made using the keyword windbreak, instead of shelterbelt which yielded the same trend as shown in Figure 3.1a. The total contribution to shelterbelt research by country varied (Figure 3.1b). The top three leading countries on shelterbelt research are (in decreasing order) China, U.S., and Canada.

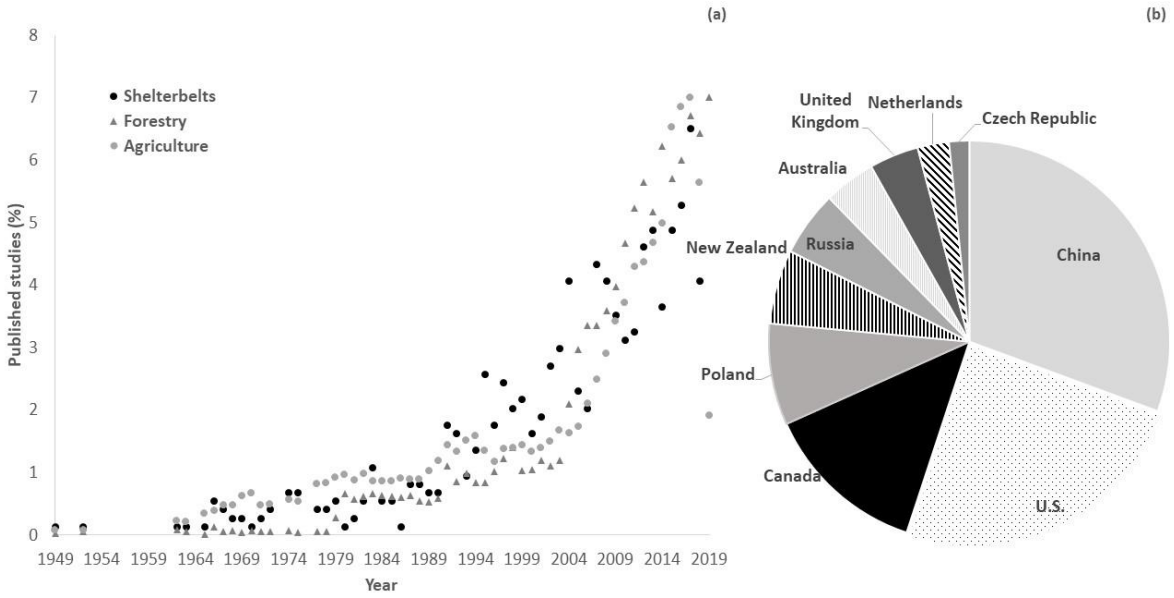

Figure 3.1 - Number of journal publications on shelterbelt agroforestry systems found on Web of Science (a), and the relative contribution by country (b).

Shelterbelt researchers in Canada have contributed much to the literature due to the great number of shelterbelts planted over the years. According to the Government of Canada, farmers in Western Canada have planted more than 600 million trees during the past century (Piwowar et al., 2017). Just in Saskatchewan alone, the total length of shelterbelts equals to 60,633 km (Amichev et al., 2015), sequestering around 4.85 Tg C in the past nine decades, more than half of which were sequestered since 1990 (3.77 Tg C) (Amichev et al., 2016).

The motivations driving farmers around the world to plant shelterbelts have been in general agreement: to protect farm yards, crops, infrastructure, and livestock from the harsh environment, and for aesthetics (Heath et al., 1999; Brandle et al., 2004). However, this general motivation has changed over the years to address the needs of each generation of farmers; thus, new reasons for planting and maintaining shelterbelts were added. For example, in New Zealand, shelterbelts planting was also focused on timber production (Ha et al., 2018). In Canada, as described above, shelterbelts have been planted mainly to protect soil from wind erosion;

however, because of new agricultural techniques, such as the no-till system, wind erosion is less of an issue than in past decades, and some farmers are currently removing their shelterbelts (Zhou et al., 2005; Strange & Brandle, 2006). In a recent study, it was determined that 29.8% of farmers in a 1400 km^2 study area in Saskatchewan, Canada, removed their shelterbelts between 2008 and 2016 (Ha et al., 2018). The main reasons that farmers were removing their existing shelterbelts were: 1) shelterbelts required additional labor for maintenance; 2) shelterbelts made it difficult to operate large farming equipment in crop fields; and 3) shelterbelts reduced the land area available for crop production (Rempel et L., 2014, 2017; Ha et al., 2018).

However, the benefits provided by the shelterbelt may be able to overcome even these new disadvantages. Some researchers have suggested that farmers are not aware of the advantages of having shelterbelts, so, they are more prone to remove them (Rempel et al., 2014, 2017). It is very likely that if education on the environmental benefits that shelterbelts provide, mainly their carbon sequestration, were projected into the long term, it would help farmers to better value them. Rewarding farmers for keeping existing, and or, planting new shelterbelts, by for example granting them a tax reduction or tax credit in a carbon trading market place (Ha et al., 2018), would make landowners more prone to stop removing them. If a carbon market were implemented, any carbon sequestered by shelterbelt trees would have a monetary value, so trees would become a part of the farm's overall budget, which could motivate future shelterbelt planting and better maintenance of existing ones.

3.3 Shelterbelt History in the Canadian Prairies

When European settlers first started to populate Western Canada in the late 1890s, they were encouraged to settle in various regions, including the driest area, known as the Palliser Triangle (Marchildon, 2014; Rempel et al., 2014). This area encompasses southern Saskatchewan, into Alberta, and Manitoba including the Canada–U.S. border, covering more than 200,000 square kilometers (Marchildon, 2014; Rempel et al., 2017). There is even a dryer area inside the Palliser Triangle, named the Dry Belt, located in southern Alberta and Saskatchewan (Anstey, 1986; Dunlop, 2000; Marchildon, 2014). This land is extremely arid, and has had many cycles of extreme dry years through time (Marchildon, 2014).

Between the 1880s and 1980s, several droughts occurred in the Canadian Prairies: in 1910, 1914, 1917–20, 1924, 1929–30 (Dunlop, 2000; Marchildon, 2014). During these dry periods, shelterbelts were useful in capturing snow, and helped increase and maintain soil

moisture. Planted trees improved the soil water regime by shading and reducing soil surface temperatures (Dunlop, 2000), all of which reduce soil evapotranspiration. At the time, there was also a false belief that planting trees would increase local rainfall (Dunlop, 2000; Marchildon, 2014), which contributed to increases in local shelterbelt planting. The 1930s drought occurred during one of the worst crises in North America, known as the Great Depression. It was a combination of drought, insect infestation, and dropping of global commodities prices (Dunlop, 2000; Marchildon, 2014). The Great Depression was so brutal that, in 1936, about 14,000 people left their farms, totaling around 12,140 km^2 of abandoned land within the Palliser Triangle alone (Dunlop, 2000; Marchildon, 2014).

To aid farmers in Western Canada facing Depression-like conditions, the Government of Canada established the Prairie Farm Rehabilitation Administration (PFRA) in 1935, in Indian Head, Saskatchewan, where 200 agrologists, engineers, field husbandmen, inspectors and administrators focused on rehabilitating farms in the Prairies after the Great Depression (Marchildon, 2014). The PFRA received $750,000 for the first year, and $1 million annually for the next four years, to help combat the consequences of drought (Marchildon, 2014). By 1939, the PFRA assisted with the construction of thousands of dugouts and earthen dams designed for stocking water (Marchildon, 2014). Additionally, the PFRA assisted farms in many ways, including the management of community pastures in Saskatchewan and Manitoba, and by conducting a soil survey covering 90% of the Palliser Triangle, at a one-mile resolution (Marchildon, 2014).

One of the most notable legacies of the PFRA activity included providing free seedlings and assistance for shelterbelt establishment to farmers, known as the Prairie Shelterbelt Program (PSP) (Amadi et al., 2017; Maillet et al., 2017). A nursery in Indian Head was created to function as a live demonstration farm to show planting options, and serve as a reference for farmers displaying the diversity of shelterbelt agroforestry systems that could be implemented on the Prairies (Dunlop, 2000). Initially, seedling demand was low, but this increased through time, from 1000 to 9.2 million trees per year, peaking in the particular years of 1961, 1970, 1981 and 1991, probably due to landowners receiving shelterbelt-related information from PFRA (i.e., hand-outs, talks at agricultural fairs and shows) related to droughts that occurred in the previous years (Amadi et al., 2017). As the demand for seedlings changed, the number of species offered also changed, increasing from five, at the beginning of the program, to 37 shelterbelt species in the

2000s (Amadi et al., 2017). It is calculated that in total, over 600 million shelterbelt trees/shrubs were provided by the PSP program (Wiseman et al., 2009; Amadi et al., 2017). Towards the end of the program, the demand for shelterbelt trees dropped, and in 2006 and 2009, 3.7 million and 2.5 million seedlings were ordered, respectively (Amadi et al., 2017). In the end, the PSP program was shut down in 2013.

The work promoted by PFRA's PSP program on implementing shelterbelts for the past nine decades showed Canada's commitment to sustainable development in the Prairies. This commitment was reaffirmed in 2009 by signing the Copenhagen Accord, when Canada committed to reduce GHG emissions by 17% by 2020, based on 2005 levels. To help with reaching the goal, the Federal government launched the Agricultural Greenhouse Gases Program (AGGP) in 2013. The goal of AGGP is to mitigate GHG emissions in the agricultural sector by creating technologies and practices that promote carbonless agriculture (Agriculture and Agri-Food Canada 2019). One of the aims of AGGP is to study shelterbelt carbon sequestration and their potential for climate change mitigation. This branch financed the majority of studies on shelterbelts in Canada since its inception. In 2016, the Paris Accord was signed by 170 countries, including Canada, which required committed countries to join efforts to keep global temperature increases under 2 °C, based on pre-industrial levels, with further efforts aimed at limiting warming to 1.5 °C (Rogelj et al., 2016). As stipulated by the AGGP program, and in the context of global efforts towards a carbonless economy, the carbon sequestration potential of shelterbelts remains a viable research priority for the Canadian Prairies.

3.4 Environmental Services Provided by Shelterbelts

Shelterbelts provide both public and private benefits, commonly referred to as environmental services (Kulshreshtha & Kort, 2009). Private benefits include protecting soil, homes, farm infrastructure, and livestock from the elements (Carroll et al., 2004; Kulshreshtha & Kort, 2009; Czerepowicz et al., 2012; Rempel et al., 2014; Amadi et al., 2017), reducing animal odor from livestock systems, lowering the risk of crop environmental damage due to pesticide spray-drift (Rempel et al., 2014; Amadi et al., 2017; Dhillon et al., 2017), reducing noise (Wight, 1988), and heating costs for households and livestock operations (Amadi et al., 2017). It is estimated that shelterbelts can save up to 18% in energy costs for heating homes (Liu & Harris, 2008).

Public benefits provided by shelterbelts include reducing soil runoff into rivers, streams and creeks, sequestering carbon dioxide from the atmosphere, enhancing and protecting animal and plant diversity, including pollinators, as well as improving water quality (Kulshreshtha & Kort, 2009; Amadi et al., 2017; Piwowar et al., 2017). Some shelterbelt benefits can be categorized as both private and public. For example, improving water quality and protecting biodiversity are more commonly classified as public environmental services; however, these can also be considered as private benefits since it would also be beneficial on the land where the shelterbelt is located.

These benefits are hard to quantify in terms of monetary value (Kulshreshtha & Kort, 2009; Piwowar et al., 2017; Rempel et al., 2017), due to the complexity of the factors affecting, and being affected by, shelterbelt systems, but there are some studies that address this question. Kulshreshtha et al. (2009) assessed public service worth provided by shelterbelt seedlings given by PFRA's PSP program from 1981 to 2001. They found that those benefits were worth $140 million, the majority provided by carbon sequestration ($73 million), and soil erosion reduction ($15 million). Similarly, Amichev et al. (2016) studied carbon sequestration of six common shelterbelt species in Saskatchewan, planted from 1925 to 2009, and estimated that the carbon additions (through CO_2 sequestration) in shelterbelt systems since 1990 (equal to 3.77 Tg C) would be worth $208 million dollars at current carbon prices.

Because shelterbelts can improve their surrounding conditions through environmental services, they can also impact crop production by retaining soil moisture, slowing wind speed, shading areas beside the trees, and reducing soil loss (Cleugh, 1998; Strange & Brandle, 2006). Shelterbelts can increase monetary gains for landowners by increasing crop yield and/or saving on chemical applications (Kulshreshtha & Kort, 2009; Amichev et al., 2016; Rempel et al., 2017). Normally, these benefits can span up to a distance of 10 H on the leeward and 0–3 H on the windward side of the trees (Mize et al., 2008). For example, it was calculated that shelterbelts planted from 1981 to 2001 in the Prairie Provinces in Canada, prevented soil erosion, equal to a benefit of $15 million (Kulshreshtha & Kort, 2009). Shelterbelts were also calculated to reduce crop production costs related to the use of pesticides, and reduce overall crop loss due to pest damage (Gámez-Virués et al., 2007; Mize et al., 2008). Gámez-Viruez et al. (2007), studying feces from birds inhabiting shelterbelts in Australia, found that birds fed on crop pests, helping as a biological control. Shelterbelts can also help to keep a more stable soil temperature range in its

surroundings. During the night, soil temperatures near shelterbelts are from 1–2 °C higher than in open fields, which can assist crops to germinate and grow faster in colder environments (Baldwin, 1988; Kort & Turnock, 1999; Strange & Brandle, 2006).

Baldwin (1988) conducted a review on the effect of shelterbelts on crop production and concluded that gains can be up to 50%. Kort (1999) completed an extensive review on how the crops respond to shelterbelt trees and found that in most cases, shelterbelts increased crop yield, and that this can be further maximized by choosing adequate shelterbelt species and designs, based on specific crops. The author concluded that wheat (*Triticum aestivum* L.), barley (*Hordeum vulgare* L.), rye (*Secale cereal* L.), millet (*Pennisetum americanum L.*), alfalfa (*Medicago sativa* L.), and hay (mixed grass and legumes) yields are more responsive to shelterbelt presence, and that oats (*Avena sativa* L.), and maize (*Zea may* L.) are affected as well, though they are less responsive. Hawke & Tombleson (1993) observed a 15% increase in pasture production on both sides of shelterbelts at distances equal to 70% of the tree height.

The general rule is that shelterbelts have positive impacts on adjacent crop yield (Tatarko, & Dickerson, 1984; Baldwin, 1988; Cleugh, 1998; Lyles et al., 2006), which are more pronounced during short-duration or more intense droughts (Kort & Turnock, 1999; Qi et al., 2001). However, there are cases where shelterbelts affect yield negatively. Land trade-off is one factor leading to decreasing yield since shelterbelts take out land area from crop production (Easterling et al., 1997; Kort & Turnock, 1999). To make shelterbelts economically viable, crop yield increases by a shelterbelt's presence should be more than compensated for the yield lost in the area that is used to plant the shelterbelt. In the long run, the benefits from the shelterbelt will therefore be felt economically (Easterling et al., 1997). According to Brandle et al. (2006) shelterbelts are economically viable if less than 6% of the land is occupied by trees.

Another factor that may decrease crop yield is allopathy on the adjacent crop, as it can inhibit seed germination and overall crop growth. Another factor is shading, created by the trees, that can reduce crop photosynthesis and growth from reduced sunlight (Cleugh, 1998; Dunlop, 2000; Amadi et al., 2017; Piwowar et al., 2017). For example, Kowalchuk & Jong, (1995) assessed the effect of shelterbelts on wheat yield and soil erosion for three years and found that when environmental conditions were dry, trees and crops competed for moisture, and yield was reduced at distances up to 10 meters from the shelterbelt edge. Singh & Kohli, (1992) studied the effect of an eight-year-old *Eucalyptus tereticornis* Sm. shelterbelt on yields of chickpea (*Cicer*

arietinum L.), lentil (*Lens culinaris* (LENCU) wheat, cauliflower (*Brassica oleracea* L.) and barseem (*Trifolium alexandrinum* L.) and concluded that yield was always reduced by shelterbelts and that chickpeas were the most affected crop from the list.

Table 3.1 shows the effect of shelterbelts on crops reported in the literature. It varies from case to case and can be positive or negative for the same crop, depending on many environmental factors, varying from year-to-year environmental inputs. In most cases, shelterbelt impact was positive. In the cases of decreasing yields, the results were mainly attributed to below-ground tree/crop competition for soil moisture and nutrients. One alternative to reducing below-ground competition is pruning the lateral tree roots (Lyles et al., 1984; Strange & Brandle, 2006). The frequency of root pruning was dependent on the shelterbelt and crop species and spacing, but is normally done every one to five years (Lyles et al., 1984; Strange & Brandle, 2006). It was calculated that in North America, root pruning can decrease competition from 10 to 44% in the adjacent shelterbelt-influenced area (Baldwin, 1988; Strange & Brandle, 2006). Onyewotu, Ogigirigi, & Stigter, (1994) found that millet yield increased after pruning roots at 0.25 H distance from *Eucalyptus camaldulensis* Dehnh shelterbelt roots beside the field. Lyles et al., (1984) also found that yield from 1 to 2 H distance were 1.6 higher than on the unpruned zone. However, root pruning is an expensive operation. To avoid root pruning, it is important to choose species with deep root systems, so they do not spread laterally and compete with crop root systems (Greb & Black, 1961; Lyles et al., 1984; Strange & Brandle, 2006). Greb & Black, (1961) found that American elm (*Ulmus Americana* L.), black walnut (*Juglans nigra* L.), ponderosa pine (*Pinus ponderosa* Douglas ex P. Lawson & C. Lawson, and Siberian elm (*Ulmus pumila* L.) have shallow roots, so they spread laterally in search of nutrients, and compete more with crops. Thevs et al., (2017) found that among the shelterbelt species tested (tamarack (*Tamarix)*, Siberian elm, Russian-olive (*Elaeagnus angustifolia* L.), honeysuckle (*Lonicera)*, and caragana (*Caragana arborescens* Lam., tamarack had the highest soil water uptake and caragana had the lowest, and therefore was a better suited species to be used in a shelterbelt composition.

Table 3.1 - Effect of shelterbelts on adjacent crop yield from studies around the world.

Shelterbelt Species	Crop Species	Influence	Yield (%)	Reference	Location
	Winter wheat	+	23	(Kort & Turnock, 1999)[a]	
	Spring wheat	+	8	(Kort & Turnock, 1999)	
	Barley	+	25	(Kort & Turnock, 1999)	
	Oat	+	6	(Kort & Turnock, 1999)	
	Rye	+	19	(Kort & Turnock, 1999)	
	Millet	+	44	(Kort & Turnock, 1999)	
	Alfalfa	+	99	(Kort & Turnock, 1999)	
Ponderosa pine	Winter wheat	+	4.19	(Greb & Black, 1961)	Colorado, U.S.
Caragana, Chokeckerry (*Prunus virginiana* L.)	Winter wheat	+	12.25	(Greb & Black, 1961)	Colorado, U.S.
Black walnut, Black locust (*Robinia pseudoacacia* L.)	Winter wheat	–	12.89	(Greb & Black, 1961)	Colorado, U.S.
Ponderosa pine	Sorghum	–	2.4	(Greb & Black, 1961)	Colorado, U.S.
Siberian pea, Chokeckerry	Sorghum	–	13.5	(Greb & Black, 1961)	Colorado, U.S.
Black walnut, Black locust	Sorghum	–	3.75	(Greb & Black, 1961)	Colorado, U.S.
(Populus × euramericana)	Soybeans (*Glycine max* L.)	+	23	(Qi et al., 2001)	Great Plains, U.S.
Green ash, Austrian pine (*Pinus nigra*), Eastern red cedar *(Juniperus virginiana* L.*)*	Soybeans	+	26	(Ogbuehi & Brandle, 1982)	Nebraske, U.S.
Eastern red cedar	Beans	+	21	(Rosenberg, 1966)	Nebraske, U.S.
Indian rosewood (*Dalbergia sissoo*)	Cotton (*Gossypium hirsutum* L.)	+	10	(Puri, Singh, & Khara, 1992)	Dhiranvas, India
Corymbia intermedia (R.T.Baker) K.D.Hill & L.A.S.Johnson, *Corymbia tessellaris* (F.Muell.) K.D.Hill & L.A.S.Johnson	Potato (*Solanum tuberosum* L.)	+	6.7	(Sun & Dickinson, 1994)	Atherton Tablelands, Australia
Arizona cypress (*Cupressus arizonica*)		–	25	(Campi, Palumbo, & Mastrorilli, 2009)	Rutigliano, Italy
Aleppo pine (*Pinus halepensis* Miller)	Wheat	+	44	(Nuberg, Mylius, Edwards, & Davey, 2002)	Southern Australia
Aleppo pine	Faba beans (*Vicia faba* L.)	+	49	(Nuberg et al., 2002)	Southern Australia
Aleppo pine	Oat	+	25	(Nuberg et al., 2002)	Southern Australia
Populus canadensis Mönch, *P. Beijingensis* W.Y. Hsu, *P. xiaozuanrica, P. Simonii* Carrière, *P. pseudo-simonii*	Mayze	+	6.13	(Zheng, Zhu, & Xing, 2016)	Western China, Heilongjiang, Jilin, Liaoning and Inner Mongolia

[a] Shelterbelt species and location are not provided because this numbers were summarized by (Kort & Turnock, 1999) after an extensive literature review from variety of studies (including a variety of locations and shelterbelt species).

Even though shelterbelt tree roots can compete with crops, they impact the overall ecosystem in a positive manner, due to their significant role on soil health and structure. It is calculated that global land degradation annually costs about $300 billion U.S. dollars (Nkonya et al., 2015). A study conducted in England and Wales illustrated that soil compaction alone was responsible for 39% of all costs of soil recovery (Graves et al., 2015). Soil compaction is one of the most serious issues faced by agricultural producers today (Carroll et al., 2004). Soil compaction is caused by a variety of factors, such as overuse of heavy machinery and short crop rotations, which reduces crop yield and soil health in the long term. In contrast, shelterbelt systems can ameliorate crop growing conditions by improving soil structure and adding organic matter into the soil by means of growing extensive and deep tree root systems, thus enhancing soil porosity, which increases soil water infiltration and recharge, and improving the overall soil health. Carrol et al. (2004) studied the effect of shelterbelts in pastures and observed that water

infiltration under and near shelterbelts was 60 times greater compared to open areas on the pasture, and that significant changes in the rate of soil water infiltration happened soon after planting, as early as two years after shelterbelt establishment.

Besides water infiltration, crop water-use efficiency is also affected by shelterbelts. The treed barrier reduces wind speed, thus slowing heat transfers from the crops to the air, and slowing down evapotranspiration. Davis & Norman (1988) reviewed the effects of shelterbelts on crop water-use and found a significant reduction in turbulent air which decreased evapotranspiration, improving water-use efficiency. Similarly, Ogbuehi & Brandle (1982) found that sheltered (shaded) soybeans had greater photosynthesis rate, stomatal conductance and deeper light penetration than non-sheltered plants. Thevs et al., (2017), studying corn, potato, wheat, and barley production, found that crop water consumption was 10–12% lower in areas in the proximity of shelterbelts, compared to open field conditions.

Environmental services provided by shelterbelts, as previously discussed, modify the micro environment, and can be seen as a useful tool to mitigate the effects of climate change that will impact agricultural production worldwide in the near future (Easterling et al., 1997; Strange & Brandle, 2006). For example, Easterling et al. (1997) used a model to simulate the effects of climate change related stress on maize planted in dry environments in Nebraska, comparing yield on sheltered and unsheltered crops. They concluded that sheltered crops yields were greater, and that shelterbelts are an important tool to ameliorate global warming consequences.

3.4.1. Shelterbelt Carbon Sequestration Potential

Shelterbelts are useful not just to mitigate local weather extremes caused by climate change, but are also useful tools to mitigate global warming, thanks to their carbon sequestration potential. The Inter-Governmental Panel on Climate Change indicated that there were about 630 million hectares of unproductive land on the planet in 2000, and they suggested that if it was used for agroforestry, it would sequester 1.43 and 2.15 Tg CO_2 every year by 2010 and 2040, respectively (IPCC, 2000).

Carbon sequestration in agroforestry varies among the different types of agroforestry practiced, ecological regions where it takes place, and soil type, ranging from 0.29 to 15.21 Mg ha^{-1} $year^{-1}$ for above-ground, and 30–300 Mg C ha^{-1} $year^{-1}$ up to 1 m depth in the soil (Nair et al., 2009, 2010). Currently, the global area under agroforestry systems is 1023 million ha and as previously stated, there is approximately 630 million ha of unproductive lands in the world that

could be used to promote carbon sequestration through agroforestry practices (IPCC, 2000). Carbon sequestration potential tends to be greatest in natural forests, then in agroforestry systems, followed by tree plantations, and finally in cropped lands (Onyewotu et al., 1994; Nair et al., 2009). Table 3.2 shows the land use and its carbon sequestration potential reported in the literature around the world. Land use systems that include trees have a great potential in comparison with agriculture alone. Schoeneberger (2009) and Wang & Feng, (1995) values are already in hectares, and they considered that shelterbelts occupied 5 and 2.5% of the cropland area, respectively.

Table 3.2 - Carbon sequestration potential of diverse land use classes using different tree species around the world.

Land Use	Species	Total Mg C (km^{-1} $year^{-1}$)	Above-ground Mg C (ha^{-1} $year^{-1}$)	Below-ground Mg C (ha^{-1} $year^{-1}$)	Total Mg C (ha^{-1} $year^{-1}$)	Location	Reference
Shelterbelt	Hybrid Poplar	6.03–6.54	0.79*Total	0.21*Total	3.3–5.2	Saskatchewan, Canada	(Amichev et al., 2015) [a]
Shelterbelt	Scots Pine (*Pinus sylvestris* L.)	1.90–2.17	0.90*Total	0.10*Total	1.4–3.3	Saskatchewan, Canada	(Amichev et al., 2015)
Shelterbelt	Manitoba Maple	2.39–2.60	0.80*Total	0.20*Total	2.8–5.3	Saskatchewan, Canada	(Amichev et al., 2015)
Shelterbelt	White Spruce (*Picea glauca* Moench)	2.43–2.75	0.81*Total	0.19*Total	2.2–4.1	Saskatchewan, Canada	(Amichev et al., 2015)
Shelterbelt	Green Ash	1.78–1.98	0.77*Total	0.23*Total	2.0–3.9	Saskatchewan, Canada	(Amichev et al., 2015)
Shelterbelt	Caragana	1.73–2.03	0.74*Total	0.26*Total	1.3–2.7	Saskatchewan, Canada	(Amichev et al., 2015)
Shelterbelt			0.58-1.17			Nebraska	(Schoeneberger, 2009) [b]
Shelterbelt	*Poplar canadensis* Mönch, *Paulownia elongala*		0.38			China	(Wang & Feng, 1995) [c]
Woodlots for firewood, fodder, land reclamation			1.0–5.0	1.0–6.0	2.0–11	Asia/Africa	(Nair et al., 2009)
Shade tree system	*Cordia alliodora* (Ruiz & Pav.) Oken, *Theobroma cacao* L.		3			Costa Rica	(Montagnini & Nair, 2004)
Shade tree system	*Erythrina poeppigiana* (Walp.) O.F. Cook*)*, *Theobroma cacao* L.		4.4			Costa Rica	(Montagnini & Nair, 2004)
Forest	*Dipteryx panamensis* (Pitt.) Rec. & Mell		20.26			Costa Rica	(Montagnini & Nair, 2004)
Monoculture	Cooffe *(Coffea arabica* L.*)*		2.14		2.14	Brazil	(Palm et al., 1999)
Imporved fallow	*Crotalaria grahamiana* Wight & Arn		8.5	2.7	11.2	Kenya	(Albrecht & Kandji, 2003)
Imporved fallow	*Eucalyptus saligna* Sm.		21.7	9.55	31.25	Kenya	(Albrecht & Kandji, 2003)
Silvipasture			6.1		6.1	North America	(Udawatta & Jose, 2011)
Alley crop			3.4		3.4	North America	(Udawatta & Jose, 2011)
agriculture	Fallow, Soybean, Maize		0.3		0.3	Goias, Brazil	(Bayer et al. 2006)
Intercroping	Gliricidia sepium ((Jacq.) Steud)			12.3	12.3	Zomba, Malawi	(Makumba, et al. 2007)

[a] Reported per-area data (Mg ha^{-1} $year^{-1}$) in Amichev et al., (2016) represent the area directly underneath the live shelterbelt tree crowns. For comparison purposes in this study, we assumed that the area of the shelterbelts in Amichev et al., (2016) represented 5% of the total farm area, similar to Schoeneberger (2009) [b] It was estimated that the area of shelterbelts represented 5% of the total farm area. [c] It was estimated that the area of shelterbelts represented 2.5% of the total farm area.
#*Total: value times the total biomass (Total Mg C (ha−1 year−1)).

3.4.2. Shelterbelt Carbon Sequestration Potential and Stocks Above-Ground

Carbon sequestration has been extensively discussed as one of the main strategies to keep atmospheric carbon dioxide at acceptable levels, and minimize environmental risks from climate change effects. Given the increased awareness about shelterbelt carbon sequestration, many studies have been conducted in this regard, across a variety of climatic and edaphic regions, and across different shelterbelt designs, and species mixes (Hawke & Tombleson, 1993; Carroll et al., 2004; Zhou et al., 2007; Mize et al., 2008; Wiseman et al., 2009; Czerepowicz et al., 2012; Marchildon, 2014; Amichev et al., 2016; Chu et al. 2019). The means to quantify carbon sequestration in shelterbelt systems have improved over the years, starting with the use of simple linear relationships and yield tables (Kort & Turnock, 1999), to more sophisticated, and more accurate methods, using complex modelling frameworks, such as Holos, CBM-CFS3 (Carbon Budget Model for the Canadian Forest Sector) (Amadi et al., 2016; Amichev et al., 2016), and 3PG (Physiological Principles Predicting Growth) models (Amichev et al., 2016).

The earliest research on shelterbelt carbon stocks in Canada was carried out by Kort & Turnock (1999). They used destructive sampling techniques to measure shelterbelt tree biomass, and fitted linear models to predict above-ground biomass for different shelterbelt species, ranging from 17 to 90 years, across all soil zones in the Saskatchewan Prairies. They reported an average biomass of 79 kg tree^{-1} (32 Mg km^{-1}) for green ash, 263 kg tree^{-1} (105 Mg km^{-1}) for hybrid poplar, and 144 kg tree^{-1} (41 Mg km^{-1}) for white spruce. Some early work was also done to understand the interaction between shelterbelts and the adjacent crops in terms of C sequestration. Peichl (2006) compared carbon sequestration within three systems in Ontario, Canada: 13-year-old hybrid poplar shelterbelt plus barley; a 13-year-old Norway spruce (*Picea abies*) shelterbelt plus barley; and a barley-only crop system. Total carbon sequestration was 15.1 and 6.4 Mg C ha $^{-1}$ higher than the barley-only system for hybrid poplar and Norway spruce, respectively. Carbon stock in the soil was also significantly different between the systems: 78, 66, and 65 Mg C ha $^{-1}$ for hybrid poplar, spruce, and barley-only systems, respectively.

Amichev et al. (2016) and Amichev et al. (2010) used the 3PG and CBM-CFS3 models to quantify tree growth and carbon stocks of shelterbelts. The CBM-CFS3 model was originally developed for the Canadian forest industry sector and has been used at various scales of analysis, from stand to landscape levels, to simulate forest stand growth and carbon dynamics. Similarly, 3PG is a hybrid model, designed to model forest growth using 60 variables (Sands 2010), which

was also adapted for use in shelterbelt systems (Kort & Turnock, 1999), . Amichev et al. (2016) parametrized 3PG to quantify carbon stocks of white spruce shelterbelts in a large scale study extending across five soil zones in Saskatchewan and spanning several decades of planting, from 1925 to 2009. They estimated the total above-ground biomass at 117.6 Mg C km^{-1}, ranging from 106 to 195 Mg C km^{-1}, depending on the soil zone. The total ecosystem carbon flux increased from 0.33 to 4.4 Mg C km^{-1} $year^{-1}$, from year 1 to 25, reaching a peak of 5.5 C km^{-1} $year^{-1}$ Mg 39 years after planting. Average-stand biomass at age 60 was 241.3, 238.6, and 227.3 Mg km^{-1} at 2.0, 3.5, and 5.0 m tree spacing design, respectively. Overall, total carbon stocks for all white spruce shelterbelts in the province, planted over the span of eight decades, was 50,440 Mg C, sequestered in over 991 km of planted shelterbelts.

Using the same methodology, Amichev et al. (2016) estimated the growth of five additional common shelterbelt species planted across Saskatchewan—hybrid poplar, Manitoba maple, Scots pine, green ash, and Caragana planted between 1925 to 2009, in three spacing designs (2.0, 3.5, and 5.0 m), and at four different mortality rates (0, 15, 30, and 50%). They estimated total shelterbelt carbon stocks for the province at 10.8 Tg C. Overall, the average carbon sequestration rate on a length basis (per km) was estimated 1.73 to 6.54 Mg C km^{-1} $year^{-1}$. The carbon sequestration rates for the individual species were 6.03–6.54 Mg C km^{-1} $year^{-1}$ for hybrid poplar, 1.73–2.03 Mg C km^{-1} $year^{-1}$ for caragana, 1.90–2.17 Mg C km^{-1} $year^{-1}$ for Scots pine, 2.43–2.75 Mg C km^{-1} $year^{-1}$ for white spruce, 1.78–1.98 Mg C km^{-1} $year^{-1}$ for green ash, and 2.39–2.60 Mg C km^{-1} $year^{-1}$ for Manitoba maple shelterbelts. The per-unit-area C rates (Mg C ha^{-1} $year^{-1}$) represent the C sequestration rate across 1-ha cumulative land area located directly underneath the shelterbelt tree crowns. These C sequestration rates included the C locked in live and dead above- and below-ground biomass (i.e., stems, branches, leaves, roots), as well as litter layer (i.e., decomposing tree branches and leaves) on the soil surface, and soil organic matter added into the soil.

The Holos model is an empirical, process-based, farm-scale model that estimates GHGs emissions from farms based on site-specific input information (Amadi et al., 2017; Liu et al., 2012). The model relies on details such as enteric fermentation, manure management, cropping systems, energy use, and presence of planted trees (Agriculture and Agri-Food Canada, 2019). Researchers have used the Holos model for exploration of diverse farming scenarios through many simulations, aiming for minimal GHGs releases from a farm. For example, Holos was used

by Amadi et al., (2017) to calculate the potential of hybrid poplar, white spruce and caragana shelterbelts to offset GHGs emissions from cereal (*Triticum aestivum* and *Avena sativa*) production for a 60-year simulation period, at five shelterbelt planting densities. At the highest planting density (i.e., 5% of total farm area occupied by trees), hybrid poplar, white spruce, and caragana shelterbelts reduced farm GHGs emissions by 23%, 18% and 8%, respectively. The majority of this GHGs offset (95%) was attributed to C sequestered in wood biomass and the soil. The rest was attributed to lower N_2O emissions and CH_4 oxidation, commonly observed within the shelterbelt zone. For a 60-yr simulation, the estimated carbon stocks were 8712, 5581, and 1705 Mg C (at the most-dense spacing) for hybrid poplar, white spruce, and caragana, respectively.

Likewise, statistical models also have been used to estimate carbon sequestration in shelterbelts (Hawke & Tombleson, 1993; Thevs et al., 2017). Possu et al. (2016) assessed 15 allometric models on Ponderosa pine windbreaks and used the best model to estimate carbon sequestration for 16 shelterbelt tree species in Nebraska, projected over 50 years in nine areas of the U.S. They found that carbon sequestration potential ranged from 1.07 ± 0.21 to 3.84 ± 0.04 Mg C ha^{-1} $year^{-1}$ for conifer species and from 0.99 ± 0.16 to 13.6 ± 7.72 Mg C ha^{-1} $year^{-1}$ for broadleaved deciduous species. Zhou et al., (2005) assessed carbon stocks in shelterbelts in Montana, U.S., with two types of statistical models: precise preferred models which required more variables from expensive data inventories (tree height, DBH); and cost preferred models (DBH), which were simpler to fit, but were less precise. The authors concluded that both sets of equations were effective to estimate shelterbelt biomass and that the precision preferred models were between 0.8 and 1.2% more precise than the cost preferred models. They found that above-ground biomass for a single row of Russian-olive shelterbelt was 110 metric tonnes km^{-1} (110 Mg km^{-1}), that converted to approximately 55 Mg C km^{-1}, 60 years after planting (equal to sequestration rate of 0.91 Mg C km^{-1} $year^{-1}$).

3.4.3. Carbon Stocks Below-Ground

Soil is the biggest organic carbon pool on Earth (Nkonya et al., 2015). It is calculated that the world's agricultural and degraded soil are able to sequester 50 to 66% of all carbon released, equivalent to 42–78 gigatons of carbon (Lal, 2004). The two major below-ground carbon pools are the soil organic carbon (SOC) and below-ground biomass (i.e., fine and coarse roots). However, even though the below-ground carbon sequestration potential is known, the methods to

quantify it are still in their infancy and there is no established standard protocol to follow when measuring it worldwide.

For determining SOC, the two main problems are the lack of standards for soil aggregate class definitions and what soil depth to sample (Nair et al., 2009). Aggregates are often classified according to their ability to resist slaking in water, and fortunately, a trend in new studies is starting to follow a standard (<53 μm, 53–250 μm, and <250μm) (Nair et al., 2010). Soil depth is the most serious issue on assessing and comparing underground carbon sequestration/stocks (Nair et al., 2009). Most studies sample up to 20 or 30 cm depth (Nair et al., 2009). For carbon stock studies in agroforestry, assessing soil to a greater depth is extremely important, since the sub-soil is a crucial part of carbon stabilization (Nair et al., 2010). A general technique that is simple and practical for any situation is needed in order to allow for comparisons among studies, facilitating better whole system shelterbelt carbon estimation. This is extremely important, given that above-ground biomass alone represents just one pool of the carbon sequestered in shelterbelt agroforestry systems and all ecosystem components need to be considered. Soil carbon sequestration is estimated to be around two-thirds of the whole carbon sequestered in the ecosystem (Rennolls & Wang, 2005; Sauer et al., 2007). For example, (Chu et al., 2019), studying shelterbelt trees planted by the Three-North Shelterbelt Program, found that 67% of the carbon was stored in the soil, with roots representing 13%, and above-ground biomass representing only 10%.

The SOC pool is in constant interaction with other C pools in shelterbelt systems, receiving inputs from above- and below-ground system components. For example, above-ground inputs include litter fall (i.e., fallen leaves and branches), animal excrements, and decomposed biomass. Below-ground carbon inputs include root litter and rhizosphere depositions (Dhillon & Rees, 2017). Higher SOC inputs help to maintain soil moisture and fertility, and is strongly affected by precipitation, temperature, soil texture, average stem and crown diameter, tree height, amount of surface litter, and shelterbelt species and age (Amadi et al., 2017; Dhillon et al., 2017).

Below-ground biomass measurement techniques for shelterbelt systems also have not been thoroughly explored, since they tend to be resource demanding and time consuming, and there is no well-established methodology to sample the below-ground system. Because of this, comparison between studies is problematic (Montagnini & Nair, 2004; Rennolls & Wang, 2005; Nair et al., 2009; Amichev et al., 2016; Amadi et al., 2017). Aiming to facilitate below-ground

carbon estimation, the IPCC recommended below-ground biomass estimations using established relationships with above-ground biomass (Campi et al., 2009). Similarly, Kort and Turnock (1999) recommended root biomass estimations to be done by considering constant ratios of 40%, 30% and 50% of above-ground biomass for deciduous, coniferous, and shrub shelterbelts, respectively, which were also prescribed by Freedman & Keith (1996) and Grier et al., (1981). However, this method is problematic, since root systems vary with species, climatic zone, and environmental conditions within the region (Nair et al., 2009). To be more comprehensive, more methods need to be tested for many species across many site conditions. For example, a dry environment would stimulate a deeper root system, while a less dry environment would produce shallower roots for the same tree species.

Numerous studies have observed a trend of soil carbon loss occurring when a new shelterbelt is first planted, most likely due to site preparation and land use change, which is offset years later, as the trees grow more extensive roots systems (Rennolls & Wang, 2005; Amichev et al., 2016; Dhillon & Rees, 2017; Amadi et al., 2017). This is a natural process that usually takes place when land use is changed. For example, when a natural ecosystem is replaced by agriculture, around 60% and 75% of SOC is lost in temperate and tropical climate, respectively (Rennolls & Wang, 2005). Amichev et al. (2016) found that soil carbon stocks decreased during the first 10 years following shelterbelt implementation, losing about 3.5% within the first five years. Their model simulations illustrated that carbon emissions due to land cover change were completely offset by the ages of 17, 18, and 21 for shelterbelts planted at 2.0, 3.5, and 5.0 m spacing, respectively.

Even though it takes years to compensate carbon loss due to shelterbelt planting, in dry environments, such as the Prairies, where biomass production is not very high, shelterbelts can be an important source of organic matter for the soil. Shelterbelts increase SOC, moisture, and fertility, and consequently, increase carbon sequestration into the soil pool. Research has demonstrated that SOC under shelterbelt trees canopies is greater than SOC under crops, and that this difference tends to be less pronounced in deeper layers of the soil (Amadi et al., 2017; Dhillon et al., 2017), but vary according to the species considered (Liu et al., 2012). For example, Amadi et al. (2017) studying the carbon sequestration potential of different shelterbelt species in Saskatchewan in the 0–7.5 cm and 7.5–15 cm soil layers, reported higher SOC stocks within the top soil layer. Similar were the results reported by Dhillon and Van Rees (2017), who studied the

SOC sequestration potential of six common shelterbelt species planted in Saskatchewan (green ash, hybrid poplar, Manitoba maple, white spruce, Scots pine and caragana), ranging from five to 63 years of age. Their results showed that soil organic matter concentration was 30% greater under shelterbelts than adjacent cropped fields, and that the SOC stock was 19% greater under shelterbelts than under crops. This difference is due to lower bulk density of soils under shelterbelts than under cropped fields. This lower bulk density is attributed to the presence of organic matter, extensive tree root systems, and due to the absence of heavy machinery traffic for the years since the shelterbelt was implemented. This finding was corroborated by Sauer et al. (2007) who also reported lower bulk density under shelterbelts than under the adjacent cropped field. The bulk density in this case was 13% lower in the 0–10 cm layer, and 7% lower in the 10–30 cm layer. They also found that soil under shelterbelts had 18.6 Mg C ha^{-1} more SOC than the soil under crop production within the top 50 cm of soil, and that litter under shelterbelts contained an additional 3–8 Mg C ha^{-1}. The SOC stocks vary greatly by species because of differences in litter composition leading, to differences in litter decomposition rates. For example, these authors found that white spruce shelterbelts had 20.8 g C kg^{-1} more SOC in the 0–5 cm soil layer than the adjacent cropped field, while green ash had only 0.8 g C kg^{-1} more SOC than the adjacent cropped field.

An important aspect of the shelterbelt SOC pool is the long residence time, which emphasizes the shelterbelts' role as an effective climate mitigation tool from a global perspective. Needless to say, the longer the added soil carbon remains in the soil pool, the better. Organic carbon compounds in the soil can be classified as either labile, with residence time in the soil of a few months, or as recalcitrant, with residence time in the soil of a few decades. Dhillon and Van Rees (2017) analyzed the effect of shelterbelts and cropped fields in Saskatchewan on the distribution of soil organic carbon density fractions. They found an increase in the SOC labile light fraction (71%) and the stable heavy fraction (22%) for soils under shelterbelts compared to cropped fields. The majority of SOC added in the 0–10 cm layer belonged to the labile light fraction, and the majority of the SOC added in the 10–30 cm layer belonged to the heavy fraction. The SOC light fraction was generally associated with conifer shelterbelts, whereas the SOC heavy fraction was associated with deciduous trees. For example, Manitoba maple litter was abundant with more resistant forms of soil organic matter (i.e., needing more time to decompose) (IPCC 2000).

Shelterbelt management practices also influence SOC stocks, and more specifically, the type of soil organic matter compounds, and consequently their residence time within the soil pool. The chemical composition of these soil compounds affects microorganisms-enzymes interactions and determine their stability and residence time in the soil (Dhillon & Rees, 2017). The soil under shelterbelts have more processed C forms, such as aliphatic C, aromatic C, and ketones, that are harder for microbes to break down, while the soil under cropped fields have more sugars and alcohols (Nair et al., 2009, 2010).

Soil greenhouse gases flux studies are also important to better understand below-ground carbon dynamics. Amadi et al., (2017) compared soil CO_2, CH_4 and N_2O fluxes in shelterbelt systems with adjacent cropped field in Prince Albert, Saskatchewan, using non-steady state vented chambers. Even though they found greater CO_2 fluxes under shelterbelts than in crop fields (probably due to higher microbial activity, root respiration and litter decomposition), soil organic carbon under the shelterbelts was 27% greater than under the adjacent cropped field. Shelterbelts contributed to the offset of other GHGs released from farming activities, not just CO_2, by enlarging the CH_4 soil sink, absorbing 58% and 81% more CH_4 than soil in cropped fields, in 2013 and 2014, respectively. Cumulative seasonal N_2O emissions from shelterbelt areas were two- to five-times lower than emissions by cropped fields nearby. A similar study by Amadi et al. (2016) investigated whether a two-row 31-year-old hybrid poplar-caragana shelterbelt influenced the soil organic carbon and GHG flux dynamic on its surrounding area, compared to an adjacent cropped field. They found that soil organic carbon concentration in the soil was greater in the proximity to shelterbelts, and that CH_4 uptake decreased with increasing distance away from the shelterbelt. The N_2O release was smaller under the shelterbelt and increased towards the cropped field, and the CO_2 flux between soil and atmosphere was more intense in the proximity to shelterbelts, which was in agreement with Amadi et al. (2016). Higher fluxes were attributed to higher organic matter concentration, microbial activity, and tree root respiration in the proximity of the shelterbelts (Amadi et al., 2017, 2016).

3.5. Conclusions

This review paper summarized the currently available research-based knowledge surrounding shelterbelt agroforestry systems, and aimed to increase the awareness of researchers, farmers, industry, and policymakers of the climate change mitigation potential of planted shelterbelts throughout Canada and the world. The current knowledge-base clearly indicates that

shelterbelts have a great potential for carbon sequestration, both in above- and below-ground pools of the system. As the trees in the shelterbelts continue to grow, they are able to reduce and offset a significant portion of the carbon released from agricultural practices, while providing several other social and environmental benefits, both for the public and private sectors.

In order to preserve existing shelterbelts, and promote the planting of new ones, new effective policies are needed in Canada that would provide farmers with the necessary economic incentives, and cost recovery for shelterbelt establishment and maintenance. This is especially important in the post-Paris Accord era, as the Government of Canada is steadily transitioning towards a carbonless economy, at the forefront of which are the farming communities in the Canadian Prairies. To better understand the budgetary impact of a carbonless economy on the Canadian farmer, whole-farm cost analysis studies, and shelterbelt decision-support tools for farmers that account for shelterbelt establishment and decades-long maintenance costs (i.e., time, machinery, and labor), will be needed. New policies that will help farmers meet shelterbelt-related costs will likely have a significant impact on the carbon mitigation potential of these systems in the long term. All these actions, if executed and coordinated effectively, can provide a major step for Canada, and for the world, towards a truly decarbonized economy.

CHAPTER 4

ESTIMATING DBH THROUGH TIME USING A VARYING NUMBER OF INCREMENT CORES AND METHODS

4.1 Abstract

Dendrochronology is the science of using tree rings to interpret past growing environments in a tree's life history. It has been used as a tool in many disciplines, such as climatology, archeology, and ecology; however, when studying radial-tree growth (e.g., diameter at breast height), and subsequent biomass and carbon stock calculations, dendrochronology has been underutilized. There is no consensus on methods for using increment cores to determine DBH over the life of a tree's growth history in a precise and controlled way. Doing so would allow this type of data to be used in allometric models, estimating past changes in biomass, and carbon stocks. The objective of this study is to explore different methods used to determine DBH derived from increment cores and report errors associated with the methods.

Ninety-three trees were harvested by cutting cross sections that were then sanded smooth until the rings were clearly visible. Annual rings were measured and the observed actual DBHs through time were determined from each sample. Hypothetical increment core paths were drawn on each cross section creating 28 different sampling modes to estimate DBH on the samples, and then DBH was calculated in two directions (from the bark to the pith and from the pith to the bark), summarizing 56 variations tested.

It was found that it was better to calculate past DBH from the bark to the pith because it yielded less extreme error than calculating DBH from the pith to the bark, except when the tree is young (less than 30-year-old). In this case, it is better to calculate DBH from the pith to the bark. Using increment cores that reach the pith yielded more precise estimates than using off-pith increment cores. Using more increment cores provided more precision, but time, budget and health of the tree need to be considered when deciding how many cores to sample, since sampling more increment cores may hurt the tree, and require more time and resources to process them. In this study, the average error is provided for all combinations of increment cores, which may help in the decision of how many increment cores to sample in a given study.

4.2 Introduction

Tree rings are a rich proxy for growth and subsequently changes in carbon stocks over the life of a tree's growth history. This surrogate is especially important when annual forest inventories are not conducted, and information is believed to be lost. Tree-ring widths are more easily available than the many successive resource-intensive and time-consuming inventory campaigns that would be needed to acquire a significant amount of incremental data, essential for modeling purposes. Despite a strong potential to be used for carbon stock estimates, the science behind using tree rings as a proxy for tree growth has been underutilized by modelers because the link between ring widths and changes in annual growth are not yet seen as sound (Bakker, 2005; Dolph, 1981; Klesse & Frank, 2016; Shi et al., 2015; Alexander et al., 2018).

Dendrochronology techniques to measure ring widths have been used as a surrogate for diameter at breast height (DBH) in many forest productivity studies (Biondi, 1999; Pape, 1999; Stahle et al., 1999; Worbes et al., 2003; Brienen & Zuidema, 2006; Beck et al., 2011; Nehrbass-ahles et al., 2014; Dye et al., 2016; Klesse & Frank, 2016; Alexander et al., 2018); despite these studies, there is still no established technique to sample and process tree-ring widths to estimate past DBH. When tree rings are used to estimate DBH, dendrochronology techniques usually bias any increment estimates. For example, in many dendrochronology studies, the oldest and or largest tree is normally targeted for sampling (Véronique, 1998; Motta & Nola, 2001; Duchesne et al., 2002; Brienen et al., 2012; Babst et al., 2014b; Nehrbass-ahles et al., 2014; Dye et al., 2016; Hember et al., 2019), which can overestimate biomass and carbon stock by up to 459% (Nehrbass-ahles et al., 2014). In addition, in dendrochronology, ring-width data is commonly processed into an index (Girardin et al., 2011) or cross-dated with other trees to produce a single main chronology (Motta & Nola, 2001; Fraver & White, 2005; Jump et al., 2006; Altman et al., 2013; Dye et al., 2016; Klesse & Frank, 2016). These procedures eliminate tree-to-tree variability, which is important for forest mensuration assessments, because sizing heterogeneity helps to determine the statistical limits of average biomass and carbon stocks.

If establishing a technique for adapting dendrochronology measurements for precise tree growth assessments can be developed, forestry and dendrochronology sciences could be better bridged, which would bring advances for forest management focused on carbon stock assessments (Bakker, 2005; Nehrbass-ahles et al., 2014). There are a few published methodologies that have been applied to retrieve tree growth from increment cores (Iles, 1974; Dolph, 1981; Biging &

Wensel, 1988; Duncan, 1989; Villalba & Veblen, 1997; Bakker, 2005;). However, these authors assume proportional growth around the pith, which is not realistic (Applequist, 1958; Norton et al., 1987; Allen, 1988; Akachuku & Abolarin, 1989; Duncan, 1989; Villalba & Veblen, 1997; Stokes & Berthier, 2000; Colbert et al., 2004; Bakker, 2005; Lupi et al., 2014; Shi et al., 2015), and requires that the increment core must pass close enough to the pith to present a complete inner-ring arc (Duncan, 1989). In some cases, authors have proposed methods when the pith is missed (Villalba & Veblen, 1997), but this too becomes very subjective, and is not seen as reliable.

A method allowing precise DBH estimations from increment cores and providing the range of errors associated with the estimation is important because DBH and basal area (BA) are the main variables related to tree biomass calculations (Biging & Wensel, 1988; Bakker, 2005; Yang et al., 2009; Klesse & Frank, 2016; Hember et al., 2019). Precise DBH estimates are crucial to make BA calculations reliable, to then serve as input variables, since allometric models have their own inherent uncertainties (Babst et al., 2014a; Nehrbass-ahles et al., 2014; Klesse & Frank, 2016; Alexander et al., 2018). Once a method to retrieve diameter through time from an increment core is established, and the yielded biases are known, carbon stock changes through time can be estimated for a location in the past, by simply assessing increment cores once from a site, and then future-tree growth can be predicted over the years based on climate scenario projections.

Defining a method would allow predicting carbon stocks through time for species and management location specifically, which would allow optimized administration selecting the most suitable species for the aimed carbon stock, and goal for each landowner. A location-specific assessment would support policies to combat global warming, by motivating individuals to plant trees, and would also benefit local economies. For example, in the province of Saskatchewan in Canada, farmers have planted over 600 million shelterbelt trees through the years, providing important public and private environmental services (Kulshreshtha & Kort, 2009; Piwowar et al., 2017). However, these same farmers are starting to remove their shelterbelts, which would end these environmental services that include carbon sequestration (Rempel et al., 2014, 2017; Ha et al., 2018; Amichev et al., 2020). Implementing such a policy could reduce this removal while rewarding for carbon sequestered, diversifying the economy.

The objective of this study is to provide a method of using increment cores taken in the field to more precisely determine DBH and BA through time, and to especially inform the error

yielded from any subsequent calculations for shelterbelt trees in Saskatchewan. A series of traditional sampling possibilities when collecting increment cores in the field will be tested in a controlled experiment in the lab. Phantom cores will be randomly 'taken' in the lab, on actual shelterbelt grown trees from the field, and the phantom cores will mimic many of the potential field sampling possibilities (e.g., extracting a core that intersects the pith of a tree, or extracting a core that misses the pith by varying amounts and in varying directions from the pith). If the study is successful, then information gleaned from increment core derived DBH and BA across the lifespan of a tree during one field visit, can replace having to visit the same tree annually through time to obtain the same information. The hypotheses tested were: i) the more increment cores that are used to calculate the DBH, the more accurate the results will be; ii) increment cores that reach the center of a tree will yield more accurate estimates; and iii) the farther estimates go back in a tree life towards the pith, the higher the associated error.

4.3 Material and methods

4.3.1 Data

Landowners from across the province of Saskatchewan, Canada, that owned established shelterbelts were contacted for permission to cut and sample one of their living shelterbelt trees. Farmers that agreed with the destructive sampling protocol were visited, and in most cases picked the tree/trees that they allowed to be cut. A total of 93 shelterbelt trees were donated for the project consisting of 10 species of varying ages (Table 4.1). A cross section was cut using a chainsaw from each live tree at the DBH (1.3 m from the ground) position and transported to the Mistik Askiwin Dendrochronology Laboratory (MAD Lab), at the University of Saskatchewan. The cross-sections were air-dried, and then a flat face was cut on the disc before the being sanded with progressively finer sandpaper until the annual rings were clearly visible on each cross-section.

Table 4.1 - Number of trees sampled (n), and minimum-maximum range for age, diameter and basal area for each shelterbelt grown species.

Species	N	Age	Diameter	Basal area
Chokecherry (*Prunus virginiana*)	1	12-12	1.4 - 1.4	1.4 - 1.4
Colorado spruce (*Picea pungens*)	1	33 - 33	13.4 - 13.4	141.4 - 141.4
Siberian elm (*Ulmus pumila*)	7	6.0 - 50.0	6.8 - 13.8	36 - 151
Green ash (*Fraxinus pennsylvanica*)	5	24.0 - 48.0	3.4 - 7.0	9.3 - 38.5
Manitoba maple (*Acer negundo*)	3	21.0 - 33.0	5.7 - 10.0	26.2 - 78.1
Hybrid poplar (*Populus deltoids* x *Populus nigra*)	46	4.0 - 38.0	2.0 - 12.0	3.2 - 114.4
Scots pine (*Pinus sylvestris*)	5	14.0 - 41.0	5.8 - 29.2	26.8 - 64.2
Eastern larch (*Larix laricina*)	9	10.0 - 16.0	6.0 - 9.9	28.4 - 77.1
Acute willow (*Salix alba*)	1	19.0 - 19.0	2.8 - 2.8	6.5 - 6.5

White spruce (*Picea glauca*)	15	8.0 - 45.0	0.0 - 10.8	0.6 - 98.2
Total	93			

4.3.2 DBH estimation methods

After sanding, the cross sections were scanned at high resolution (Figure 4.1a) and all annual rings were drawn on the image (Figure 4.1b). Each ring length was measured with the software program ImageJ (Rasband, 2018). The ring lengths were divided by π, so that the actual DBH of each year i (DBH_{r_i}) of each cross section was known. Actual basal area (BA) was also determined using ImageJ, as the area inside each ring drawn, on the year i (BA_{r_i}) for each cross section (Rasband, 2018) (Figure 4.1b).

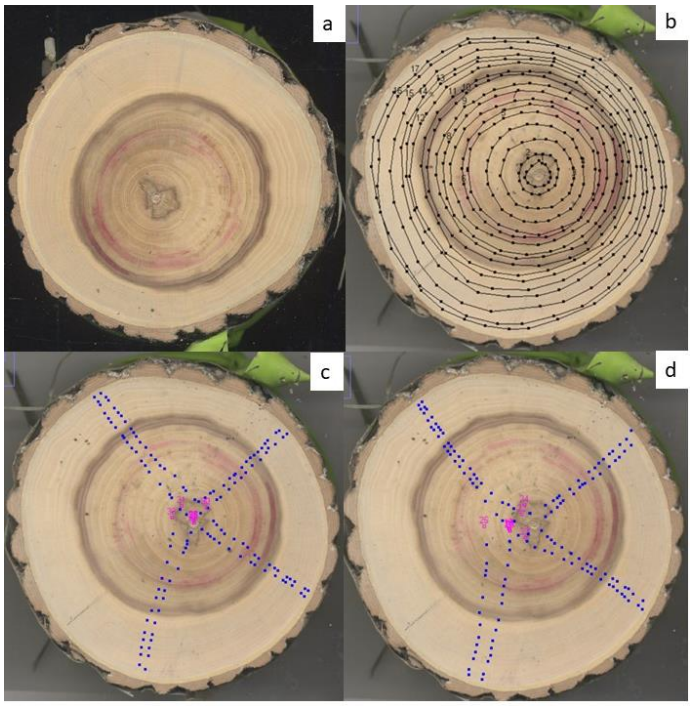

Figure 4.1 - a) Example of a 17-year-old Manitoba maple cross section; b) annual-ring lengths were drawn and measured with ImageJ; c) the "pith approach": increment core paths were aimed at the cross-section's pith; d) the "center approach" increment core paths were aimed at the cross-section's center.

DBH (DBH_i) and BA (BA_i) for each year (i) on each cross section were determined by testing methods varying in three factors: direction (2 levels), approach (2 levels) and mode (14 levels). The directions were calculating DBH_i from the bark to the pith (B to P) or from the pith to the bark (P to B). It was felt to be important to test the direction of the calculations, to better

understand how compounding error occurs over the years across a cross-section. The different direction affects the calculation of the error term on each ring, its distribution, and extent across the cross section. Annual increments are greatest near the pith and smallest near the bark for most trees (due to several factors, such as larger radius of the tree, lower tree growth rate as the tree ages, and competition), therefore there is higher uncertainty associated with estimating DBH and BA near the pith than near the bark. For the P to B direction, the uncertainty related to these increments is highest at the start of the calculation, and the variability is accumulated forward. Conversely, for the B to P method, the DBH calculation starts by using the increment estimations from near the bark, which are smaller, so they have a lower level of uncertainty related to them. These error measurements start to compound at a smaller rate, and only tend to rise with the increase of the average increment as the compounding calculation moves towards the larger estimations near the pith.

For each direction, two approaches were tested, the pith approach (Figure 4.1c) or the center approach (Figure 4.1d). The center and the pith approaches were tested because these two areas of a tree are locations on a cross sections commonly aimed at and reached when coring a tree. On each approach, one to four theoretical increment cores were drawn on each cross section following the two approaches, the pith and the center. Cores could either reach the pith of the tree (p_j) or miss the pith (off-pith or op_k), for the pith approach; or reach the center of the tree (c_j), or miss the center of the tree (off-center or oc_k), for the center approach. For each approach, the combination of one to four theoretical increment cores created 14 possible modes of calculation. Thus, in each mode, j and k varied from 0 to 4, and $j + k \leq 4$ (Table 4.2). In sum, 56 (2 (direction) x 2 (approaches) x 14 (modes)) combination of methods were tested. Appendix Table A1 details the direction, approach, mode, and the number of increment core used in each case.

Table 4.2 - Description of the two approaches tested. All options were applied to calculate DBH using the increment core paths. Variable p_j indicates j increment cores reached the pith; variable op_k indicates that k increment cores missed the pith; variable c_j indicates that j increment cores reached the center; and oc_k indicates that k increment cores missed the center. Variable in_i indicates an increment core calculation. Note: P to B indicates pith to bark direction and B to P indicates bark to pith direction.

Direction	Approach	Mode	Description
B to P P to B	Pith	$P_j O P_k$	in_i was calculated as the average of j increment core paths terminating at the exact pith, and k increment core paths terminating near the pith without reaching it.

B to P P to B	Center	C_jOC_k	in_i was calculated as the average of j increment core paths terminating at the exact center, and k increment core paths terminating near the center without reaching it.

For the pith approach ($p_j op_k$) one to four increment cores were drawn on the cross section towards the pith starting at a randomized location on the bark (1° to 360°). Either the drawn path reached the pith (p_j) or it missed (op_k) by a randomized deviation of up to 15% of the outermost DBH, and then randomized to miss either to the left or right of the pith. Thus, DBH_i and BA_i were calculated by using one to four increment cores reaching the pith (p_j), off-pith (op_k), or a combination of both on-pith and off-pith increment cores ($p_j op_k$) (Table 4.2, Appendix Table A1.). Likewise, for the center approach ($c_j oc_k$), one to four increment cores were drawn on the cross section towards the center of the disk starting at a randomized location on the bark (1° to 360°). Either the path reached the exact center (c_j) or it did not (oc_k) by a deviation of up to 15% of the outermost DBH to the left or right, all randomly determined. The DBH_i and BA_i were calculated by using one to four increment cores reaching the center (c_j), off-center (oc_k), or a combination of both on-center and off-center increment cores ($c_j oc_k$) (Table 4.2, Appendix Table A1).

For the Pith to Bark direction, DBH for the year i (DBH_i) was calculated (1) as two times the accumulated increment of the core (in_i) at year i, for the cases when using only one core, or the average accumulated increment for the year i (in_i) from all increment cores, according to the mode ($p_j op_k$ or $c_j oc_k$). For the Bark to the Pith direction, to calculate DBH for the year i (DBH_i) the last DBH measured outside the bark DBH_{Last} was subtracted by two times the increment on the year i (in_i) or two times the average increment on the year i (in_i) (2) (Fule et al., 1997; Colbert et al., 2004; Metsaranta & Lieffers, 2009; Goodsman et al., 2010; Babst et al., 2014b; Shi et al., 2015; Dye et al., 2016; Alexander et al., 2018; ; Teets et al., 2018). The estimated BA of the year i (BA_i) was calculated (3) using the estimated DBH for the year i (DBH_i) (Girardin et al., 2016).

$$DBH_i = 2 * in_i \quad (1)$$

$$DBH_i = DBH_{Last} - (2 * in_i) \quad (2)$$

$$BA_i = \frac{DBH_i^2 \pi}{4} \quad (3)$$

4.3.3 Assessment

A mixed model was used to assess the significance of mode and species and their interactions. All methods were also assessed by the mean absolute error (MAE), Bias, and Bias in percentage (Bias%), MAE (% Last ring) (calculating the mean absolute error in relation to the last ring, the increment closest to the bark, to assess all rings) and Bias (% Last ring) (bias calculated in relation to the last ring, the increment closest to the bark, to assess all rings) for both DBH_i (4, 5, 6, 7, and 8, respectively) and BA_i (9, 10, 11, 12, and 13 respectively).

$$MAE = \left|DBH_{r_i} - DBH_i\right| \quad (4)$$

$$Bias = DBH_{r_i} - DBH_i \quad (5)$$

$$Bias\% = \frac{DBH_{r_i} - DBH_i}{DBH_{r_i}} * 100 \quad (6)$$

$$MAE_{DBH}\ (\%\ Last\ ring) = \frac{MAE}{DBH_{Last\ ring}} * 100 \quad (7)$$

$$Bias_{DBH}\ (\%Last\ ring) = \frac{Bias}{DBH_{Last\ ring}} * 100 \quad (8)$$

Where DBH_{r_i} is the observed actual DBH for year i, DBH_i is the estimated DBH for year i and $DBH_{Last\ ring}$ is the DBH closest to the bark.

$$MAE = \left|BA_{r_i} - BA_i\right| \quad (9)$$

$$Bias = BA_{r_i} - BA_i \quad (10)$$

$$Bias\% = \frac{BA_{r_i} - BA_i}{BA_{r_i}} * 100 \quad (11)$$

$$MAE_{BA}\ (\%\ Last\ ring) = \frac{MAE}{BA_{Last\ ring}} * 100 \quad (12)$$

$$Bias_{BA}\ (\%Last\ ring) = \frac{Bias}{BA_{Last\ ring}} * 100 \quad (13)$$

Where BA_{r_i} is the real BA for the year i, BA_i is the estimated BA for the year i and $BA_{Last\,ring}$ is the BA closest to the bark.

It is important to note that MAE and MAE (%Last ring) are more reliable than Bias, Bias% and Bias (%Last ring), because all MAE values are positive, so opposite signs cannot cancel each other out, unlike Bias, Bias % and Bias (%Last ring). These calculated values can underestimate the error. However, Bias, Bias (%) and Bias (% Last ring) are still important elements because they help illustrate overall trends for over- or under-estimations and can be used to compare modes to see errors in a more holistic perspective.

Modes were also assessed by rank, ordering them from the best to the worst for estimating the real DBH and BA according to MAE. All values for all modes were divided by their maximum value, so each mode for each statistic was scaled from 0 to 1. These scaled values were then summed, for both DBH and BA. The summed totals were then ranked, with the best method determined to be the mode with the lowest overall summed score.

4.3.4 Rings compactness

The main problem when calculating DBH using increment cores is the cross-section shape. If all cross-section rings were perfect circles, measuring DBH increment by using one increment core reaching the pith would be flawless. Unfortunately, rings are not as round as theoretically possible because growth around the pith is often uneven, which is normally explained by their individual genetics and growing environment (Liu, 1986; Salminen and Varmola, 1993; Biondi, 1999; Bakker, 2005; Barthélémy & Caraglio, 2007; Lupi et al., 2014; Shi et al., 2015; Dye et al., 2016; Alexander et al., 2018). To measure how the shape of the ring affects the error in DBH and BA determinations, correlations between MAE, Bias, Bias %, MAE (%Last ring), Bias (%Last ring) and compactness of each ring were calculated. Compactness is defined as the ratio of the area of an object, to the area of a circle with the same perimeter (14). In other words, how the shape of an object is similar or dissimilar to a perfect circle. The higher the compactness value, the more similar to a perfect round circle the existing ring path was found to be. The lower the compactness value, the more eccentric the ring path was found to be.

$$Compactness = \frac{4*\pi*BA}{\frac{DBH^2}{\pi}} \quad (14)$$

4.4 Results

Direction, approach, mode, number of increment cores used, tree age, species and cross section shape significantly affected MAE, MAE (% Last ring), Bias and Bias (%), and Bias (% Last ring) for both DBH and BA estimates. All calculations were based on the strategy of using accumulated increments to calculate DBH and subsequently BA. The different directions of calculating DBH (P to B or B to P) and then summing all increments, resulted in the same values being found for the diameters. The difference between the two directions of the calculations is the uncertainty levels associated with these calculations.

It is important to emphasize that the greater the increment (wider rings near the pith in most cases), the greater the uncertainty associated with its DBH estimation. This bias will accumulate over subsequent DBH estimations across a cross section. The end point of the calculation is therefore not as important as the starting point, since the bias from the beginning will be accumulated and summed over the cross section, while those at the end will not be carried as far in the iterative calculation.

4.4.1 Directional Error: P to B vs B to P

Direction was the first factor addressed because the other factors tested are nested within direction and therefore are affected by the property. P to B yielded lower average errors in comparison with B to P. P to B yielded lower errors on rings near the pith and B to P yielded lower errors on rings near the bark. Despite P to B resulting in lower average errors, the errors can be extreme near the bark for all statics assessed (Figure 4.2 and Appendix Figure A1 in the Appendix illustrates the number of rings used in each year to build Figure 4.2). Regardless of the origin of the start of the calculation (the pith for P to B or the bark for B to P), errors tend to compound as DBH and BA are calculated over the years for all approaches and modes. Bias (%) is calculated in relation to the respective ring. For the P to B direction, the most accumulated error (%) will be on the largest ring on the cross section. On the other hand, for the B to P direction, the most accumulated error (%) would be on the smallest ring on the disk. You can see this in the data for MAE % (Last ring) and Bias % (Last ring) for both DBH and BA (Figure 4.2b, 4.2e, 4.2g and 4.2j, respectively). For Bias %, as the error is calculated in relation to the respective ring, the error can also be very high for the P to B method (Figure 4.2d, and 4.2i) in comparison with Bias % for the B to P method, and also when the last ring is considered for both DBH and BA (Figure 4.2e, 4.2j).

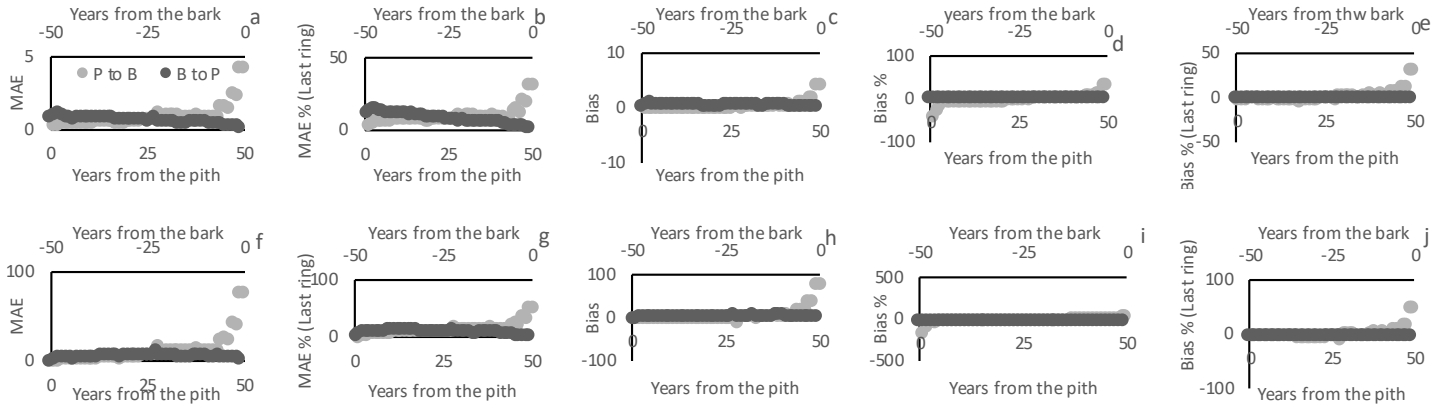

Figure 4.2 - a) Ring average MAE (Mean Absolute Error); b) ring average MAE % (Last ring) (Mean absolute error based on the last ring); c) ring average Bias; d) ring average Bias % (Bias in percentage); e) ring average Bias % (Last ring) (Bias in percentage based on the last ring) for DBH for B to P (Bark to Pith) and P to B (Pith to Bark) directions; f) ring average MAE (Mean Absolute error); g) ring average MAE % (Last ring) (Mean absolute error based on the last ring); h) ring average Bias; i) ring average Bias % (Bias in percentage); j) ring average Bias % (Last ring) (Bias in percentage based on the last ring) for BA for the B to P (Bark to Pith) and P to B (Pith to Bark) directions.

4.4.2 Comparing Modes

Average error yielded from each mode and direction of the calculations for DBH and BA are listed in Table 4.3. Figure 4.3 illustrates average MAE (a and c) and Bias (b and d) for each mode for DBH and BA respectively, calculated using the P and B and B to P directions. The lowest MAEs were normally from P_j, $P_j OP_k$ modes, and OP_k and OC_k *and* C_j increment core paths tended to yield the worst estimates for both DBH and BA (Table 4.3). To make the comparison between the different modes more straightforward, Table 4.4 ranked the sums based on MAE and MAE (% Last ring) for DBH and BA. For both DBH and BA, the best modes were P_4, P_3 and $P_3 OP_1$ and the worst were C_1, OC_1 and OP_1, respectively. As the species differed significantly (Appendix Table A2), Table 4.5 shows the best and worst modes according to the rank by species with more than one tree in the database (Appendix Table A3). For all species the best and worst modes followed the same general trend, with P_4, P_3 and $P_3 OP_1$ ranked as the best, and C_1, OC_1 *and* OP_1C1 ranking as the worst. The only species diverging from this result were the ones with only one individual sampled. Figure 4.4 illustrates the effect of mode and direction calculated for a random green ash tree, where the actual observed DBH is plotted against the estimated DBH. The calculations for P_4, P_3 and $P_3 OP_1$ were the best modes, yielding most

estimated values at or near the observed DBH values. To analyze the effect of the best and worst modes on the last DBH estimated for each tree, Figure 4.5 illustrates each tree's observed DBH plotted against each tree's estimated DBH. The best modes yielded more data points aligned to a perfect correlation than the worst methods. For all modes B to P tended to yield data points more closely aligned with the x=y line, indicating more precision in the estimations.

Table 4.3 - Mean Absolute Error (MAE), Mean Absolute error last ring (MAE (%Last ring)), Bias, Bias (%) and Bias (% Last ring) for DBH and BA estimates from the bark to pith (B to P) and from the pith to bark (P to B).

Method	DBH										BA									
	MAE		MAE(% Last ring)		Bias		Bias (%)		Bias (% last ring)		MAE		MAE(% Last ring)		Bias		Bias (%)		Bias (% last ring)	
	B to P	P to B	B to P	P to B	B to P	P to B	B to P	P to B	B to P	P to B	B to P	P to B	B to P	P to B	B to P	P to B	B to P	P to B	B to P	P to B
C_1	0.87	0.70	11.63	9.28	0.58	-0.13	0.14	-12.38	0.08	-2.84	6.16	6.25	12.04	11.84	3.90	-0.56	-0.45	-42.54	0.09	-3.37
C_1OC_1	0.85	0.62	11.39	8.35	0.60	-0.18	0.16	-14.40	0.09	-3.41	5.95	5.59	11.66	10.62	3.94	-0.73	-0.46	-45.24	0.09	-3.64
C_1OC_2	0.84	0.59	11.24	7.98	0.61	-0.19	0.17	-15.08	0.09	-3.58	5.84	5.31	11.46	10.09	4.01	-0.75	-0.41	-45.80	0.09	-3.67
C_1OC_3	0.83	0.57	11.12	7.76	0.61	-0.20	0.17	-15.42	0.09	-3.67	5.74	5.13	11.34	9.77	4.05	-0.76	-0.33	-46.01	0.10	-3.69
C_2	0.83	0.62	11.05	8.27	0.59	-0.14	0.15	-12.39	0.08	-2.86	5.78	5.63	11.25	10.50	4.00	-0.46	-0.71	-38.88	0.09	-3.10
C_2OC_1	0.83	0.59	11.07	7.96	0.60	-0.16	0.16	-13.72	0.09	-3.22	5.71	5.38	11.23	10.09	4.02	-0.59	-0.62	-41.73	0.09	-3.36
C_2OC_2	0.83	0.58	11.06	7.76	0.60	-0.18	0.16	-14.38	0.09	-3.39	5.71	5.20	11.22	9.80	4.04	-0.63	-0.69	-43.05	0.09	-3.45
C_3	0.82	0.59	10.83	7.90	0.59	-0.14	0.15	-12.37	0.08	-2.85	5.61	5.40	10.94	9.99	4.01	-0.40	-1.02	-37.61	0.09	-3.00
C_3OC_1	0.82	0.58	10.93	7.73	0.60	-0.16	0.16	-13.41	0.09	-3.14	5.61	5.23	11.02	9.77	4.04	-0.52	-0.95	-40.18	0.09	-3.22
C_4	0.82	0.58	10.79	7.72	0.59	-0.14	0.14	-12.37	0.08	-2.85	5.58	5.29	10.89	9.74	4.05	-0.38	-1.36	-36.99	0.09	-2.95
OC_1	0.90	0.68	12.06	9.15	0.62	-0.22	0.17	-16.31	0.09	-3.90	6.43	6.00	12.64	11.73	4.00	-1.02	0.08	-55.17	0.10	-4.35
OC_2	0.86	0.61	11.45	8.32	0.62	-0.23	0.18	-16.55	0.09	-3.99	5.98	5.44	11.82	10.56	4.08	-1.03	0.10	-51.93	0.10	-4.13
OC_3	0.84	0.58	11.22	7.93	0.62	-0.22	0.19	-16.42	0.09	-3.95	5.83	5.16	11.54	9.99	4.11	-0.90	0.11	-49.72	0.10	-3.98
OC_4	0.82	0.57	11.08	7.73	0.62	-0.22	0.18	-16.42	0.09	-3.95	5.73	5.02	11.40	9.71	4.12	-0.87	0.13	-48.85	0.10	-3.92
OP_1	0.82	0.73	10.85	9.29	0.40	0.08	0.07	-8.41	0.06	-0.50	6.17	6.94	11.86	12.33	2.93	1.55	-0.18	-32.66	0.08	-0.46
OP_2	0.79	0.60	10.59	7.61	0.46	0.08	0.11	-8.40	0.07	-0.51	5.59	5.62	10.92	9.80	3.06	1.79	-0.17	-29.80	0.08	0.00
OP_3	0.76	0.55	10.29	7.06	0.46	0.07	0.13	-8.54	0.07	-0.65	5.28	5.17	10.52	9.13	2.98	1.79	-0.16	-29.21	0.08	-0.18
OP_4	0.73	0.53	10.09	6.71	0.45	0.07	0.14	-8.54	0.07	-0.65	5.02	4.94	10.26	8.59	2.87	1.84	-0.14	-28.71	0.08	-0.08
P_1	0.79	0.50	10.71	6.38	0.51	0.08	0.09	0.08	0.07	0.51	5.74	5.14	11.70	9.28	3.97	0.78	-0.11	-2.30	0.09	0.21
P_1OP_1	0.79	0.49	10.62	6.31	0.51	0.08	0.13	-4.15	0.08	0.01	5.42	4.90	10.86	8.54	3.57	1.40	-0.13	-13.43	0.08	0.34
P_1OP_2	0.77	0.49	10.43	6.27	0.50	0.07	0.14	-5.56	0.08	-0.23	5.28	4.73	10.59	8.32	3.39	1.51	-0.17	-17.62	0.08	0.09
P_1OP_3	0.75	0.47	10.22	6.06	0.49	0.08	0.15	-6.35	0.08	-0.34	5.12	4.55	10.39	7.96	3.25	1.68	-0.22	-20.11	0.08	0.17
P_2	0.77	0.38	10.49	4.97	0.58	0.08	0.17	0.09	0.08	0.51	5.25	3.95	10.69	7.10	4.13	0.95	-0.02	-1.43	0.09	0.57
P_2OP_1	0.77	0.41	10.43	5.31	0.55	0.08	0.17	-2.60	0.08	0.19	5.24	4.17	10.56	7.33	3.81	1.35	-0.09	-8.13	0.09	0.49
P_2OP_2	0.76	0.43	10.30	5.47	0.53	0.08	0.17	-4.21	0.08	-0.06	5.14	4.22	10.43	7.38	3.59	1.49	-0.15	-12.69	0.08	0.36
P_3	0.75	0.34	10.27	4.39	0.60	0.08	0.19	0.08	0.08	0.51	5.17	3.47	10.46	6.24	4.24	1.01	0.02	-1.17	0.09	0.67
P_3OP_1	0.75	0.37	10.24	4.80	0.57	0.08	0.19	-2.05	0.08	0.24	5.13	3.78	10.38	6.65	3.92	1.29	-0.07	-6.29	0.09	0.56
P_4	0.73	0.31	9.99	4.01	0.60	0.08	0.20	0.08	0.09	0.51	5.05	3.12	10.21	5.67	4.27	1.04	0.06	-1.02	0.09	0.73

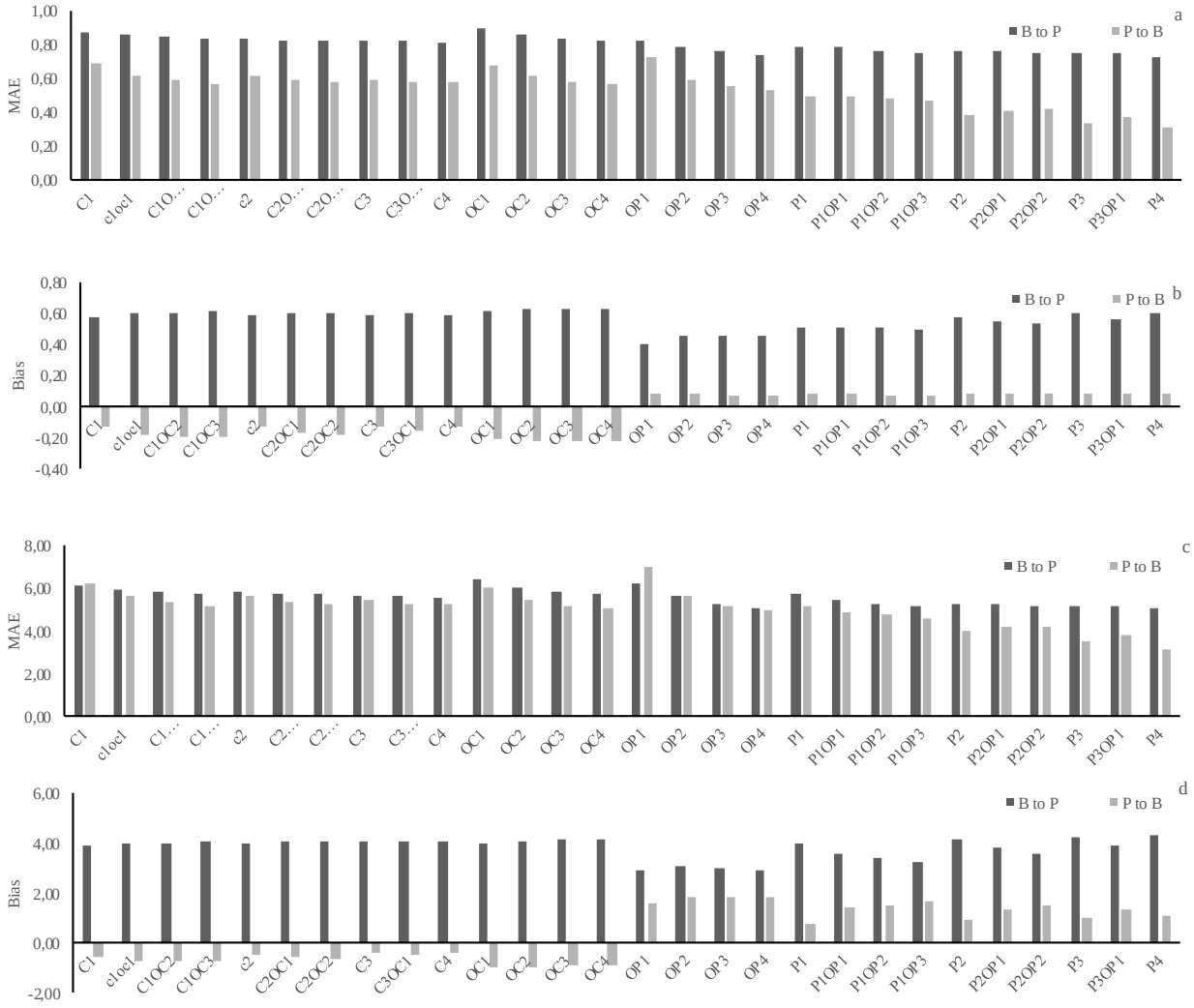

Figure 4.3 - MAE (mean absolute error) and Bias for DBH (a, b) and BA (c, d) according to the approach for the B to P (bark to pith) and P to B (pith to bark) directions.

Table 4.4 - Modes ranked based on MAE and MAE (% Last ring) for DBH and BA. The best three methods are highlighted in red, while the worst three methods are highlighted in blue.

	DBH						BA							
	MAE		MAE (% Last ring)		SUM	RANK	MAE		MAE (% Last ring)		SUM	RANK	SUM	RANK
	B to P	P to B	B to P	P to B			B to P	P to B	B to P	P to B				
C_1	0.97	0.96	0.96	1.00	3.89	27	0.96	0.90	0.95	0.96	3.77	26	7.66	26
C_1OC_1	0.95	0.85	0.94	0.90	3.64	25	0.93	0.81	0.92	0.86	3.52	25	7.16	25
C_1OC_2	0.93	0.81	0.93	0.86	3.54	22	0.91	0.76	0.91	0.82	3.40	22	6.94	22
C_1OC_3	0.92	0.79	0.92	0.83	3.46	18	0.89	0.74	0.90	0.79	3.32	17	6.79	18
C_2	0.92	0.85	0.92	0.89	3.58	23	0.90	0.81	0.89	0.85	3.45	23	7.03	23
C_2OC_1	0.92	0.82	0.92	0.86	3.51	21	0.89	0.78	0.89	0.82	3.37	20	6.88	20
C_2OC_2	0.92	0.79	0.92	0.84	3.46	17	0.89	0.75	0.89	0.80	3.32	16	6.78	17

C_3	0.91	0.81	0.90	0.85	3.47	19	0.87	0.78	0.87	0.81	3.33	18	6.79	19
C_3OC_1	0.91	0.79	0.91	0.83	3.44	15	0.87	0.75	0.87	0.79	3.29	13	6.73	14
C_4	0.90	0.80	0.89	0.83	3.43	14	0.87	0.76	0.86	0.79	3.28	12	6.71	13
OC_1	1.00	0.93	1.00	0.98	3.92	**28**	1.00	0.86	1.00	0.95	3.82	**27**	7.73	**28**
OC_2	0.95	0.84	0.95	0.90	3.63	24	0.93	0.78	0.94	0.86	3.51	24	7.14	24
OC_3	0.93	0.80	0.93	0.85	3.51	20	0.91	0.74	0.91	0.81	3.37	21	6.88	21
OC_4	0.91	0.78	0.92	0.83	3.44	16	0.89	0.72	0.90	0.79	3.30	14	6.74	16
OP_1	0.91	1.00	0.90	1.00	3.81	**26**	0.96	1.00	0.94	1.00	3.90	**28**	7.71	**27**
OP_2	0.88	0.82	0.88	0.82	3.39	13	0.87	0.81	0.86	0.79	3.34	19	6.73	15
OP_3	0.84	0.76	0.85	0.76	3.21	12	0.82	0.74	0.83	0.74	3.14	11	6.35	11
OP_4	0.81	0.72	0.84	0.72	3.10	9	0.78	0.71	0.81	0.70	3.00	8	6.10	9
P_1	0.87	0.68	0.89	0.69	3.13	11	0.89	0.74	0.93	0.75	3.31	15	6.44	12
P_1OP_1	0.87	0.68	0.88	0.68	3.11	10	0.84	0.71	0.86	0.69	3.10	10	6.21	10
P_1OP_2	0.85	0.67	0.87	0.67	3.06	8	0.82	0.68	0.84	0.67	3.01	9	6.07	8
P_1OP_3	0.83	0.65	0.85	0.65	2.98	7	0.80	0.66	0.82	0.65	2.92	7	5.90	7
P_2	0.85	0.53	0.87	0.53	2.78	4	0.82	0.57	0.85	0.58	2.81	4	5.59	4
P_2OP_1	0.85	0.57	0.86	0.57	2.86	5	0.82	0.60	0.84	0.59	2.85	6	5.71	6
P_2OP_2	0.84	0.59	0.85	0.59	2.87	6	0.80	0.61	0.82	0.60	2.83	5	5.70	5
P_3	0.83	0.47	0.85	0.47	2.62	**2**	0.80	0.50	0.83	0.51	2.64	**2**	5.26	**2**
P_3OP_1	0.83	0.51	0.85	0.52	2.71	**3**	0.80	0.54	0.82	0.54	2.70	**3**	5.42	**3**
P_4	0.81	0.42	0.83	0.43	2.49	**1**	0.79	0.45	0.81	0.46	2.50	**1**	4.99	**1**

Table 4.5 - Best and worst sampling modes for each species according to total rank

Species	N	Best	Worst
Siberian elm (*Ulmus pumila*)	7	P_3OP_1, P_4, P_3	OP_1, C_1, OC_1
Green ash (*Fraxinus pennsylvanica*)	5	P_3OP_1, P_4, P_3	OP_1, C_1, OC_1
Manitoba maple (*Acer negundo*)	3	P_3OP_1, P_4, P_3	OP_1, C_1, OC_1
Hybrid poplar (*Populus deltoids* x *Populus nigra*)	46	P_3OP_1, P_4, P_3	OP_1, C_1, OC_1
Scots pine (*Pinus sylvestris*)	5	P_3OP_1, P_4, P_3	OP_1, C_1, OC_1
Eastern larch (*Larix laricina*)	9	P_3OP_1, P_4, P_3	OC_1, OC_2, OC_3
White spruce (*Picea glauca*)	15	P_3OP_1, P_4, P_3	C_1, OC_1, OC_2

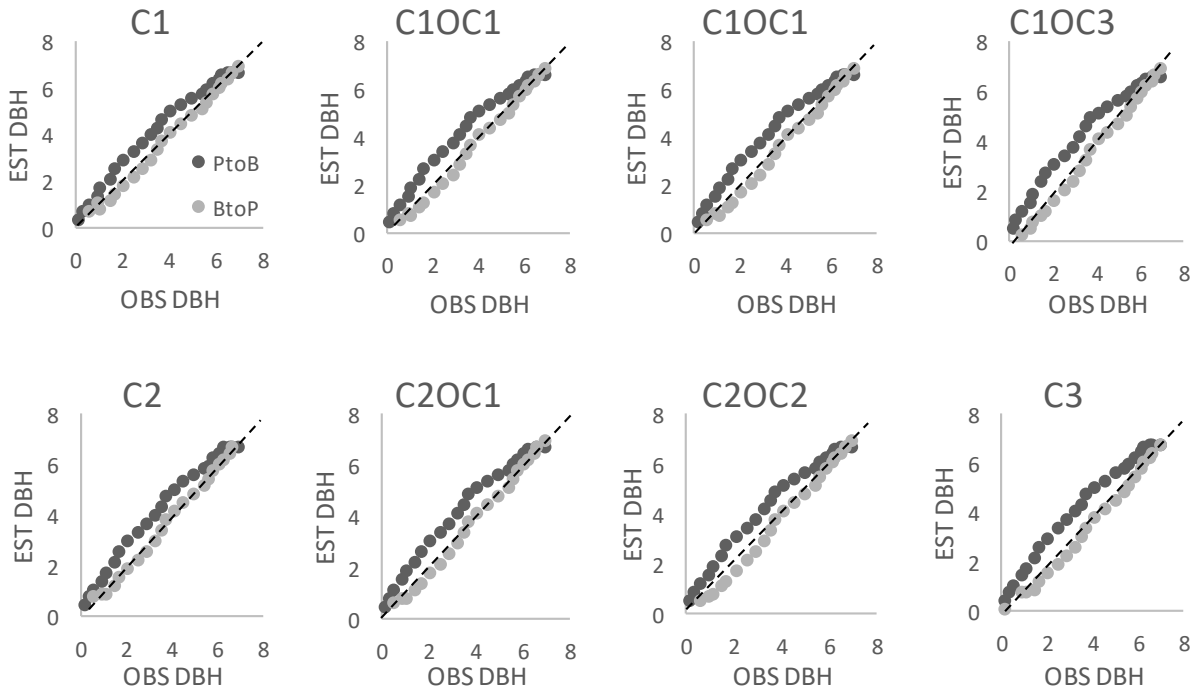

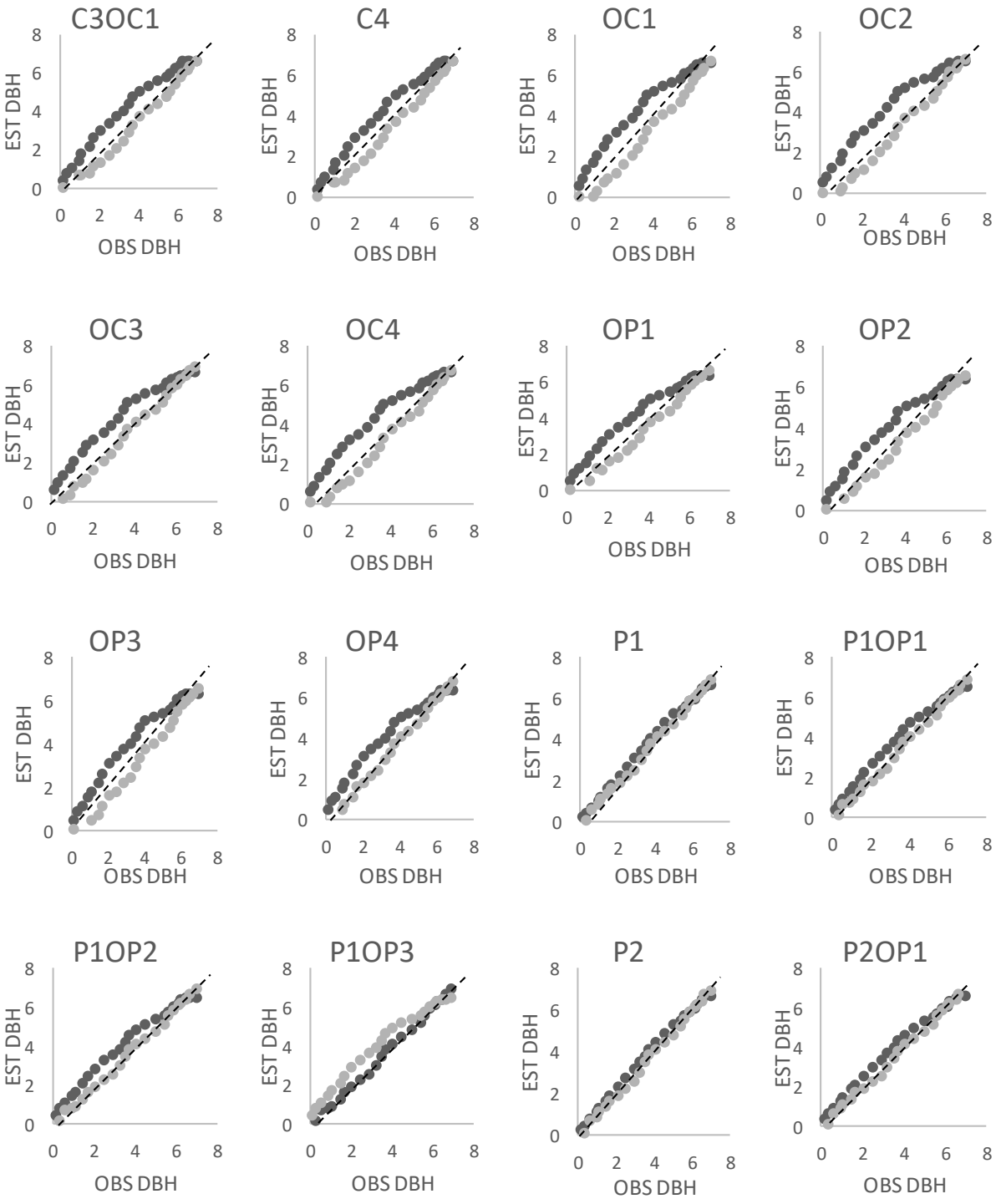
C3OC1
C4
OC1
OC2
OC3
OC4
OP1
OP2
OP3
OP4
P1
P1OP1
P1OP2
P1OP3
P2
P2OP1
EST DBH
OBS DBH
0
2
4
6
8

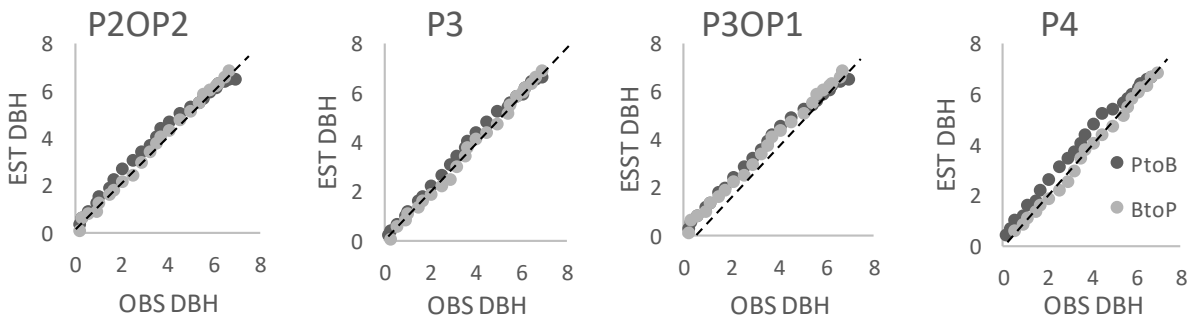

Figure 4.4 - Observed and estimated DBH according to the mode for a 40-year-old green ash. The dashed line is the x=y equation.

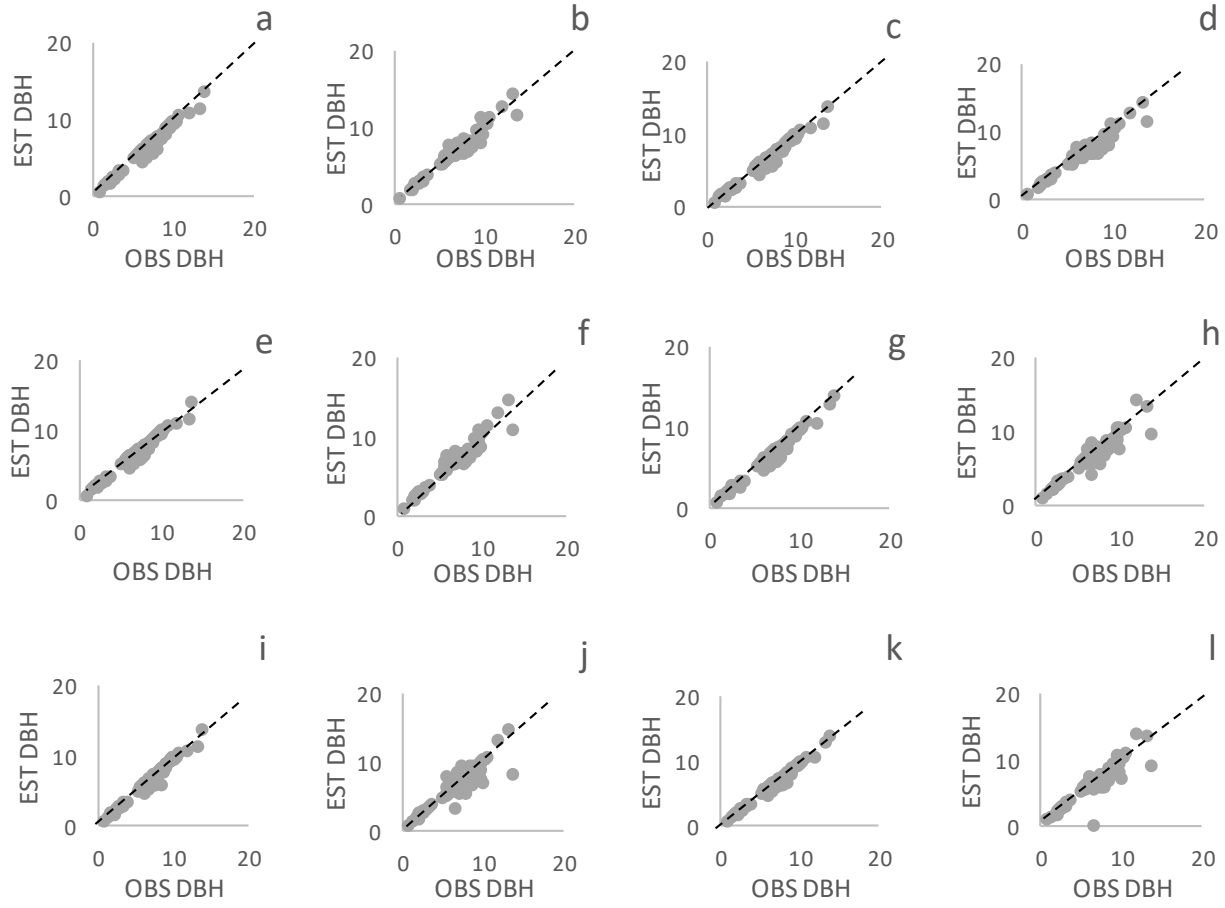

Figure 4.5 - Observed DBH versus estimated last DBH for each tree according to the best (a)P4 B to P; b)P4 P to B; c) P3 B to P; d) P3 P to B) and worst methods (e)P3OP1 B to P; f) P3OP1 P to B; g) OC1 B to P; h) OC1 P to B; i) OP1 B to P; j) OP1 P to B; k) C1 B to P; and l) C1 P to B). The dashed line is the x=y equation.

4.4.3 Number of increment cores used

Table 4.6 lists average MAE and MAE (%Last ring) obtained from using 1, 2, 3 or 4 increment core paths to calculate DBH and BA for each 10-year age class in each direction. As a general trend, the more increment cores used, the better. See Appendix Table A4 for more statistics that consider Bias, Bias (%) and Bias (%Last ring) as well.

4.4.4 Age

Regardless of the mode and direction, the older a tree's age class was, the higher the error was for all statistics observed (Table 4.6). To facilitate the visualization of an age effect on different modes, Figure 4.6 illustrates plots of MAE in DBH over the years for the three best (PP_4, P_3 and P_3OP_1) and three worst modes (C_1, OC_1 and OP_1) in both directions (B to P and P to B, respectively). The errors are higher at the age of 1 in the B to P direction, and the errors are higher at age 50 for the P to B direction, for all modes. B to P did not yield the same level of extreme values as P to B. For the B to P method (Figure 4.6a), similar MAE values are seen at the bark and diverge later near the pith. For the P to B direction (Figure 4.6b), the error differed more at the beginning of the estimates near the pith, at age 1.

Table 4.6 - MAE, MAE (% based on the last ring) yielded by using, 1, 2, 3 and 4 increment cores for classes of age ranging from 0–10, 10–20, 20–30, 30–40, 40–50 years for DBH and BA.

Class	Cores	B to P				P to B			
		DBH		BA		DBH		BA	
		MAE	MAE (% Last ring)	MAE	MAE (% Last ring)	MAE	MAE (% Last ring)	MAE	MAE (% Last ring)
0 - 10	1	1	15.69	6.27	17.08	0.6	9.82	4.65	13.12
	2	0.97	15.46	5.92	16.24	0.51	8.42	3.88	10.99
	3	0.95	15.18	5.86	16.07	0.47	7.9	3.6	10.22
	4	0.94	15.03	5.83	16.02	0.45	7.58	3.43	9.79
10-20	1	0.71	11.32	4.47	12.52	0.45	7.1	3.2	9.2
	2	0.7	11.11	4.27	12.04	0.38	6.1	2.74	7.81
	3	0.69	11.05	4.21	11.9	0.36	5.72	2.56	7.28
	4	0.69	11.01	4.17	11.82	0.35	5.51	2.46	6.98
20 - 30	1	0.75	10.49	5.43	10.78	0.59	9.27	5.34	12.54
	2	0.77	10.46	5.28	9.93	0.52	8.05	4.64	10.6
	3	0.77	10.49	5.28	9.78	0.5	7.8	4.44	10.41
	4	0.77	10.43	5.24	9.64	0.47	7.44	4.15	9.85
30 - 40	1	1.05	10.64	8.5	10.62	0.81	8.58	8.28	11.39
	2	0.97	9.54	7.51	8.94	0.67	7.04	6.98	9.49
	3	0.92	8.96	7.12	8.33	0.62	6.53	6.57	8.88
	4	0.89	8.58	6.79	7.92	0.59	6.15	6.32	8.5
40 - 50	1	0.89	9.62	7.46	10.07	0.91	9.3	10.13	12.38
	2	0.83	9.08	6.64	9.08	0.77	7.89	8.64	10.28
	3	0.81	8.91	6.36	8.75	0.72	7.4	8.1	9.49
	4	0.8	8.81	6.21	8.6	0.69	7.02	7.77	9

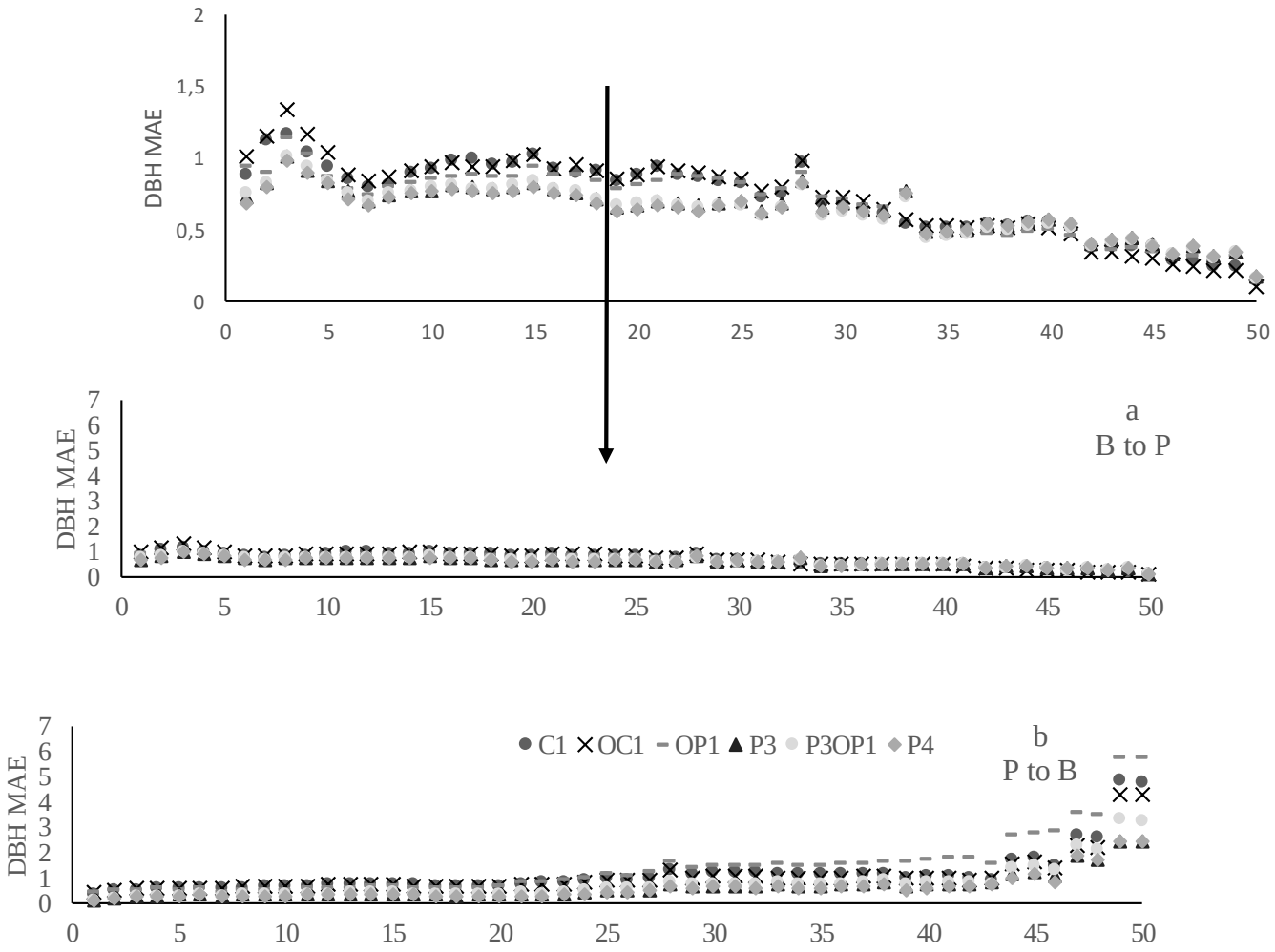

Figure 4.6 - MAE for DBH over the years for the best (P4, P3OP1 and P3) and worst (C1, OC1 and OP1) modes using the B to P (a) and P to B directions (b). The upper part of the Figure zooms (a) to better illustrate the data in a smaller scale allowing to differentiate the modes.

4.4.5 Species

Species significantly affected MAE, MAE (%Last ring), Bias, Bias % and Bias (%Last ring) for DBH and BA (Table 4.7). Acute willow and chokecherry were the species yielding the lowest error in MAE for both DBH and BA. Colorado Spruce and Manitoba Maple yielded the highest error in MAE for DBH and Colorado Spruce and Siberian elm yielded the highest error in MAE for BA. Only one young willow and chokecherry were sampled, so a larger sample size assessment is required for further conclusions on species.

Table 4.7 - MAE (Mean Absolute Error) (SD – standard deviation between the rings), MAE (%Last ring) (SD), Bias (SD), Bias (%) (SD) and Bias (% Last ring) for DBH and BA for each species.

	DBH					BA				
Species	MAE	MAE (% Last ring)	Bias	Bias (%)	Bias (% last ring)	MAE	MAE (% Last ring)	Bias	Bias (%)	Bias (% last ring)
Chokecherry	0.11 (0.08)	7.98 (5.67)	-0.01 (0.13)	-8.32 (13.61)	-3.84 (6.44)	0.13 (0.11)	8.87 (7.51)	-0.03 (0.17)	-19.22 (31.38)	-4.62 (9.21)
Colorado spruce	1.18 (1.21)	8.83 (9.04)	0.61 (1.58)	-5.33 (10.82)	-2.00 (3.54)	12.32 (14.00)	8.78 (9.98)	3.76 (18.27)	-13.00 (28.44)	-2.75 (6.41)
Siberian elm	0.88 (0.99)	8.35 (8.14)	0.29 (1.29)	-0.13 (15.07)	0.65 (8.00)	9.02 (13.98)	9.64 (10.60)	3.29 (16.31)	-2.67 (36.59)	0.81 (11.62)
Green ash	0.41 (0.33)	7.34 (5.52)	-0.06 (0.52)	-10.09 (23.73)	-3.30 (5.82)	1.97 (2.16)	7.87 (7.66)	-0.61 (2.86)	-27.07 (81.01)	-4.08 (8.65)
Manitoba maple	1.01 (0.98)	14.12 (13.35)	0.13 (1.41)	0.67 (16.67)	0.55 (11.09)	7.27 (9.43)	15.80 (16.53)	0.91 (11.87)	-1.89 (35.65)	0.04 (18.68)
Hybrid poplar	0.76 (0.75)	9.85 (8.77)	0.41 (0.99)	-3.17 (19.81)	-0.33 (6.54)	5.98 (8.14)	11.46 (11.98)	3.04 (9.63)	-10.51 (74.12)	-0.06 (9.87)
Scots pine	0.42 (0.46)	6.50 (7.24)	0.10 (0.62)	-6.17 (20.89)	-1.16 (4.77)	2.51 (2.71)	7.38 (7.96)	0.87 (3.59)	-19.39 (88.45)	-1.05 (6.91)
Eastern larch	0.52 (0.41)	7.04 (5.35)	0.26 (0.61)	-4.28 (24.63)	-0.28 (5.22)	3.51 (3.86)	7.99 (7.53)	2.03 (4.80)	-14.90 (105.67)	0.23 (7.36)
Acute willow	0.30 (0.28)	10.78 (10.02)	0.23 (0.33)	-1.94 (8.02)	-0.51 (3.07)	0.74 (0.69)	12.41 (11.57)	0.53 (0.87)	-4.65 (17.91)	-0.93 (4.94)
White spruce	0.45 (0.49)	8.18 (7.60)	0.14 (0.66)	-9.53 (30.95)	-2.02 (7.19)	2.97 (4.30)	9.04 (9.56)	1.24 (5.08)	-29.73 (120.66)	-1.93 (9.66)

4.4.6 Compactness

Average correlations between compactness and MAE, MAE (% Last ring), Bias, Bias (%) and Bias (% Last ring) were negative (Table 4.8), indicating that when compactness is low (ring shape is more oval), the error is high. Correlations were higher for Bias (%) DBH and BA, then for MAE (%Last ring) and MAE for BA (Appendix Table A5). Although there were some minor changes in correlations between species, the values did not change much, which indicates that the tree compactness seemed to alter on an individual tree basis, and not species by species (Appendix Table A5).

Table 4.8 - Correlation between the compactness of the rings on the cross section and MAE, MAE (% Last ring), Bias, Bias (%) and Bias (% Last ring) for DBH and BA.

Atribute	MAE	MAE (%Last ring)	Bias	Bias (%)	Bias (%Last ring)
DBH	-0.36	-0.08	-0.33	-0.84	-0.35
BA	-0.48	-0.69	-0.35	-0.89	-0.25

4.5 Discussion

4.5.1 Direction, approach and mode: pith vs shape

B to P yielded fewer extreme values than P to B, despite P to B generating lower average errors than B to P, when considering all age classes. This can be attributed to the fact that near the bark, the ring widths are generally smaller than the ring widths near the pith, so these small ring widths will result in a less significant difference between the estimated annual DBH and therefore, less expressive errors. On the other hand, beginning the calculations with larger ring widths near the pith potentially leads to more significant errors, which will accumulate over the set of cross-section calculations, causing more extreme errors for the annual DBHs near the bark. The P to B direction of calculation is only recommended when young trees are being sampled, up to approximately 30-year-old trees, on average (see Figure 4.2). For a year-by-year assessment throughout the life of a tree, B to P is a more preferable direction to calculate variables, since errors do not increase as much in a specific area of the cross section, like they do in the P to B direction. In addition, B to P calculations do not overestimate values (Figure 4.3b, 4.3d), as was seen in the P to B direction errors.

Besides direction, both approach and mode also affect the estimates. Increment cores containing the pith, p_j and $p_j op_k$, yielded the lowest MAE and MAE (%Last ring) for DBH and BA estimates. This highlights both the importance of reaching the pith when coring for better

DBH and BA estimates, and any subsequent biomass and carbon stocks estimates made from the values. Realistically, the pith is more attainable on trees presenting round cross sections. Hence, the rounder a cross section, and the more even the growth around the pith, the more reliable the estimates, when using increment cores. This was again illustrated by the negative correlation between compactness and MAE, MAE (%Last ring), Bias, Bias % and Bias % (Last ring) for both DBH and BA (Table 4.8, Appendix Table A5). Perfectly round cross sections are not common in nature, because tree architecture is affected by many factors, such as competition (Salminen & Varmola, 1993; Shi et al., 2015), wind (Nicoll & Ray, 1996; Skatter & Kucera, 1998; Stokes & Berthier, 2000), spiral grain (Shi et al., 2015), slope (Shi et al. 2015), species (Rozas, 2003) and genetic commands. Inner ring-shape pattern is not obvious by observing the outside of a tree, hence it is often difficult to determine the exact pith location when coring, resulting in a high possibility of increment cores being off-pith (Liu, 1986; Biondi, 1999; Motta & Nola, 2001; Colbert et al., 2004; Pirie et al., 2015; Altman et al., 2016). If limited by time or budget, it is better to seek high quality increment cores, for example, long increment cores, with no rotten parts or broken pieces (Norton et al., 1987; Rozas, 2003; Altman et al., 2016), that reach the pith, rather than low-quality cores but attaining a higher sample size per tree. In many cases, rotten and broken pieces cannot be avoided, since this factor relies on interior wood quality of the tree. Therefore, reaching the pith, although not always easy in the field, is a skill that can be improved upon with experience.

Some authors have tried to overcome the absence of a pith in an increment core by testing methods to estimate the pith location on off-pith increment cores (Applequist, 1958; Liu, 1986; Allen, 1988; Duncan, 1989; Villalba & Veblen, 1997; Rozas, 2003; Pirie et al., 2015), but all of these methods default to circular growth around the pith, which is not reasonable, since most cross sections are not perfectly round. No research evidence has been found associating any degree of off-pith coring to determine the effect on the error when estimating DBH and BA. There are studies relating the degree of off-pith coring and their error when estimating tree age. For example, Duncan (1989) estimated the age for *Dacrycarpus dacrydioides* and reported that off-pith increment cores were one of the main sources of error (35%). In addition, Duncan (1989) found that the errors increased with increasing offset from the true pith, and that even larger errors were associated with greater eccentricity within the stem. Similarly, Rozas (2003) estimated ages

with increment cores for *Fagus sylvatica* and *Quercus robur* and concluded that the closer the increment core was to the pith, the more accurate the age estimate.

4.5.2 Number of increment cores vs shape, age and mode

In general, most studies utilize two increment cores (e.g., dendroclimatology, dendroecology, dendrochronology) (Iles, 1974; 2014b; Bouriaud & Popa, 2009; Duchesne et al., 2002; Worbes et al., 2003; Tatarinov et al., 2007; Goodsman et al., 2010; Babst et al., 2014a; Nehrbass-ahles et al., 2014; Dye et al., 2016; DeRose et al., 2017; Tenzin et al., 2017; Alexander et al., 2018), and there are studies using a varying number of cores, depending on field conditions (Biging & Wensel, 1988; Véronique, 1998; Rozas, 2003; Clark & Hallgren, 2004; Bakker, 2005; Fraver & White, 2005; Brienen & Zuidema, 2006; Jump et al., 2006; Barry, 2014; Klesse & Frank, 2016;). In general, this study found that the more increment cores used, the more precise the estimates for both DBH and BA. Using fewer increment cores to calculate diameters for very round trees may be acceptable, but these types of trees are uncommon. Fewer increment cores may also be tolerable for young trees, for three reasons. First, young trees yield less errors than older trees because it is harder to miss the pith when the trees are smaller in diameter (Clark & Hallgren, 2004). Second, coring less harms the tree less, which is very important for small trees, since they can be more easily injured. Third, younger trees have less rings to accumulate error in successive calculations, thus estimates will be more precise, even when using less increment cores in a calculation. For example, in the B to P direction, for the 20 to 30-year age class, using one increment core yielded lower DBH MAE error (0.75 cm) than using 2 increment cores at the immediate larger 30 to 40-year age class (0.97 cm) (Table 4.6).

To cope with non-round cross-sectional shapes, ideally, diameters should be measured from the cross section, so the errors would be minimal to non-existent. However, cutting trees to measure DBH is not feasible in most cases, because it is expensive, time consuming, and most importantly destroys the tree (Rozas, 2003). To attain a close-to ideal situation, the general recommendation from this study and others is the more cores that can be successfully obtained, the better (Iles, 1974; Rozas, 2003). Although I did not test all possibilities, five cores would have likely increased the precision more, and ten cores would have increased it even higher. In this study, the most precise estimation outcomes were found by using four increment cores. In a time-limited or budget-limited situation, using less increment cores, for example 3, may be equally acceptable, to bridge the gap of obtaining the highest precision versus the time and effort spent on

collecting and processing more cores. This recommendation also takes into account that by the third attempt at coring towards the pith of a tree in the field, you have a much higher likelihood of reaching the pith, as earlier attempts all assist the person in determining where an off-center pith is probably located. For almost all species for example, using 3 and 4 increment cores that reached the pith yielded the same precise estimates (e.g., Figure 4.5a vs Figure 4.5c). Similarly, Babst et al. (2014b) estimated biomass using 1 and 2 increment cores and found that no significant difference was found among the estimates. Biging and Wensel (1988) also used one and two increment cores and found similar results. Biging and Wensel (1988) attributed this similarity to the round shape of the cross sections. Klesse and Frank (2016) studying a forest in the Swiss Alps found that 4 radii accounted for better estimates when encountering eccentric cross sections, but concluded that using two is more reasonable, given that this difference was not sufficiently pronounced to offset the extra work and budget required to sample two more increment cores.

In addition to cross section shape and age, the best number of increment cores used relies on factors such as budget, available time, and precision required for the calculation, since increasing the number of cores used increases processing time, effort, core storage space, and tree damage (Bakker, 2005). The degree of precision gained from coring and processing one, two, or three extra increment cores should be considered before sampling, on a case-by-case basis. Table 4.3 provide approximations of the additional accuracy yielded by adding increment core sample depth for each possible mode.

4.5.3 Advantages and limitations of the dendrochronology method

Dendrochronology has been used as a tool to assist in a number of different sub-disciplines, such as climate (Jump et al., 2006; Bouriaud & Popa, 2009; Salzer et al., 2009; Beck et al., 2011), carbon fertilization (Véronique, 1998; Salzer et al., 2009; Silva et al., 2010; Beck et al., 2011; Girardin et al., 2016; Hember et al., 2019), tree age estimation (Duncan, 1989; Rozas, 2003; Worbes et al., 2003, Clark & Hallgren, 2004; Fraver et al., 2011; Bergin & Kimberley, 2012; Altman et al., 2016), forest ecology (Motta & Nola, 2001), forest disturbance (Altman et al., 2013; Fraver & White, 2005), forest fertilization (Véronique, 1998; Duchesne et al., 2002; Goodsman et al., 2010) and forest management (Biondi, 1999; Pape, 1999; Stahle et al., 1999; Worbes et al., 2003; Brienen & Zuidema, 2006; Beck et al., 2011; Nehrbass-ahles et al., 2014; Dye et al., 2016; Klesse & Frank, 2016; Alexander et al., 2018). However, when studying forest

management focused on quantifying carbon stocks, dendrochronological tools have traditionally been viewed as not very suitable in terms of sampling and processing, because they bias the estimates. Some studies have focused on finding the best sampling technique (Brienen et al., 2012; Babst et al., 2014b; Nehrbass-ahles et al., 2014; Alexander et al., 2018; Hember et al., 2019;), and others have combined data from increment cores with traditional inventory methods, or dendrometer bands, to help predict growth (Biondi, 1999; Clark et al., 2007; Tatarinov et al., 2007; Metsaranta & Lieffers, 2009; Nehrbass-ahles et al., 2014; Cuny et al., 2015; Dye et al., 2016; Klesse & Frank, 2016; Alexander et al., 2018; Hember et al., 2019). Eddy covariance towers have also been used to predict carbon stocks (Gower et al., 2001; Rocha et al., 2006; Ilvesniemi et al., 2009; Zweifel et al., 2010; Babst et al., 2014c; Teets et al., 2018) and some studies have found loose agreement between eddy towers and increment cores (Zweifel et al., 2010; Teets et al., 2018). But no eddy covariance-, dendrometer- or inventory-related studies have sampled trees individually to calculate the individual error from using increment cores to calculate DBH, as this study has achieved. Hence the main objective of this study was to question the reliability of using increment core data for deriving past DBH values and other associated estimates, such as within allometric equations (Shi et al., 2015; Alexander et al., 2018).

Understanding the precision of all input data in allometric equations is important because each equation has its own source of built-in uncertainty, as well as uncertainty built into the process of acquiring data (Metsaranta & Lieffers, 2009; Dye et al., 2016; Alexander et al., 2018). Error from calculating DBH from increment cores is normally underestimated as trees are generally considered round (Fule et al., 1997; Colbert et al., 2004; Ahmed et al., 2009; Metsaranta & Lieffers, 2009; Goodsman et al., 2010; Babst et al., 2014c; Shi et al., 2015; Dye et al., 2016; Alexander et al., 2018), which is a common misconception. This study reveals that the error from using increment cores can be significantly high: it was 16.55% for DBH and 55.17% for BA (Table 4.3), and these measurements were made from shelterbelt trees, that normally have limited tree-to-tree and tree-understory competition, which probably lead to more round cross sections, therefore, less error if compared to trees grown in forests. In most studies, forest-grown tree rings have underestimated carbon stocks (Biondi 1999; Metsaranta & Lieffers, 2009; Klesse & Frank, 2016; Hember et al., 2019). Carbon stocks were underestimated in this study too in B to P, but overestimated in P to B for both DBH and BA, as in Biging and Wensel (1988), and in Dye et al., (2016) who found that tree-ring data overestimated net primary production for two sites, and

underestimated for one site, in comparison with data from permanent plots. More studies are needed to fully increase precision on DBH retrieved from increment cores.

Being able to retrieve DBH from increment cores in a precise and reliable manner is important for local carbon stock assessment, which could have a global impact if used for climate change mitigation planning. Global impact could be achieved by using tree-growth data in models to predict growth (and carbon stock gains) based on climate scenarios that maximize the selection of species and management protocols for carbon sequestration (Davis et al., 2013; Howat, 2020).

In this study, the weakness of the method is that the error accumulates over the years on the successive rings in the cross section, but this can be minimized if the pith is reached, since the errors tend to be minimal. The strength of the method is based on its simplicity and ease-of-use to calculate tree growth over the years using increment cores and the error yielded. This methodology allows DBH or BA estimated data to be used to calculate biomass and carbon stocks, which could affect forestry, dendrochronology and global warming mitigation disciplines. It can be used as a tool allowing socioeconomic policies by rewarding landowners for carbon sequestration (Amichev et al., 2020), which would be a positive effort towards combating global warming for Saskatchewan as well as globally. This methodology can be used with any tree producing identifiable annual rings, but it is especially reliable for shelterbelts, where plant dynamics are somewhat controlled, different from the forest dynamic, where mortality, regrowth, and competition are uncontrolled (Biondi, 1999; Brienen & Zuidema, 2006; Babst et al., 2014b, 2014a; Dye et al., 2016; Alexander et al., 2018).

4.6 Conclusions

This study concludes that the best direction to calculate DBH is starting from the bark moving towards the pith and that reaching the pith with increment cores is very important to increase the precision of estimates. The hypothesis that increment cores that reach the center of the tree would yield more precise estimates was proven wrong. Instead, reaching the pith was found to be more important than reaching the center, but these two elements can coincide for more circular shaped cross sections, where precise calculated estimates can be made for both DBH or BA. The hypothesis that older aged trees would yield more error was proven true. The older the tree, the higher the error. The hypothesis that the more increment cores used, the better the estimates is also accurate. In fact, using four increment cores yielded the lowest error in

almost every case, but this might be reconsidered in cases where time is limited, or processing resources are limited, as well as when small trees are being sampled.

As this is the first study to more deeply explore the range of field sampling outcomes when extracting increment cores to retrieve past DBH values, the gap between classic forestry and classic dendrochronology utilization has been lessened. By better understanding how the values are derived, and how their associated error values change, the newly understood information makes calculating DBHs from increment cores more reliable. As a result, the large amount of data stored in regional and global data banks from cored trees is one step closer to being more fully used for things like allometric models and carbon stock assessment studies. Information that can ultimately serve as a tool to assist in combating global warming and help by assisting in planning and mitigation in the future.

Mitigation planning can now incorporate a local focus. Increment cores can be sampled at each farm's shelterbelts by small crews, taken to a laboratory, measured, and used to create a farm-specific carbon footprint, which could support at least two powerful tools aiming to decrease carbon emissions. First, a local carbon market could be more easily created once a landowner knew how much carbon they were accruing. This would help to motivate farmers to annually sequester more carbon by growing a crop of trees, and potentially offset emissions that they might accrue from growing other crops, or having cattle within their farm operation. Second, a policy rewarding carbon sequestration could also be developed by a federal or provincial government. Such a policy would motivate carbon sequestration as well. In both cases, carbon credits or tax benefits would contribute to trees be considered as a valuable asset in the farming operation, not just a random landscape component. This study helps reach an important milestone that assures that increment-core-derived data in such a system would be reliable for carbon assessments. It also implies that such markets and/or incentivized policies could be applied broadly to reach many farms in Saskatchewan, Canada, and even perhaps the world. Linking these sound ecological benefits, with the growing climate awareness of landowners, would be a great stimulus to a greener food production chain, and towards a decarbonized economy for this, and for the next generation.

CHAPTER 5

EXPLORING THE CANOPY QUANTUM EFFICIENCY PARAMETER FOR MODELING FUTURE GROWTH USING 3-PG IN SHELTERBELTS IN SASKATCHEWAN

5.1 Abstract

Shelterbelts are an agroforestry mechanism with great potential to sequester carbon into its biomass and surrounding soil matrix. This carbon sequestration capacity makes shelterbelts a valuable tool to mitigate climate change while utilizing a relatively small amount of land and still providing other important environmental services. Published studies have modeled future shelterbelt growth across a wide geographic spectrum, and a few have modeled it with the 3-PG model, but none have assessed how geographically specific a modelled fit, needs to be. The goal of this study was to fit shelterbelt tree growth in the 3-PG model across a wide and narrow geographic area in Saskatchewan, to assess the alpha parameter (the canopy quantum efficiency) within the model for fitting accuracy over time.

It was found that model fitting should be tree- or locally-specific, and not regionally-specific or from a wide geographic region. The older the tree, and the farther in the past the model runs, the larger the estimated error. The 3-PG model is reliable for shelterbelt's local carbon stocks modeling, which is seen as a significant benefit for two reasons. First, as the environment varies, the model varies along with the changes, which is convenient for modeling growth under past and future changing climates. Second, a local assessment can serve as a carbon footprint tool on a farm specific basis, which ultimately could lead to a landowner being rewarded for the carbon they sequestrate on an annual basis. These financial incentives could possibly reduce emissions by motivating individuals to practice better land stewardship by perhaps planting more trees, leading towards a more sustainable future for everyone.

5.2 Introduction

Conventional models, also known as statistical models, are site specific (Landsberg and Hingston, 1996), cannot simulate growth for un-forested areas, and are not sensitive to climate variations in the short term (Stape et al., 2004). Conversely, process-based models simulate growth based on physiological principles considering the environment and its fluctuations, which leads to more precise growth estimates (Battaglia and Sands, 1998; Stape et al., 2004). This is

especially important when considering changes through time, as exacting future estimates are difficult to make with statistical models (Gupta and Sharma, 2019), as environmental conditions do not follow past records as precisely. The model 3-PG estimates growth based on plant efficiency to transform light into energy and then, into matter (Landsberg and Waring, 1997), all of which is specially affected by one parameter, the canopy quantum efficiency (known as alpha (α_c)). Alpha depicts how well a tree canopy is able to capture the sun's energy and turn it into mass, specifically, how the leaves capture sunlight to feed into the photosynthesis process (Baldocchi and Amthor, 2001), to produce matter to be allocated into various tree compartments (Feikema et al., 2010). Several factors affect quantum canopy efficiency, which are described by the environmental constraints in the model, also known as environment modifiers (1).

$$a_c = f_T f_N f_F \varphi a_{cx} \quad (1)$$

The modifier a_{cx} is the theoretical maximum canopy efficiency, f_T, f_N and f_F are the temperature, nutritional, and frost modifiers, respectively, and φ is the physiological modifier (PhysMod) (2) which assumes the value of the most restrictive modifier, either vapor pressure deficit (f_D) or soil water modifier (f_θ), times the age-dependent modifier (f_{AGE}), that depicts hydraulic features that change with the age of the tree.

$$\varphi = f_{AGE} min\{f_D f_\theta\} \quad (2)$$

Alpha is a very sensitive parameter, highly affecting tree growth (Almeida et al., 2004; Esprey et al., 2004; Alexandre, 2009; Headlee et al., 2013; Amichev et al., 2016c), so its precise determination is crucial for model precision. For example Amichev, Bentham, Kurz, et al., (2016c), when parameterizing 3-PG for white spruce, conducted a sensitivity analysis for DBH by varying k (Extinction coefficient for PAR absorption by canopy), fullCanAge (age at full canopy), alpha, and Y (Ratio NPP/GPP) in a +/- 40% range, and found that alpha was the most sensitive parameter affecting tree biomass (+/- 49.5%). Thus, although Landsberg et al., (2003) recommended alpha as 0.05 mol C (mol quanta)$^{-1}$ for conifers and 0.07 mol C (mol quanta)$^{-1}$ for deciduous trees, precisely quantifying alpha will raise accuracy estimates within the 3-PG model.

For model runs, fitting alpha precisely is important because it is highly probable that the modifier could vary with environment, a factor that changes from site to site, and from species to species. For example, trees growing in the same province (Saskatchewan, Canada) had their alpha values varying from 0.0177 mol C (mol quanta)$^{-1}$ to 0.05 mol C (mol quanta)$^{-1}$, depending on the species (Amichev et al., 2016a). Alpha also differed on trees of the same species growing under

different geographic conditions. Amichev, Johnston, & Van Rees (2010a) tested hybrid poplar trees, and the alpha varied from 0.0177 mol C (mol quanta)$^{-1}$ for their study trees growing in Canada, to 0.08 mol C (mol quanta)$^{-1}$ for the same species of tree growing in Minnesota and Wisconsin, in the USA (Headlee et al., 2013). Alpha is also sensitive enough to differ for plants growing at the same site, and from the same species, but in different plantation rotations: over seven willow rotations, alpha varied from 0.0530 mol C (mol quanta)$^{-1}$ to 0.1119 mol C (mol quanta)$^{-1}$ (Amichev et al., 2011).

These reasons lead to the conclusion that it is crucial to explore and determine an accurate alpha value for the 3-PG model in order to obtain precise estimates. The goal of this paper is twofold. First, to fit tree-specific alpha values and validate them by using tree-specific alpha values from other same-species trees at the same site. I will then compare these results to species-specific literature values (Amichev et al., 2016a) established from a much wider geographic area. This will allow the assessment of the effect of alpha on 3-PG precision estimates moving from a site-specific fitting to a wider geographic fitting. The second goal is to assess the precision of the modelled growth over the age of the tree to better understand how far into the past estimates are reliable, and conversely, have an idea of how far in the future estimates might hold true. I hypothesize that; i) local-specific fitting is more accurate than regional-specific fitting; and; ii) the farther back in time estimates go, the higher the associated error will compound through time.

5.3 Methods

5.3.1 Data

Twenty-nine healthy trees were either selected by a landowner or randomly selected and cut down and measured in the province of Saskatchewan, using the randomized branch sampling procedure (Amichev et al. 2015), encompassing six species [caragana (CG), green ash (GA), Manitoba maple (MM), hybrid poplar (HP), white spruce (WS) and Scots pine (SP)], from 8 to 56-year-old (Appendix B details the sampling process regarding number and location of the trees sampled). Variables assessed included total height, diameter at breast height, diameter at every one metre up to the total tree height, leaf area, branch and foliage biomass (following the Valentine et al. (1984) procedure, modified by Amichev et al. (2015)), spacing between trees and tree rows, and crown width. A disc was cut at the diameter breast height from each tree (1.3 m) and diameters through time for each tree were retrieved as described in Chapter 4 (mode P3), as it was proven a reliable method. Mean annual increment (MAI) of each tree was calculated by

dividing the last diameter (nearest the bark) by the age of the tree (cm year^{-1}). Relations to biomass was not included in the analysis for simplicity, because diameter and biomass behave in a very similar manner.

5.3.2 Tree-level Fitting

Model parameterization was completed for each tree individually using data from this study and parameter values from Amichev et al., (2010, 2016b, 2017), who studied the same shelterbelt tree species in the same province (Saskatchewan, Canada). For each tree, the best alpha value was fitted by multiple iterations, until the smallest Root Mean Square Error (RMSE), bias, and highest Coefficient of Determination (R^2) was achieved (in that order of priority), for each predicted tree diameter.

5.3.3 Validation

The effect of alpha on the precision of 3-PG modeled diameter estimates was assessed by two validation approaches: *Local Validation* and *Regional Validation*. For local validation, alpha fitted for a specific tree was used for other trees of the same species from the same site. For regional validation, species-specific alpha values from the literature (Amichev et al., 2016b) were used on each tree. Tree-specific fitting was validated over time by observing the RMSE and bias for every 5-year age class from the most immediate year at the bark, moving back through time towards the pith.

5.3.4 Assessment

Fitting and validation were assessed by the RMSE (3), bias (%) (4) and R^2 (5), where y_i was the observed diameter data, $\hat{y}$ was the estimated diameter values, $\bar{y}$ was the average of the observed diameter data. Graphs of the predicted versus observed diameter were built to observe the fitting as well.

$$RMSE = \sqrt{\sum_{i=1}^{n} \frac{(\hat{y}_i - y_i)^2}{\bar{y}}} \quad (3)$$

$$\text{Bias (\%)} = \left(\frac{(y_i - \hat{y}_i}{y_i}\right) * 100 \quad (4)$$

$$R^2 = \left(\frac{n(\sum y_i \hat{y}_i) - (\sum y_i)(\sum \hat{y}_i)}{\sqrt{[n\sum {y_i}^2 - (\sum y_i)^2][n\sum {\hat{y}_i}^2 - (\sum \hat{y}_i)^2]}}\right)^2 \quad (5)$$

5.4 Results

5.4.1 Fitting

Table 5.1 describes the trees sampled, their location, spacing, N (number of trees per hectare), MAI (mean annual increment), FCA (full canopy closure age, calculated from species-specific linear regressions using age and crown size), age, cluster, species, alpha, RMSE (root mean square error), bias and R^2 (coefficient of determination) for predicted tree diameter across classes of DBH estimated in 5, 10, 15, 20, 25, 30, 40, 45 years into the past since the last DBH near the bark. Most trees were fitted well by the 3-PG model. RMSE ranged from 1.2 to 68.53, bias ranged from 0.00 to the negative and positive extremes of -291.24 and 33.09, and R^2 ranged from 0.80 to 0.99 (Table 5.1). Since the most extreme bias was negative, in general, the models tended to overestimate real DBH. Observed and predicted DBH for a random tree from each species were plotted (Figure 5.1) so the fitting could be assessed. Similarly, predicted and observed biomass was plotted in Figure 5.2. In general, predicted and observed DBH were similar, and almost always followed a straight line (see R^2 in Table 5.1).

Table 5.1 - Location, spacing, N (number of trees per hectare), MAI (mean annual increment), FCA (full canopy closure age), age, soil cluster, species, alpha, RMSE (root mean square error), bias and R^2 (coefficient of determination) for predicted tree diameter across classes of DBH at 5, 10, 15, 20, 25, 30, 40, 45 years into the past.

									All classes			45		40		35		30		25		20		15		10		5	
Species	Loccation	Spacing	N	MAI	FCA	Age	Cluster	Alpha	RMSE	Bias	R2	RMSE	Bias	RMSE	Bias	RMSE	Bias	RMSE	Bias	RMSE	Bias	RMSE	Bias	RMSE	Bias	RMSE	Bias	RMSE	Bias
GA	53.03632, -105.84488	4.68	456.6	0.35	20	56	BLK-2	0.006	6.627	-2.95	0.978			6.627	-2.95	5.317	-1.28	4.649	-3.56	4.743	-3.83	4.879	-4.14	5.219	-5.02	5.377	-5.28	5.76	-5.73
GA	49.76691, -105.91942	4.1	608	0.76	15	29	BRN-1	0.012	13.15	-30.6	0.993									13.15	-30.56	9.331	-5.7	7.358	1.6	7.463	4.9	8.08	8.09
GA	50.96188, -107.23123	1.7	3508	0.69	3.5	30	BRN-2	0.012	11.81	4.902	0.94							11.81	4.9	11.98	-0.57	11.36	-4.4	10.61	-1.33	9.346	5.38	10.9	10.85
SP	49.76691,-105.91941	5	397.45	0.4	35.5	46	BRN-1	0.011	12.6	20.88	0.99			12.6	20.88	11.2	10.7	8.845	3.41	6.681	-1.62	5.805	-5	6.059	-6.05	5.624	-5.65	4.03	-4.03
MM	49.76691, -105.91942	4.7	567	0.63	13	25	BRN-1	0.009	68.53	-123	0.98											68.53	-122.79	56.69	-64.79	48.74	-51.74	38.4	-39.1
MM	51.97869, -106.67750	3.9	643.5	0.58	10	20	D-BRN-3	0.006	17.59	-1.98	0.98													17.59	-1.98	16.01	-15.36	15.8	-15.8
MM	51.26666,-105.96666	7	200	0.7	60	43	D-BRN-2	0.008	31.11	33.09	0.996			31.11	33.09	29.33	29.56	25.59	24.05	21.04	18.76	16.52	13.86	12.59	9.43	9.455	5.1	2.84	-2.78
WS	51.07475, -101.89690	2.25	4444	0.28	11.5	26	BLK-1	0.014	21.09	-45.8	0.995													21.09	-45.78	12.44	-9.64	7.26	5.19
WS	50.89850, -101.89690	1.5	4444	0.44	7.5	15	BLK-1	0.023	23.16	-52	0.985															23.16	-52	11.2	-1.71
WS	50.89850, -101.89690	7	204	0.44	35.5	49	BLK-1	0.011	14.44	-0.71	0.954	14.44	-0.71	13.71	9.32	12.88	10.18	12.53	6.35	12.34	1.98	12.76	-2.32	13.79	-5.5	14.95	-8.12	15.2	-9.66
WS	50.89850, -101.89690	4.6	472	0.75	23.5	47	BLK-1	0.019	14.7	9.319	0.96			14.7	9.32	13.63	4.9	12.11	0.44	11.09	-3.46	11.04	-7.1	12.08	-10.77	13.79	-13.52	14.8	-14.76
WS	49.76691, -105.91942	2	2500	0.1	10	48	BRN-1	0.006	13.57	-26.8	0.949									13.57	-26.81	4.445	-2.25	2.738	0.96	2.893	0.89	3.3	-0.26
WS	50.89850, -101.89690	1.5	4444	0.24	8	13	BLK-1	0.016	32.85	-291	0.989															32.85	-291.24	19.7	-20.63
WS	50.96188, -107.23123	4.6	471.7	0.37	23.5	47	BRN-2	0.01	53.86	-30.5	0.993			53.86	-30.51	35.02	-66.81	27.39	-86.63	20.94	-31.37	15.64	-17.44	10.39	-9.18	5.033	-2.82	1.96	1.65
WS	49.76691, -105.91942	4.7	454.5	1.05	23.5	39	BRN-1	0.035	22.53	-26.5	0.95					22.53	-26.48	21.2	-13.05	19	-2.61	17.7	4.29	17.6	10.84	19.25	16.89	22.5	22.05
WS	49.76691, -105.91942	2	2500	0.54	10	29	BRN-1	0.032	18.86	-145	0.99									18.86	-145.49	12.19	-13.09	10.65	-10.8	9.711	-9.65	8.68	-8.44
WS	49.76691, -105.91943	2	2500	0.2	10	36	BRN-2	0.009	22.33	-42.1	0.98											22.33	-42.14	12.76	-5.69	8.855	6.8	10.3	9.91
CG	51.81263, -105.29261	6.9	210	0.23	27	18	BLK-1	0.003	29.57	26.87	0.92													29.57	26.87	19.64	4.37	16	-13.98
CG	51.2360, -103.64978	2.5	1634	0.33	6.3	21	BLK-1	0.005	24.42	31.24	0.88											24.42	31.24	21.45	20.27	10.44	1.2	9.22	-8.22
CG	51.23605, -103.64978	2	2500	0.18	4.2	23	BLK-1	0.004	34.97	31.65	0.88											34.97	31.65	30.4	17.07	18.99	-5.85	21.7	-20.24
CG	52.81969, -106.19210	2.3	1111	0.2	8.3	23	BLK-4	0.002	13.29	15.81	0.802											13.29	15.81	6.601	12.53	3.111	5.43	1.2	2.16
HP	49.76691, -105.91941	3	1111	0.73	6	25	BRN-1	0.016	11.39	11.18	0.973									11.39	11.18	10.26	6.31	9.544	4.21	9.906	7.79	10.9	10.26
HP	51.97869, -106.67749	3.3	926	1.01	16	28	D-BRN-3	0.025	7.631	-5.6	0.993									7.631	-5.6	7.111	-5.54	6.844	-5.01	5.479	-2	4.26	3.49
HP	49.76691, -105.91942	2	2500	0.37	3.5	14	BRN-1	0.012	6.229	-5.51	0.911															6.229	-5.51	6.49	-4.39
HP	49.76691, -105.91942	2	2500	0.86	3.5	12	BRN-1	0.018	8.067	-9.25	0.975															8.067	-9.25	4.91	-3.02
HP	51.97869, -106.67749	3.4	850	1.19	29	33	D-BRN-3	0.053	29.88	14.95	0.999							29.88	14.95	22.17	-28.11	18.41	-20.21	15.15	-15.11	14.99	-14.98	14.5	-14.51
HP	49.76691, -105.91941	3	1111	1.36	6	8	BRN-1	0.037	10.71	6.45	0.977																	10.7	6.45
HP	51.97869, -106.67773	3.28	926	0.61	14.4	13	D-BRN-3	0.063	4.849	6.096	0.995															4.849	6.1	2.94	-1.42
HP	49.76692, -105.91942	3	1111	1.01	6	20	BRN-1	0.021	17.08	-23.7	0.983											17.08	-23.71	14.99	-16.39	10.75	-10.2	2.94	-2

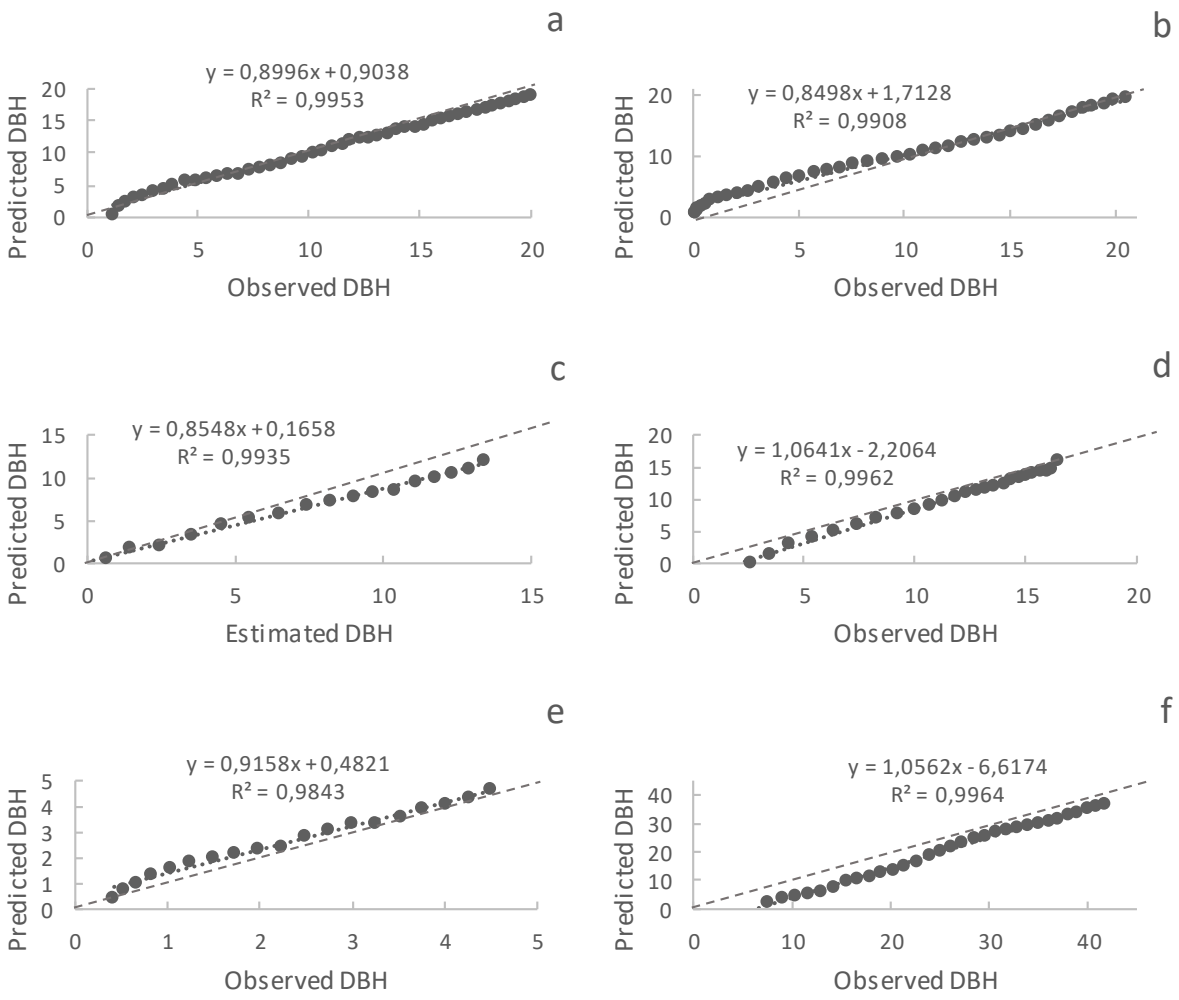

Figure 5.1 - Predicted and observed DBH from a random tree from each species. The trees are, a) Green ash; b) Scots pine; c) Manitoba maple; d) White spruce; e) Caragana; f) Hybrid poplar. Dashed line is the x=y equation.

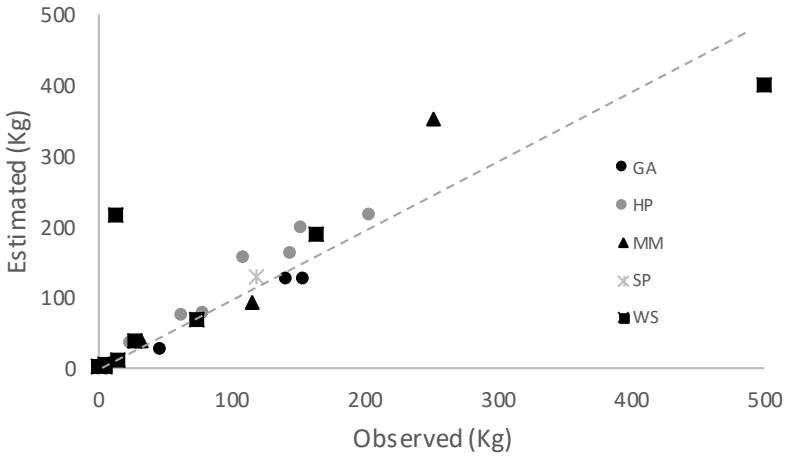

Figure 5. 2 – Predicted and observed biomass (Kg) for green ash (GA), hybrid poplar (HP), Manitoba maple (MM), Scots pine (SP), white spruce (WS).

5.4.2 Geographic Validation (Local vs Regional)

To assess how different alpha values affect their precision estimates, tree-specific fitting was compared by using alpha from the same-species of tree with another tree from the same site of the same species (Local validation), and then by using an average alpha value for a wider geographic region derived from the literature for that species (Regional validation) (Table 5.2). Validations for RMSE, bias, and R^2 were assessed (Table 5.2). For all species, RMSE and bias were lowest for tree-specific fitting, followed by local-specific validation, and then for regionally derived values available from the literature (Amichev et al., 2016b). R^2 did not differ among most fitted parameters, except for caragana, which presented lower values for both local and regionally derived validations (0.20) in comparison with the tree-specific fitting value (0.87) (Table 5.2).

Table 5.2 - Average alpha, difference between average alpha at fitting (tree) and at the validation (local and regional) (Dif), root mean square error (RMSE), bias, and coefficient of determination (R^2) for predicted DBH. Note: The standard deviation for tree fitting, local, and regional value validations are listed beside each calculation in parentheses; Green ash (GA), Manitoba maple (MM), white spruce (WS), caragana (CG) and hybrid poplar (HP) trees sampled in SK, Canada.

	Species	alpha	Dif	RMSE	Bias	R^2
Tree	GA	0.0098 (0.0038)		10.53 (3.45)	-9.54 (18.63)	0.97 (0.03)
	SP	0.011		12.6	20.88	0.98
	MM	0.0077 (0.0015)		39.07 (26.39)	-30.56(81.78)	0.99 (0.01)
	WS	0.0175 (0.0098)		23.75 (12.00)	-65.19 (89.76)	0.97 (0.02)
	CG	0.0033 (0.0012)		25.56 (9.25)	26.39 (7.38)	0.87 (0.05)
	HP	0.0306 (0.0186)		11.98 (8.16)	-0.67(12.72)	0.98 (0.03)
Local	GA	0.012 (0)	-0.002	12.23 (0.59)	-10.36 (21.58)	0.97 (0.04)
	SP					
	MM	0.007 (0.01)	0.001	28.64 (15.62)	-5.11 (34.36)	0.99 (0.01)
	WS	0.019 (0.02)	-0.002	114.07 (128.73)	-94.12 (238.20)	0.96 (0.05)
	CG	0.0042 (0.01)	-0.001	41.54 (6.37)	29.3 (29.30)	0.20 (0.06)
	HP	0.027 (0.02)	0.004	58.35 (48.74)	-23.19 (89.57)	0.98 (0.02)
Regional	GA	0.03	-0.02	137.58 (90.66)	-197.38 (128.68)	0.97 (0.03)

SP	0.05	-0.039	229.42	-252.62	0.99
MM	0.03	-0.0223	198.98 (65.81)	-220.07 (75.09)	0.99 (0.01)
WS	0.05	-0.0325	262.65 (182.61)	-537.44 (289.35)	0.95 (0.05)
CG	0.0177	-0.014	444.98 (240.45)	-432.81 (377.14)	0.20 (0.08)
HP	0.03	-0.0006	60.92(104.08)	-50.44 (152.18)	0.97 (0.03)

Predicted DBH and stem biomass (Kg tree^{-1}) from validations (tree and regional) and fitting were compared. Table 5.3 shows average DBH and stem biomass (Kg tree^{-1}) estimated at age 60 for each species. Figures 5.2 and 5.3 illustrate average DBH and stem biomass, respectively, predicted for each species from age 1 to 60. DBH and biomass at 60 were similar for local validation and fittings, and significantly different for the regional validation, except for HP, which presented similar values for tree-specific fitting, local, and regional validations (Table 5.3; see Appendix B, Figure B1 and B2 for tree-specific DBH and biomass estimates, respectively, from the year 1 to year 60).

Table 5.3 - Average DBH and tree stem biomass at the age of 60 for each species for tree fitting, local and regional validations. Note: The standard deviation for tree fitting, local, and regional value validations are listed beside each calculation in parentheses.

		Green ash	Scots pine	Manitoba maple	White spruce	Caragana	Hybrid poplar
DBH (cm)	Tree	23.33(8.79)	26.5	39.13(8.32)	20.23(11.70)	16.25(4.10)	43.30(17.97)
	Local	23.40(12.44)		37.14(3.08)	20.89(10.32)	16.15(2.75)	39.34(13.53)
	Regional	44.33(16.61)	66.81	82.03(13.38)	39.15(20.47)	83.27(13.04)	41.57(5.67)
Kg tree^{-1}	Tree	183.43(133.99)	209.74	318.97(120.44)	206.94(240.82)	44.46(24.40)	652.68(583.47)
	Local	193.83(187.77)		281.85(43.30)	199.15(283.27)	35.94(2.36)	498.47(440.57)
	Regional	714.26(457.13)	1201.27	1284.67(390.91)	752.24(760.32)	2606.43(912.76)	496.94(133.74)

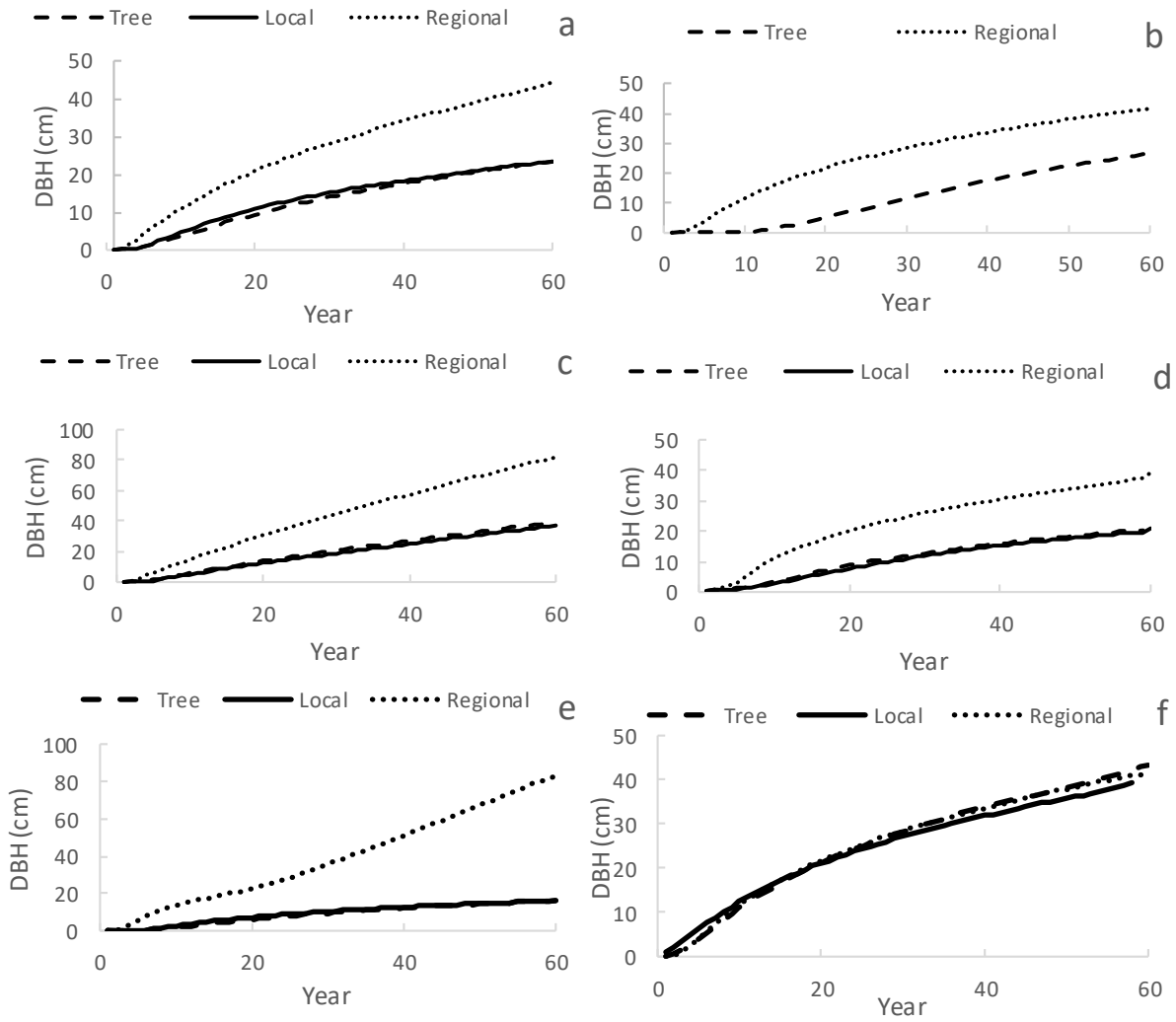

Figure 5.3 – Average (averaged over 8 runs) predicted diameters over time for each species for fitting, local, and regional validations. The trees are, a) Green ash (n=3); b) Scots pine (n=1); c) Manitoba maple (n=3); d) White spruce (n=10); e) Caragana (n=4); f) Hybrid poplar (n=8). Note: n = number of trees from each species.

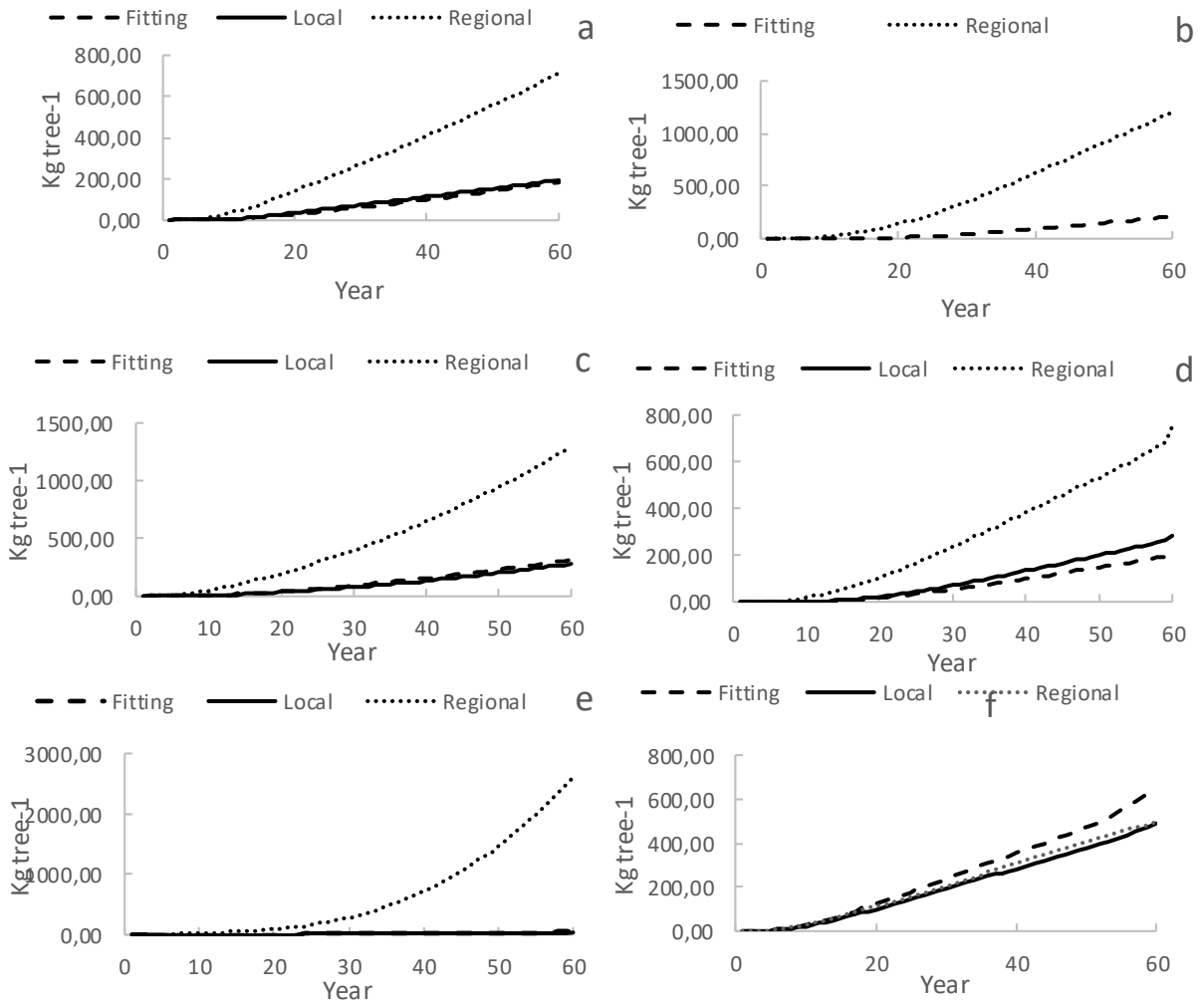

Figure 5.4 -Average (averaged over 8 runs) predicted tree biomass (kg tree^{-1}) over time for each species for fitting, local and regional validations. The trees are, a) Green ash (n=3); b) Scots pine (n=1); c) Manitoba maple (n=3); d) White spruce (n=10); e) Caragana (n=4); f) Hybrid poplar (n=8). Note: n = number of trees from each species.

5.4.3 Time validation

Table 5.4 lists the RMSE and bias for DBH estimates for every 5-year-age class from the last DBH at the bark moving back through time towards the pith. The value listed in the column refers to the age at the base of the tree, and the classes at the top row refers to the age at the DBH, so age in the column and row do not coincide. The general trend was that RMSE increased from bark to pith, for all classes from age 5 to 45. A similar and less defined trend was found for bias, even though in bias, positive and negative signals can cancel each other. Bias does not reflect the real average error, but it is useful to assess the overall trend of the method, especially

in terms of over- or under-estimation. Appendix B, Figures B3 and B4 illustrate tree-specific RMSE and bias over the classes of age. The general trend was that the older the tree, the higher the RMSE and bias.

Table 5.4 - RMSE and bias for trees at each 5-year age class into the past. Note: the number of trees used in the average calculation for that class is in parentheses. If there are no parentheses, it indicates that only one tree was used for the calculation.

	RMSE									Bias								
Age	45	40	35	30	25	20	15	10	5	45	40	35	30	25	20	15	10	5
8									10.71									6.45
12								8.07	4.91								-9.25	-3.02
13								18. 85 (2)	11.31								-142.57	-11.03
14								6.23	6.49								-5.51	-4.39
15								23.16	11.21								-52.00	-1.71
18							29.57	19.64	16.04							26.87	4.37	-13.98
20						17.08	16. 29 (2)	13.38	9.35						-23.71	-9.18	-12.78	-8.90
21						24.42	21.45	10.44	9.22						31.24	20.27	1.20	-8.22
23						24.13 (2)	18.50	11.05	11.48						23.73	14.80	-0.21	-9.04
25					11.39	39.39 (2)	33.12	29.32	24.65					11.18	-58.24	-30.29	-21.97	-14.42
26							21.09	12.44	7.26							-45.78	-9.64	5.19
28					7.63	7.11	6.84	5.48	4.26					-5.60	-5.54	-5.01	-2.00	3.49
29					16.00 (2)	10.76	9.01	8.59	8.38					-88.02	-9.39	-4.60	-2.37	-0.17
30				20.85 (2)	17.07	14.89	12.88	12.17	12.70				9.93	-14.34	-12.31	-8.22	-4.80	-1.83
36						22.33	12.76	8.85	10.32						-42.14	-5.69	6.80	9.91
39			22.53	21.20	19.00	17.70	17.60	19.25	22.49			-26.48	-13.05	-2.61	4.29	10.84	16.89	22.05
43		31.11	29.33	25.59	21.04	16.52	12.59	9.45	2.84		33.09	29.56	24.05	18.76	13.86	9.43	5.10	-2.78
46		12.60	11.20	8.85	6.68	5.81	6.06	5.62	4.03		20.88	10.70	3.41	-1.62	-5.00	-6.05	-5.65	-4.03
47		34.28 (2)	24.32	19.75	16.01	13.34	11.23	9.41	8.39		-10.60	-30.96	-43.10	-17.42	-12.27	-9.98	-8.17	-6.55
48					13.57	4.44	2.74	2.89	3.30					-26.81	-2.25	0.96	0.89	-0.26
49	14.4	13.71	12.88	12.53	12.34	12.76	13.79	14.95	15.20	-0.71	9.32	10.18	6.35	1.98	-2.32	-5.50	-8.12	-9.66
56		6.63	5.32	4.65	4.74	4.88	5.22	5.38	5.76		-2.95	-1.28	-3.56	-3.83	-4.14	-5.02	-5.28	-5.73
Average	14.44	16.01	17.60	15.43	12.95	13.23	14.65	11.79	10.01	-0.71	9.95	-1.38	-2.28	-11.67	-6.95	-3.07	-12.15	-2.66

5.4.4 Correlation between alpha, RMSE, bias and R^2 and stand characteristics

Correlation between number of trees per hectare, full canopy age, age, spacing, mean annual increment, and the fitting alpha, were calculated for each species and for all species together (Table 5.5). Figure 5.4 illustrates the regression analysis between alpha and the number of trees per hectare, full canopy age, age, spacing, mean annual increment per species and for all species together. Scots pine was not used in this analysis because there was just one tree. Overall, alpha had a significant (< 0.05) positive correlations with MAI, illustrated by all species trendline slopes on Figure 5.4. A positive correlation between alpha and MAI means that the higher the tree growth rate, the greater the alpha. Overall, alpha showed a low and negative correlation with age, number of trees, and spacing. This negative correlation with age and N, although not statistically significant, are still illustrated by GA, WS, HP, and MM trendlines (Figure 5.4). This overall negative, low, and not significant correlation between alpha and spacing is overshadowed by MM and HP positive, higher, and significant (for HP) correlation between spacing and alpha (see MM and HP trendlines in Figure 5.4). Positive correlations between spacing and alpha are biologically reasonable, since the wider the tree growth spacing, the higher the tree growth rate. HP's significant positive correlation between alpha and FCA, and

alpha and spacing corroborates that the wider the spacing, the longer the tree will take to reach its canopy closure age. The older the tree and the more closely spaced the planted trees were, the less the tree grows.

Table 5.5 - Correlation between N (number of trees per hectare), FCA (full canopy age), Age, Spacing, and MAI (mean annual increment in DBH) and alpha for green ash, Manitoba maple, white spruce, caragana and hybrid poplar trees sampled in SK, Canada. Note: correlation significance is in (brackets); Values significant above 0.05 are in **bold;** n = number of trees for each species.

Species (n)	N	FCA	Age	Spacing	MAI
Green ash (3)	0.54(0.63)	-0.73(0.47)	**-1(0.02)**	-0.65(0.54)	0.98(0.10)
Manitoba maple (3)	-0.34(0.77)	0.24(0.84)	0.39(0.74)	0.43(0.71)	0.57(0.60)
White spruce (10)	-0.05 (0.89)	-0.03(0.93)	-0.32(0.36)	-0.03(0.95)	**0.79(0.005**)
Caragana (4)	0.47(0.53)	-0.25(0.74)	-0.14(0.85)	-0.13(0.86)	0.62(0.37)
Hybrid poplar (8)	-0.59(0.12)	**0.70(0.05)**	0.07(0.86)	**0.65(0.04)**	0.26(0.51)
Overall	-0.04(0.80)	0.01(0.97)	-0.25(0.20)	-0.13(0.50)	**0.63(0.003)**

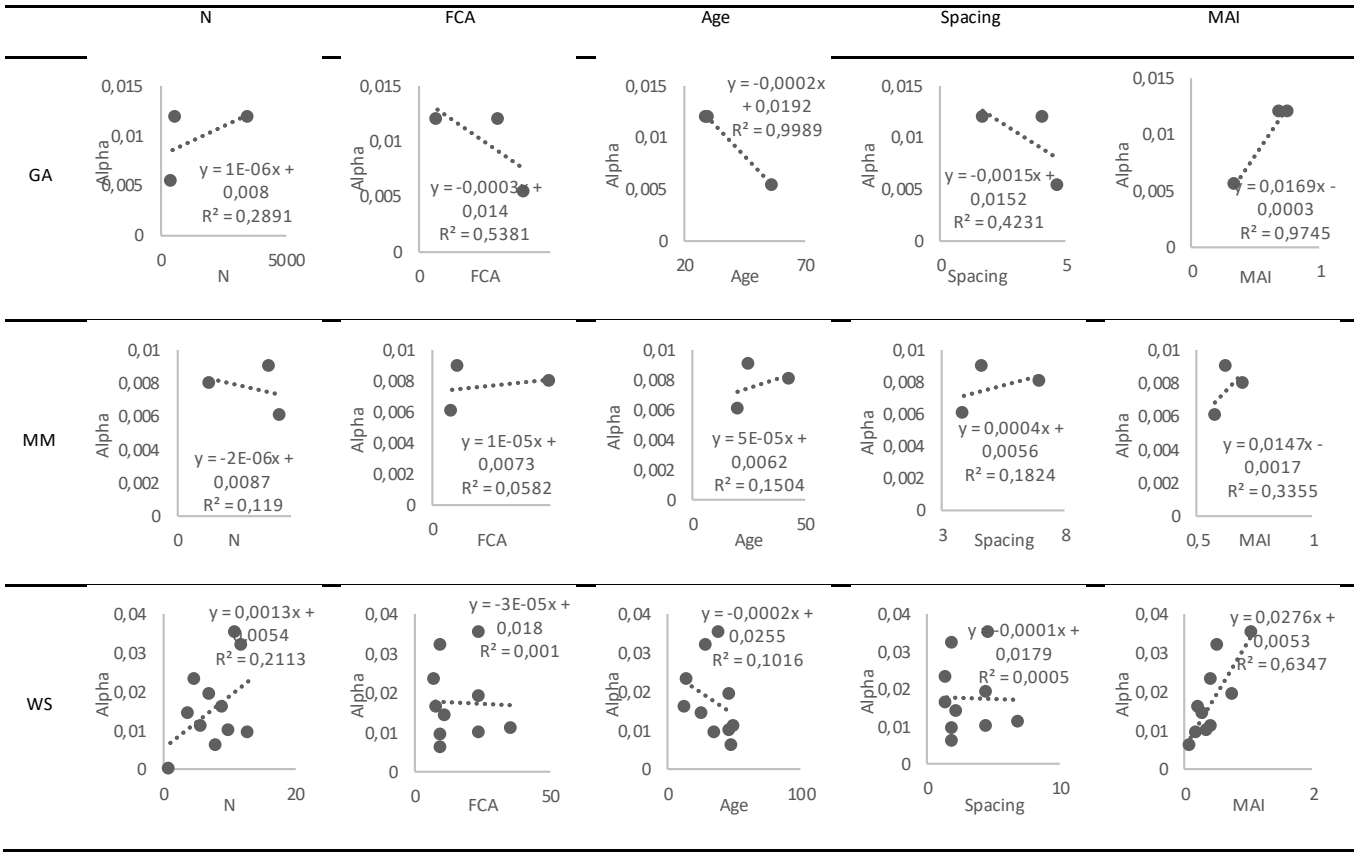

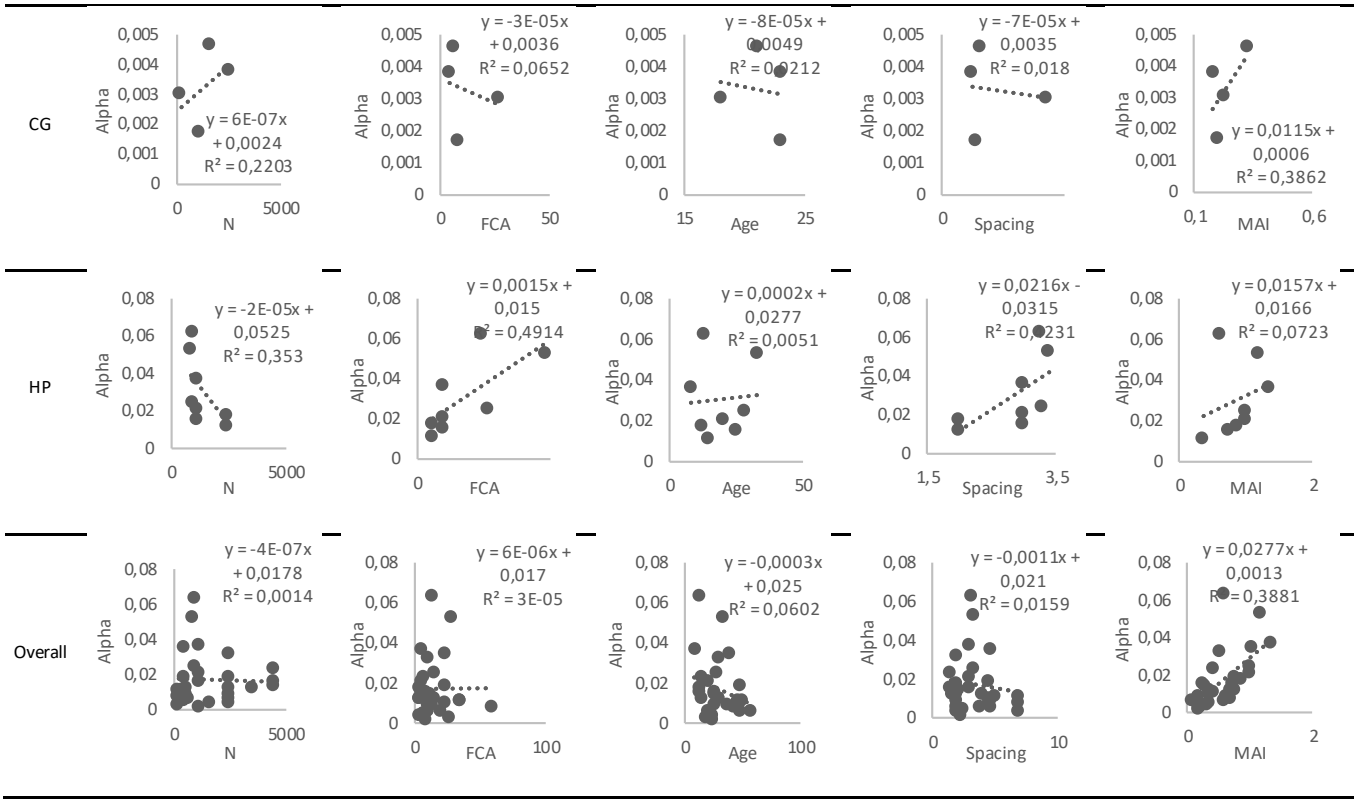

Figure 5.5 - Alpha versus N (number of trees per hectare), Alpha versus FCA (full canopy age), Alpha versus AGE, Alpha versus spacing, and Alpha versus MAI (mean annual DBH increment) for green ash (GA), Manitoba maple (MM), white spruce (WS), caragana (CG) and hybrid poplar (HP) trees sampled in SK, Canada.

5.5 Discussion

5.5.1 Fitting

The 3-PG model was able to fit the radial growth of all 29 trees, except for two individual trees, a 25-year-old Manitoba maple and a 26-year-old white spruce tree. If these two trees are excluded, the average RMSE, bias and R^2 were 17.2, -18.43 and 0.96 respectively, which is considerably lower than the respective 50 and 30 maximum RMSE and bias, found by Amichev et al., (2017) who fitted 3-PG for the same shelterbelt species in the same province. The lowest R^2 was 0.87 for caragana, which agrees with Amichev et al., (2017), who also found the lowest R^2 for the caragana species across the same six species. One factor that may be related to the uncertainty for caragana is that the famers frequently trim/cut caragana at their base, and the species is able to grow again from the rootstock. As a result, the root system may have a different age from their above-ground component, which may be one cause for more uncertainty in

growth, and subsequently their depiction in lower quality modeling when compared to other species.

5.5.2 Tree-specific vs Local-specific vs regional-specific modelling

Alpha values greatly affected 3-PG precision. Determining the appropriate alpha value for each tree yielded the lowest RMSE and bias, however, using local-specific alpha values within a given species also yielded acceptably low RMSE and bias, and similar DBH and biomass estimates (Table 5.2). No study has validated the alpha parameters as this study has, but some have tested a model's performance across a wider geographic range. For example, Landsberg et al., (2003) assessed 3-PG performance by R^2 and bias when the model was validated using the same database (data from the same site but under different treatments, and data from different locations). They found that in all cases, the model produced unbiased estimates. Gonzalez-benecke et al., (2014) fitted 3-PG to *Pinus taeda* in the USA and validated it using data from Uruguay and found agreement between fitting and validation. Tickle et al., (2001) fitted 3-PG SpatialT™ for a forest in Australia and found a small divergence between R^2 and standard error between calibration and validation for volume (0.31 to 0.67 and 243 to 174, respectively), but higher for DBH (0.77 to 0.54 and 70 to 85, respectively), and stocking (0.97 to 0.53 and 103 – 357, respectively). Some studies have tested the effect of alpha using a sensitivity analysis. For example, Esprey et al., (2004) found that varying alpha by 0.04 yielded volume divergence of 100 m^3 ha^{-1}. Amichev, Bentham, Kurz, et al., (2016) studying white spruce conducted a sensitivity analysis and found that varying alpha by 40% impacted biomass volume by 49.5%.

In this study, alpha values affected the outputs as well. The larger the divergence between the alpha parameter at the initial fitting and the alpha value used during validation, the greater were the RMSE and bias (cf. Dif, Table 5.2). For example, for WS, the difference between the fitting alpha value and the local-validation alpha value was -0.002, and the RMSE and bias were 114.07 and -94.12, respectively. For the regional validation, the difference between the fitting alpha and the validation alpha was higher (-0.033) and the RMSE and bias were 262.65 and -537.44, respectively, almost ten times the RMSE and bias at fitting, 23.75 and -65.19, respectively (Table 5.2).

HP presented similar alpha values for fitting, site and literature validations, resulting in relatively low RMSE and bias in the subsequent local and regional validation calculations. This

is probably a result of HP being a species with a greater natural geographic range that is well adapted to a larger part Saskatchewan (Joss et al. 2008), so the alpha value was similar from site to site. Alternatively, GA presented much higher differences between the calculated alphas, and hence higher RMSE and biases at validation. This is probably a result of its narrower natural geographic range, found growing towards the southern part of the province nearer to the USA border (Lowe and Greene, 1989; Wright, 1960), and is only growing north of this natural range because it was specifically planted there as a shelterbelt species.

5.5.3 Time

RMSE and bias increased from the bark towards the pith through a cross section. This is probably a result of the method used to retrieve DBH (Chapter 4) accumulates error through time, from the bark to the pith. As the area around the pith is older, errors accumulated towards the pith. The older the tree and the closer the ring is to the pith, the greater the chance of more biased 3-PG estimates. Even though this was a general trend for all species, it varied from tree to tree, and from species to species. For example, for SP, RMSE increased after 30 years towards the past (Appendix Figure B3b). For WS, the errors in the classes of age were fairly homogeneous over the years (Appendix Figure B3d). For HP there was an increase in RMSE after 30 years into the past as well, but it was for only one tree (Appendix Figure B3f).

5.5.4 Correlation

In general, alpha was positively correlated to MAI (Table 5.5 and Figure 5.4), meaning that the higher the tree's growth rate, the higher the alpha parameter. The alpha parameter tended to illustrate a negative correlation with age, meaning that the older the tree got, the lower its growth rate became, and the lower its alpha value was going to be. Spacing and FCA tended to be positively correlated to alpha (for MM and HP), so the greater the spacing, the greater the alpha. In wider spacing (low N), trees take longer to affect each other's growth because they will take longer to inter-compete with each other for available resources, so their alpha's will start to be affected by this parameter only later in a tree's life.

These correlations indicates that the main tree attribute related to alpha is growth rate. Years ago, a decreasing growth rate was believed to be caused by higher respiration rates due to increasing biomass (Kimmins, 1997; Barnes et al., 1998). It is now known that growth rate is more closely related to a tree's efficiency to produce leaves, to overcome competition, to reach the canopy closure age later, and to face reduced photosynthesis due to lower stomatal

conductance, which in turn is related to the hydraulic conditions of its vascular system (Smith & Long 2001; Binkley et al. 2002; Yoder et al., 2014). By more fully understanding the relationship between alpha and these specific tree attributes related to growth rates, alpha ranges can be better estimated site- and species-specifically for improved 3-PG predictions.

5.6 Conclusion

This study reveals that the alpha parameter in the 3-PG model needs to be tree- or locally-fitted within the same species to achieve the most precise modelling estimates, as hypothesized. Tree-specific fitting was compared to data measured directly from trees, generating accurate RMSE, bias and R^2 values. A literature review revels this study is the first time that an agroforestry system has had its DBH and biomass modeled with such a specific focus. Tree-specific fitting was validated across varying scales, at both local and regional levels. This was done as an important mechanism to check the reliability of modeling these factors beyond the scope of an individual tree, and to test the practical use of the method on a farm and regional geographic scale. By showing that the most precise estimates are tree- and site-specific, it implies that the factors affecting tree growth varies from site to site within the same region, and therefore, precise tree growth and carbon stock modeling is necessary at the same tree- or local-spatial scales, and cannot be adequately scaled up.

The localized modeling performed in this study also allows a farm to create a specific carbon footprint at the same scale. Such a farm-specific carbon footprint would support a range of new economic and global warming mitigation policies. This could motivate the creation of carbon markets encouraging producers to diversify their economy while reducing their emissions. It would allow for policies to reward producers for long-term carbon sequestration on their land, which would help offset the negative effects of current carbon pricing policies. Such a policy would increase shelterbelt planting, enhancing a suite of environmental benefits, and ultimately increase carbon sequestration across the entire provincial landscape of Saskatchewan. Even though the regional estimates can be seen as precise as well as depended upon at certain scales, in the case of using these estimates to support farm-level policies, its use is not recommended. In the case of a rewarding or a carbon market policy, each landowner should be affected individually, so the local-specific fitting is more appropriate in precision, because it better describes values for a given farm.

This study's data illustrates that 3-PG modeling reliance varies, being the most accurate for the years near the bark and less accurate for those years near the pith, as set out in the initial hypothesis. In general, the 3-PG model is trustworthy for farm-specific carbon stock estimates over time, which is advantageous. The advantage of using 3-PG is that it accounts for the ongoing environmental changes in space and in time, which makes 3-PG modeling reliable for a specific location, independent of the time-frame. This is first, because 3-PG modeling accounts for the many constantly changing environmental variables related to tree growth, which are not commonly used in most models of this type. Second, it adds to a total carbon footprint analysis on a per farm basis, which would support policies rewarding landowners for carbon sequestration. Such a policy would motivate individuals to plant trees and/or take better care of their existing trees, all of which would bring more hope for combating climate change and providing a better life for the next generations.

CHAPTER 6

CONCLUSIONS

This study bridged historical, theoretical, and practical facets of carbon assessments within agroforestry shelterbelt systems. It developed a sound footing on how and why shelterbelt systems in Canada have been grown in the past, and how these systems could be used as part of a carbon accounting system moving forward. It developed an easy and precise method to retrieve past tree growth diameters using increment cores from a single visit, and also explored the various error terms that are inherent within this process. It then validated these DBH data when they were subsequently used as input variables within a hybrid forestry model, program 3-PG. As a result, I provided a means to retrieve DBH and BA increments through time using increment cores along with a better understanding of the average errors associated with the calculations. I found that growth information from increment cores can be trusted as input variables for runs in the 3-PG model, and tree- or local-specific fitting yielded very sound estimates of growth in the past. I next summarize my main findings and discuss the implications of this study's outcomes in the context of climate change adaptation towards a more sustainable agricultural system, sequestering more carbon.

6.1 Shelterbelt's role in combating climate change

The relevance of shelterbelts, and the environmental services that they provide, including raising crop yields, protecting soils from erosion, and especially sequestering carbon is evidenced in this study (Chapter 2 and 3). Researchers from across the globe are starting to acknowledge the benefits of implementing shelterbelt systems, which was demonstrated by the rising pace of shelterbelt research over the years compared to the body of agricultural and forestry research and their publications. Conversely, farmers have not seen as many benefits, and have shifted from a trend of implementing shelterbelts up to the early 2000s, to a trend of removal since this time (Ha et al., 2019; Amichev et al., 2020b). Removals imply that the carbon previously sequestered in the system, will slowly dissipate back into the atmosphere, and the tonnes of carbon that were removed by the trees and their soil matrix has ended. This liberated carbon will now start to be released back into the atmosphere through decomposition and gas exchanges, which will begin to again affect global climates.

Climate change is affecting the entire planet, so combatting its negative effects has to be coordinated at a high level by governments. As stressed in Chapter 3, the 1901 federal initiative that created a program to initiate shelterbelt systems on the landscape was ultimately successful. Farmers initially implemented shelterbelts for crop yields, protection against wind, and to mitigate drought effects, but now these same shelterbelt systems could be the backbone of a carbon sequestration program that no one is currently monitoring. The Canadian federal government is starting to take actions to promote carbon sequestration and reduce emissions, such as launching research funding aimed at climate change mitigation (e.g., AGGP), and by implementing national policies such as the carbon tax. But these federal moves do not currently seem to be enough to bring attention to the benefits that are already growing in shelterbelts across the landscape, or to try to suppress their removal. Other actions are needed.

Solutions for this removal issue are pointed out in this study in Chapter 3, for example, by raising awareness of shelterbelt importance to motivate further tree planting. To have an even more effective outcome, farmers should be rewarded for cultivating trees and sequestering carbon. By being able to trade a positive GHG balance in a local market, and or by receiving an incentive from governments (such as a tax credit), farmer would start to care more about the carbon that is already being sequestered by their trees. To support any of these options, a highly accurate and practical method of calculating farm-specific carbon footprints is necessary. This is what was explored in this study in Chapters 4 and 5 (see Appendix C for practical details and guidance when applying the methods described in Chapter 4 and 5).

6.2 Farm-specific carbon footprints

To determine farm-specific carbon footprints, the first step a policy would need, is to be able to calculate tree growth through time; the second step it would need, is to then be able to use this growth farm-specifically to calculate how much carbon was sequestered at a given location. Chapter 4 provided a means to retrieve past DBH and BA growth from increment cores over all of the years of a tree's life. This is seen as an import step for modeling, as along with growth information, the error that the calculations yield can also be established. Reporting the error gives a better perspective surrounding any uncertainty and helps to illustrate the dependability of the method used. Being able to precisely retrieve growth values from increment cores from a single visit is an important milestone for two main reasons. First, it avoids relying on the many time- and money-consuming annual DBH inventory campaigns that would be required to acquire

the same information. Second, it allows more data sources to be incorporated into models, such as data from the International Tree Ring Data Bank (ITRDB), and any living (and in some cases, dead) tree that produced annual rings at a given location.

6.3 Does reliable data make reliable models?

Chapter 5 accomplished the second step of calculating farm-specific carbon footprints, which was modeling tree growth farm-specifically, based on climate scenarios, species, and management factors. Specifically, Chapter 5 achieved two important milestones. First, it proved that increment core-related input data yielded reliable modeling data. It implies that a broader range of potential data can be used for carbon stock modeling, instead of just traditional periodic DBH measurements. By creating better models, it allows for a better understanding of which environmental conditions, management regimes, and specific species of tree would optimize carbon sequestration at a given location. Second, fitting a farm-specific model was proven to be the most precise model available, which assures that farm-specific carbon footprint calculated in the manner of this study, is trustworthy. Reliable farm-specific carbon footprints could support the idea of local carbon markets, and/or policies rewarding carbon sequestration. If such a policy and/or such a market were developed, overall GHG emissions would drop from more sequestered carbon, with those affects felt not only locally, but also globally.

6.4 Implications of this study

This study's findings have special implication for agroforestry systems, especially those shelterbelt trees grown in Canada and in the U.S.A. Despite their high carbon sequestration potential, and their crucial importance in reducing emissions in the agricultural sector, these trees are almost never measured in any type of inventories (Perry et al., 2009; Amichev et al., 2020b). All this despite their common position across the landscape (60,633km of existing shelterbelts in SK (Amichev et al., 2015)). Now that data can be accurately retrieved through time within predictable ranges of deviations, models estimating both past and future shelterbelt growth can be fitted with this derived data from shelterbelts, making agroforestry modeling more trustworthy. More accurate fitting and accurate models would be a significant achievement, given that most models used for agroforestry-grown trees, were fitted with data from forest-grown trees (Perry et al., 2009; Schoeneberger, 2009). More accurate shelterbelt modeling allows for a better understanding and subsequently, forecasting, of shelterbelt growth under different climatic scenarios based on the different emission levels and management regimes. By

forecasting growth under different scenarios, tree carbon sequestration can be optimized by selecting the best species, best area, and best management practices, which would make shelterbelts an even more powerful tool to combat climate change (Davis et al., 2013; Howat, 2020; Amichev et al., 2020a).

Having a high level of accuracy in shelterbelt growth modeling also means that agroforestry can now be further incorporated into global warming mitigation planning and be a key factor in policies that reward carbon sequestration. Such policies and the possibility to trade sequestration credits in an open market would motivate farmers to keep and plant new shelterbelts on their lands, and potentially stop the trend of removing shelterbelts (Rempel et al., 2014; Ha et al., 2019; Amichev et al., 2020b). Such rewards would boosts carbon sequestration in rural areas, making food production more sustainable without taking land out of agricultural production (Humpenöder et al., 2016). This would create a more diversified farm economy by creating another means of income (Schoeneberger, 2009), rather than just having current commodities available to a landowner, such as crops and cattle (Strange & Brandle, 2006; Ehni, 2012; Amichev et al., 2020b, 2020b).

Past events have shown that the federal government has the power to revert the current trend of shelterbelt removal and turn it into shelterbelt planting, if the right tools and benefits are provided to landowners. For example, from 1901 to 2013, the government provided technical support and free seedlings to farmers, and as a result, over 600 million trees were planted in the prairies of Saskatchewan and today sequester at least 10.8 Tg C (Amichev et al., 2015; Amadi et al., 2016). As more land is now being required for food production, shelterbelts are being removed, and their sequestration benefits are being underestimated by landowners (Rempel et al., 2014, 2017). Still, there remains a lot of area available and suitable for shelterbelt implementation. For example, just in Saskatchewan, 8.76, 7.90, and 9.77 million ha were identified as suitable for deciduous, coniferous, and shrub shelterbelts, respectively. Eighty percent of this land was identified as being above-average in suitability, indicating that it has a high carbon sequestration potential for shelterbelt implementation, that could be added to the margins of many fields (Amichev et al., 2020a).

There are suitable and available lands in Saskatchewan to implement shelterbelts, sequester carbon, and potentially diversify the farm economy. As a complement, there is a shelterbelt decision support system (DSS) [shelterbelts-sk.ca], which is fed with data from this

study and others, all financed by AGGP. The DSS provides information about land and species suitability, ideal spacing, carbon stock changes through time, and maintenance techniques according to each farmer's goal. The DSS can also serve as a tool for both farmers as well as policy makers, allowing each to plan and manage shelterbelts, and to potentially establish federal and/or provincial incentive policies for landowners.

The essentials knowledge on how to sequester more carbon by using shelterbelts is known. There are available and suitable lands to plant even more shelterbelts, and the academic tools needed to assist and guide farmers in implementing and maintaining shelterbelts already exists. With farmers becoming more aware that their actions can assist in combating global warming, society just needs another federal or provincial intervention program to implement such a policy. In this way Canada would sequester more carbon in rural agricultural areas, have a greener agricultural sector, and most importantly, serve as a leading example for the rest of the world in innovative ways to sequester carbon.

REFERENCES

Aggarwal, P., Vyas, S., Thornton, P., & Campbell, B. M. (2019). How much does climate change add to the challenge of feeding the planet this century? *Environmental Research Letters*, *14*(4), 1-11.

Agriculture and Agri-Food Canada. (2008). Circling the Globe with Tree, retrieved on December 2, 2020 from www.agr.gc.ca/shelterbelt

Agriculture and Agri-Food Canada (2015). Shelterbelt Planning and Establishment, retrieved on October 6, 2019 from http://www.agr.gc.ca/eng/science-and-innovation/agricultural-practices/agroforestry/shelterbelt-planning-and establishment/?id=1344636433852

Agriculture and Agri-Food Canada (2019). Agricultural Greenhouse Gases Project, retrieved October 6, 2019 from http://www.agr.gc.ca/eng/programs-and-services/agricultural-greenhouse-gases-program/?id=1461247059955

Ahmed, M., Wahab, M., Khan, N., Muhammad, F.S., Uzair Khan, M., & Tariq Husain, S. (2009). Age And Growth Rates Of Some Gymnosperms Of Pakistan: A Dendrochronological Approach. *Pak. J. Bot.*, 41(2), 849-860.

Akachuku, A.E., & Abolarin, D.A.O. (1989). Variations in pith eccentricity and ring width in teak (Tectona grandis L. F.). *Trees*, 3, 111–116.

Albrecht, A., & Kandji, S. T. (2003). Carbon sequestration in tropical agroforestry systems. *Agriculture, Ecosystems and Environment*. 99(1-3), 15-27.

Alexander, M.R., Rollinson, C.R., Babst, F., Trouet, V., & Moore, D.J.P. (2018). Relative influences of multiple sources of uncertainty on cumulative and incremental tree-ring-derived aboveground biomass estimates. *Trees*, 32, 1–12.

Alexandre, P.M. de M. (2009). Calibração do modelo 3-PG para povoamentos de pinheiro bravo (*Pinus pinaster*) em Portugal. M. S. dissertation. Universidade Tecnica de Lisboa, Lisboa, Portugal.

Allen, R.B. (1988). A forest succession in the Catlins ecological region, south-east Otago, New

Zealand. *N. Z. J. Ecol.*, 11, 21–29.

Almeida, A.C., J.J. Landsberg, and P.J. Sands. (2004). Parameterisation of 3-PG model for fast-growing Eucalyptus grandis plantations. *For. Ecol. Manage.* 193(1–2): 179–195

Altman, J., Doležal, J., Černý, T., & Song, J.S. (2013). Forest response to increasing typhoon activity on the Korean peninsula: Evidence from oak tree-rings. G*lob. Chang. Biol.*, 19, 498–504.

Altman, J., Doležal, J., & Čížek, L. (2016). Age estimation of large trees: New method based on partial increment core tested on an example of veteran oaks. *For. Ecol. Manage.*, 380, 82–89.

Amadi, C.C., van Rees, K.C.J., & Farrell, R.E. (2016). Soil-atmosphere exchange of carbon dioxide, methane and nitrous oxide in shelterbelts compared with adjacent cropped fields. *Agric. Ecosyst. Environ*. 223, 123–134.

Amadi, C. C., Farrell, R. E., & Van Rees, K. C. J. (2017). Greenhouse gas emissions along a shelterbelt-cropped field transect. *Agriculture, Ecosystems and Environment*, *241*, 110–120.

Amichev, B.Y., Johnston M., & K.C.J. Van Rees. (2010). Hybrid poplar growth in bioenergy production systems: Biomass prediction with a simple process-based model (3PG). *Biomass and Bioenergy* 34(5): 687–702.

Amichev, B.Y., Hangs, R. D., & K.C.J. Van Rees. (2011). A novel approach to simulate growth of multi-stem willow in bioenergy production systems with a simple process-based model (3PG). *Biomass and Bioenergy* 35(1): 473–488.

Amichev, B. Y., Bentham, M. J., Cerkowniak, D., Kort, J., Kulshreshtha, S., Laroque, C. P. & Van Rees, K. C. J. (2015). Mapping and quantification of planted tree and shrub shelterbelts in Saskatchewan, Canada. Agroforestry Systems, 89(1), 49–65.

Amichev, B.Y., Bentham, M.J., Kulshreshtha, S.N., Laroque, C.P., Piwowar, J.M., & Van Rees, K. (2016). Carbon sequestration and growth of six common tree and shrub shelterbelts in Saskatchewan, Canada. *Canadian Journal of Soil Science*, 97, 368–381.

Amichev, B.Y., Laroque, C.P., Belcher, K.W., Bentham, M.J., & Van Rees, K.C.J., (2020a). Shelterbelt systems establishment in Saskatchewan, Canada: a multi-criteria fuzzy logic approach to land suitability mapping, *New Forests*, 51, 933-963.

Amichev, B.Y., Laroque, C.P., & van Rees, K.C.J. (2020b). Shelterbelt removals in Saskatchewan, Canada: implications for long-term carbon sequestration. *Agrofor. Syst.* 94, 1665–1680.

Amichev, B. Y., Bentham, M. J., Kurz, W. A., Laroque, C. P., Kulshreshtha, S., Piwowar, J. M., & van Rees, K. C. J. (2016). Carbon sequestration by white spruce shelterbelts in Saskatchewan, Canada: 3PG and CBM-CFS3 model simulations. *Ecological Modelling*, 325, 35–46.

Anstey, T.H. (1986). One Hundred Harvests. Agriculture and Agri-Food Canada, Ottawa.

Applequist, M.B. (1958). A Simple Pith Locator for Use With Off-Center Increment Cores 0–5.

Babst, F., Alexander, M.R., Szejner, P., Bouriaud, O., Klesse, S., Roden, J., Ciais, P., Poulter, B., Frank, D., Moore, D.J.P. (2014a). A tree - ring perspective on the terrestrial carbon cycle *Oecologia*, 307–322.

Babst, F., Bouriaud, O., Alexander, R., Trouet, V., &Frank, D. (2014b). Toward consistent measurements of carbon accumulation: A multi-site assessment of biomass and basal area increment across Europe. *Dendrochronologia* 32, 153–161.

Babst, F., Bouriaud, O., Papale, D., Gielen, B., Janssens, I.A., Nikinmaa, E., Ibrom, A., Wu, J., Bernhofer, C., Köstner, B., Grünwald, T., Seufert, G., Ciais, P., Frank, D. (2014c). Above-ground woody carbon sequestration measured from tree rings is coherent with net ecosystem productivity at five eddy-covariance sites. *New Phytol.* 201, 1289–1303.

Bakker, J.D. (2005). A new, proportional method for reconstructing historical tree diameters. *Can. J. For. Res.* 35, 2515–2520.

Baldocchi, D.D., & Amthor, J. S. (2001). Canopy Photosynthesis: History, Measurements, and Models. Academic Press.

Baldwin, C. S. (1988). The influence of field windbreaks on vegetable and specialty crops. *Agriculture, Ecosystems and Environment*, 22–23, 191–203.

Barnes, B.V., Zak, D.R., Denton, S.R., Spurr, S. (1998). Forest ecology. New York: Wiley.

Barry, D. (2014). Refining dendrochronology to evaluate the relationship between age and diameter for dominant riparian trees in the Redwood Creek watershed. M. S. thesis. Universsity of San Francisco.

Barthélémy, D., & Caraglio, Y. (2007). Plant Architecture: A Dynamic, Multilevel and Comprehensive Approach to Plant Form, Structure and Ontogeny. *Ann. Bot.* 99, 375–407.

Batish, D. R., Kohli, R. K., Jose, S., & Singh, H. P. (1976). *Ecological Basis of Agroforestry*. Taylor and Francis Group. *Spring* (72). 400 p.

Battaglia, M., & P.J. Sands. (1998). Process-based forest productivity models and their application in forest management. *Forest Ecology and Management*, 102(1), 13-32

Bayer, C., Martin-Neto, L., Mielniczuk, J., Pavinato, A., & Dieckow, J. (2006). Carbon sequestration in two Brazilian Cerrado soils under no-till. Soil and Tillage Research, 86(2), 237–245.

Beach, R. H., DeAngelo, B. J., Rose, S., Li, C., Salas, W., & DelGrosso, S. J. (2008). Mitigation potential and costs for global agricultural greenhouse gas emissions. *Agricultural Economics*, *38*(2), 109–115.

Beck, P.S.A., Juday, G.P., Alix, C., Barber, V.A., Winslow, S.E., Sousa, E.E., Heiser, P., Herriges, J.D., & Goetz, S.J. (2011). Changes in forest productivity across Alaska consistent with biome shift. *Ecol. Lett.*, 14(4), 373-379

Bennetzen, E. H., Smith, P., & Porter, J. R. (2016). Decoupling of greenhouse gas emissions from global agricultural production: 1970-2050. *Global Change Biology*, *22*(2), 763–781.

Bergin, D.O., & Kimberley, M.O. (2012). Reliability of increment core growth ring counts as estimates of stand age in totara (Podocarpus totara D.Don). *New Zeal. J. For. Sci.* 42, 131–141.

Biging, G.S., & Wensel, L.C. (1988). Estimation of basal area and basal area increment of coniferous trees. *Nature Proceedings*. 1-26.

Binkley, D., Stape, J. L., Ryan, M. G., Barnard, H. R., & Fownes, J. (2002). Age-related decline in forest ecosystem growth: an individual-tree, stand-structure hypothesis. *Ecosystems*, 5(1), 58-67.

Biondi, F. (1999). Comparing tree-ring chronologies and repeated timber inventories as forest monitoring tools. *Ecol. Appl.* 9, 216–227.

Bizikova, L., Larkin, P., Mitchell, S., & Waldick, R. (2019). An indicator set to track resilience to climate change in agriculture: A policy-maker's perspective. *Land Use Policy*, *82*, 444–456.

Bouriaud, O., & Popa, I. (2009). Comparative dendroclimatic study of Scots pine, Norway spruce, and silver fir in the Vrancea Range, Eastern Carpathian Mountains. *Trees*, 3, 95–106.

Boyce, J. K. (2018). Carbon Pricing: Effectiveness and Equity. *Ecological Economics*, 150, 52–61

Brandle, J. R., Hodges, L., & Zhou, X. H. (2004). Windbreaks in North American agricultural systems. *Agroforestry Systems*. 61–62, 65–78.

Brienen, R.J.W., Gloor, E., & Zuidema, P.A. (2012). Detecting evidence for CO_2 fertilization from tree ring studies: The potential role of sampling biases. *Global Biogeochem*, 26(1), 1-13.

Brienen, R.J.W., & Zuidema, P.A. (2006). The use of tree rings in tropical forest management: Projecting timber yields of four Bolivian tree species. *For. Ecol. Manage*. 226, 256–267.

Bush, E., & Lemmen, D. (2019). *Canada's Changing Climate Report*. Ottawa.

Campi, P., Palumbo, A. D., & Mastrorilli, M. (2009). Effects of tree windbreak on microclimate and wheat productivity in a Mediterranean environment. *European Journal of Agronomy*, 30(3), 220–227.

Carlson, K. M., Gerber, J. S., Mueller, N. D., Herrero, M., MacDonald, G. K., Brauman, K. A., … West, P. C. (2017). Greenhouse gas emissions intensity of global croplands. *Nature Climate Change*, *7*(1), 63–68.

Carroll, Z. L., Bird, S. B., Emmett, B. A., Reynolds, B., & Sinclair, F. L. (2004). Can tree shelterbelts on agricultural land reduce flood risk. *Soil Use and Management*, *20*, 357–359.

Chu, X., Zhan, J., Li, Z., Zhang, F., & Qi, W. (2019). Assessment on forest carbon sequestration in the Three-North Shelterbelt Program region, China. *Journal of Cleaner Production*, 215, 382–389.

Clark, J.S., Wolosin, M., Dietze, M., Ibáñez, I., LaDeau, S., Welsh, M., & Kloeppel, B. (2007). Tree Growth Inference and Prediction From Diameter. *Ecol. Appl*. 17, 1942–1953.

Clark, S.L., & Hallgren, S.W. (2004). Age estimation of Quercus marilandica and Quercus stellata: applications for interpreting stand dynamics. *Can. J. For. Res*. 34, 1353–1358.

Cleugh, H. A. (1998). Effects of windbreaks on airflow, microclimates and crop yields. *Agroforestry Systems*, 41(1), 55–84.

Colbert, J.J., Schuckers, M., Fekedulegn, D., Rentch, J., MacSiúrtáin, M., & Gottschalk, K., (2004). Individual tree basal-area growth parameter estimates for four models. *Ecol. Modell*. 174, 115–126.

Conforti, P. (2011). Looking ahead in world food and agriculture: perspectives to 2050. Food and Agriculture Organization of the United Nations (FAO).

Cortus, B. G., Jeffrey, S. R., Unterschultz, J. R., & Boxall, P. C. (2011). The Economics of Wetland Drainage and Retention in Saskatchewan. *Canadian Journal of Agricultural Economics*, *59*(1), 109–126.

Crossley, D. I. (1935). Shelterbelts for the prairies. *The Forestry Chronicle*, 11(1), 8-19.

Cuny, H.E., Rathgeber, C.B.K., Frank, D., Fonti, P., Makinen, H., Prislan, P., Rossi, S., Del Castillo, E.M., Campelo, F., Vavrčík, H., Camarero, J.J., Bryukhanova, M. V., Jyske, T., Gricar, J., Gryc, V., De Luis, M., Vieira, J., Cufar, K., Kirdyanov, A. V., Oberhuber, W.,

Treml, V., Huang, J.G., Li, X., Swidrak, I., Deslauriers, A., Liang, E., Nojd, P., Gruber, A., Nabais, C., Morin, H., Krause, C., King, G., & Fournier, M. (2015). Woody biomass production lags stem-girth increase by over one month in coniferous forests. *Nat. Plants* 1, 1–6.

Czerepowicz, L., Case, B. S., & Doscher, C. (2012). Using satellite image data to estimate aboveground shelterbelt carbon stocks across an agricultural landscape. *Agriculture, Ecosystems & Environment*, 156, 142–150

Das, P., & Horton, R. (2018). Pollution, health, and the planet: time for decisive action. *The Lancet*, *391*, 407–408.

Davis, E. L., Laroque, C. P., & van Rees, K. (2013). Evaluating the suitability of nine shelterbelt species for dendrochronological purposes in the Canadian Prairies. *Agroforestry Systems*, *87*(3), 713–727.

DeRose, R.J., Shaw, J.D., & Long, J.N. (2017). Building the forest inventory and analysis tree-ring data set. *J. For.* 115, 283–291.

Dhillon, G. S. (2016). Sequestration And Characterization Of Soil Organic Carbon For Shelterbelt Agroforestry Systems In Saskatchewan. PhD dissertation, University of Saskatchewan.

Dhillon, G. S., Gilespie, A., Peak, D., & Van Rees, K. C. J. (2017). Geoderma Spectroscopic investigation of soil organic matter composition for shelterbelt agroforestry systems. *Geoderma*, 298, 1–13.

Dhillon, G. S., & van Rees, K. C. J. (2017). Soil organic carbon sequestration by shelterbelt agroforestry systems in Saskatchewan. *Can. J. of Soil Sci.*, 97(3), 394-409

Dolph, K.L. (1981). Estimating past diameters r species Sierra Nevada. Sierra 1–4.

Duchesne, L., Ouimet, R., & Houle, D. (2002). Basal Area Growth of Sugar Maple in Relation to Acid Deposition, Stand Health, and Soil Nutrients. *J. Environ. Qual.* 31, 1676–1683.

Duncan, R.P. (1989). An Evaluation Of Errors In Tree Age Estimates Based On Increment Cores

In Kahikatea *(Dacrycarpus Dacrydioides*). *New Zeal. Nat. Sci*., 1-9.

Dunlop, A. (2000). Spatial and temporal aspects of Saskatchewan Field Shelterbelts, 1949-98 1–222. Master thesis, Geograpy department, University of Saskatchewan.

Dye, A., Plotkin, A.B., Bishop, D., Pederson, N., Poulter, B., & Hessl, A. (2016). Comparing tree-ring and Permanent plot estimates of aboveground net primary production in three eastern U.S. forests. *Ecosphere* 7, 1–13.

Easterling, W. E., Hays, C. J., Easterling, M. M. K., & Brandle, J. R. (1997). Modelling the effect of shelterbelts on maize productivity under climate change: An application of the EPIC model. *Agriculture, Ecosystems and Environment*, 61(2–3), 163–176.

Ehni, A., 2012. Windbreak Renovation Presentation. University of Nebraska–Lincoln Extension EC1777

Esprey, L.J., Sands, P. J., & Smith, C. W. (2004). Understanding 3-PG using a sensitivity analysis. F*or. Ecol. Manage*. 193(1–2), 235–250.

Feikema, P.M., J.D. Morris, C.R. Beverly, J.J. Collopy, T.G. Baker, et al. (2010). Validation of plantation transpiration in south-eastern Australia estimated using the 3PG+ forest growth model. *For. Ecol. Manage*. 260(5), 663–678.

Fitzsimmons, M. J., Pennock, D. J., & Thorpe, J. (2004). Effects of deforestation on ecosystem carbon densities in central Saskatchewan, Canada. *Forest Ecology and Management*, *188*(1–3), 349–361

Franks, J.R., & Hadingham, B. (2012). Reducing greenhouse gas emissions from agriculture: Avoiding trivial solutions to a global problem. *Land use policy* 29, 727–736.

Fraver, S., Bradford, J.B., & Palik, B.J. (2011). Improving Tree Age Estimates Derived from Increment Cores: A Case Study of Red Pine. *For. Sci.*, 57(2), 164-170.

Fraver, S., & White, A.S. (2005). Identifying growth releases in dendrochronological studies of forest disturbance. *Can. J. For. Res.* 35, 1648–1656.

Freedman, B., & Keith, T. (1996). Planting trees for carbon credits: A discussion of context,

issues, feasibility, and environmental benefits. *Environmental Reviews*, 4(2), 100–111.

Fule, P., Covington, W., & Moore, M.M. (1997). Determining Reference Conditions for Ecosystem Management of Southwestern Ponderosa Pine Forests. *Ecological Apliccations*, 7(3), 895-908

Gámez-Virués, S., Bonifacio, R. S., Gurr, G. M., Kinross, C., Raman, A., & Nicol, H. I. (2007). Arthropod prey of shelterbelt-associated birds: Linking faecal samples with biological control of agricultural pests. *Australian Journal of Entomology*, *46*(4), 325–331.

Girardin, M.P., Bernier, P.Y., Raulier, F., Tardif, J.C., & Jing Guo, X. (2011). Testing for a CO_2 fertilization effect on growth of Canadian boreal forests 2. *Journal of Geophysical Research*, 116, 1-6

Girardin, M.P., Bouriaud, O., Hogg, E.H., Kurz, W., Zimmermann, N.E., Metsaranta, J.M., De Jong, R., Frank, D.C., Esper, J., Büntgen, U., Jing Guo, X., & Bhatti, J. (2016). No growth stimulation of Canada's boreal forest under half-century of combined warming and CO_2 fertilization. *PNAS*, 113(52).

Gonzalez-benecke, C.A., E.J. Jokela, W.P. Cropper, R. Bracho, & D.J. Leduc. (2014). Parameterization of the 3-PG model for *Pinus elliottii* stands using alternative methods to estimate fertility rating , biomass partitioning and canopy closure. *For. Ecol. Manage*. 327, 55–75.

Goodsman, D.W., Lieffers, V.J., Landhäusser, S.M., & Erbilgin, N. (2010). Fertilization of lodgepole pine trees increased diameter growth but reduced root carbohydrate concentrations. *For. Ecol. Manage*. 260, 1914–1920.

Gower, S.T., Krankina, O., Olson, R.J., Apps, M., Linder, S., & Wang, C. (2001). Net Primary Production and Carbon Allocation Patterns of Boreal Forest Ecosystems. *Ecol. Appl.* 11, 1395.

Graves, A. R., Morris, J., Deeks, L. K., Rickson, R. J., Kibblewhite, M. G., Harris, J. A., & Truckle, I. (2015). The total costs of soil degradation in England and Wales. *Ecological Economics*, 119, 399–413.

Greb, B. W., & Black, A. L. (1961). Effects of Windbreaks Plantings on Adjacent Crops. *Soil and Water Conservation,* 16 (5), 223-227.

Grier, C. C., Vogt, K. A., Keyes, M. R., & Edmonds, R. L. (1981). Biomass distribution and above- and below-ground production in young and mature *Abies amabilis* zone ecosystems of the Washington Cascades. *Canadian Journal of Forest Research,* 11(1), 155–167.

Gupta, R., & Sharma, L. K. (2019). The process-based forest growth model 3-PG for use in forest management : A review. *Ecol. Modell.* 395, 55–73.

Ha, T. V., Amichev, B.Y., Belcher, K.W., Bentham, M.J., Kulshreshtha, S.N., Laroque, C.P., & Van Rees, K.C.J. (2018). Shelterbelt Agroforestry Systems Inventory and Removal Analyzed by Object-based Classification of Satellite Data in Saskatchewan, Canada. *Can. J. Remote Sens.*, 45(2), 246-263.

Hawke, M. F., & Tombleson, J. D. (1993). Production and interaction of pastures and shelterbelts in the central North Island. *Proceedings of the New Zealand Grassland Association*, 197 (55), 193-197.

He, W., Yang, J. Y., Qian, B., Drury, C. F., Hoogenboom, G., He, P., … & Zhou, W. (2018). Climate change impacts on crop yield, soil water balance and nitrate leaching in the semiarid and humid regions of Canada. *PLoS ONE*, *13*(11), 1-19.

Headlee, W.L., Zalesny, R. S. Jr, Donner, D. M. & Hall, R. B. (2013). Using a Process-Based Model (3-PG) to Predict and Map Hybrid Poplar Biomass Productivity in Minnesota and Wisconsin, USA. *Bioenerg. Res*. 6, 196–210.

Heath, B. A., Maughan, J. A., Morrison, A. A., Eastwood, I. W., Drew, I. B., & Lofkin, M. (1999). The influence of wooded shelterbelts on the deposition of copper, lead and zinc at Shakerley Mere, Cheshire, England. *Science of the Total Environment*, 235, 415–417.

Helmers, G., & Brandle, J.R. (2005). Optimum windbreak spacing in Great Plains agriculture. *Great Plains Research*, 179-198.

Hember, R.A., Kurz, W.A., & Girardin, M.P. (2019). Tree Ring Reconstructions of Stemwood Biomass Indicate Increases in the Growth Rate of Black Spruce Trees Across Boreal

Forests of Canada. J. G*eophys. Res. Biogeoscience*s 124, 2460–2480.

Howat, B. (2020). The effects of climate change on the radial growth of four shelterbelt species across the brown, dark brown, and black soil zones of saskatchewan. M. S. thesis, Soil Science Department, University of Saskatchewan, Saskatoon

Humpenöder, F., Popp, A., Philip Dietrich, J., Klein, D., Bauer, N., Fuss, S., Lamb, W.F., Callaghan, M.W., Kreidenweis, U., Stevanović, M., Leon Bodirsky, B., Kriegler, E., & Lotze-Campen, H. (2016). Afforestation to mitigate climate change: impacts on food prices under consideration of albedo effects. *Environ. Res. Lett* 11, 85001.

Iles, K. (1974). Geometrical considerations affecting the determination of basal area growth by increment boring methods. Partial fulfiment Requir. M. S. Oregon State University.

Ilvesniemi, H., Levula, J., Ojansuu, R., Kolari, P., Kulmala, L., Pumpanen, J., Launiainen, S., Vesala, T., & Nikinmaa, E. (2009). Long-term measurements of the carbon balance of a boreal Scots pine dominated forest ecosystem. *Boreal Environ. Res.* 14, 731–753.

Izaurralde, R. C., Lemke, R. L., Goddard, T. W., McConkey, B., & Zhang, Z. (2004). Nitrous oxide emissions from agricultural toposequences in Alberta and Saskatchewan. *Soil Science Society of America Journal*, 68(4), 1285-1294.

Joss, B. N., Hall, R. J., Sidders, D. M., & Keddy, T. J. (2008). Fuzzy-logic modeling of land suitability for hybrid poplar across the Prairie Provinces of Canada. *Environmental Monitoring and Assessment*, 141(1-3), 79-96.

Jump, A.S., Hunt, J.M., & Peñuelas, J. (2006). Rapid climate change-related growth decline at the southern range edge of Fagus sylvatica. *Glob. Chang. Biol.* 12, 2163–2174.

Kimmins J.P. (1997). Forest ecology. New York: Prentice-Hall

Klenert, D., Mattauch, L., Combet, E., Edenhofer, O., Hepburn, C., Rafaty, R., & Stern, N. (2018). Making carbon pricing work for citizens. *Nature Climate Change*, *8*(8), 669–677.

Klesse, S., & Frank, S.E.D. (2016). Integrating tree-ring and inventory-based measurements of aboveground biomass growth : research opportunities and carbon cycle consequences from

a large snow breakage event in the Swiss Alps. *Eur. J. For. Res*. 135, 297–311.

Kompas, T., Pham, V. H., & Che, T. N. (2018). The Effects of Climate Change on GDP by Country and the Global Economic Gains From Complying With the Paris Climate Accord. *Earth's Future*, *6*(8), 1153–1173.

Kooten, G. C. van, Binkley, C. S., & Delcourt, G. (1995). Effect of Carbon Taxes and Subsides on Optimal Forest Rotation Age and Supply of Carbon Services. *Amer. J. Agr. Econ*, 77, 365-374.

Komanoff, C., & Gordon, M. (2015). British Columbia's Carbon Tax: By The Numbers, A Carbon Tax Center Report. Carbon Tax Center, New York.

Kort, J., & Turnock, R. (1999). Carbon reservoir and biomass in Canadian prairie shelterbelts. *Agroforestry Systems*, *44*, 175–186.

Kowalchuk, T. E., & Jong, E. de. (1995). Shelterbelts and their effect on crop yield. *Canadian Journal of Soil Science*, 75(4), 543–550.

Kreidenweis, U.; Humpenöder, F.; Stevanovic, M.; Bodirsky, B. L.; Kriegler, E.; & Lotze-Campen, H.; Popp, A. (2016). Afforestation to mitigate climate change: impacts on food prices under consideration of albedo effects. *Environmental Research :Letters*, 11, 1-12.

Kujawa, A., & Kujawa, K. (2008). Effect of young midfield shelterbelts development on species richness of macrofungi communities and their functional structure. *Polish Journal of Ecology*, 56(1), 45.

Kulshreshtha, S., & Kort, J. (2009). External economic benefits and social goods from prairie shelterbelts. *Agrofor. Syst.* 75, 39–47.

Lal, R. (2004). Soil carbon sequestration impact on global climate change and food security. *Science*, 304(5677), 1623-7

Landsberg, J.J., & Hingston, F. J. (1996). Evaluating a simple radiation/dry matter conversion model using data from *Eucalyptus globulus* plantations in Western Australia. *Tree Physio*l., 801–808.

Landsberg, J.J., and R.H. Waring. (1997). A generalised model of forest productivity using simplified concepts of radiation-use efficiency, carbon balance and partitioning. *For. Ecol. Manage*. 95(3), 209–228.

Landsberg, J.J., Waring, R. H., & N.C. Coops. (2003). Performance of the forest productivity model 3-PG applied to a wide range of forest types. *For. Ecol. Manage.*, 172, 99–214.

Liu, C.J. (1986). Rectifying radii on off-center increment cores. *For. Sci.* 32, 1058–1061.

Liu, L., Huang, G., Baetz, B., Huang, C. Z., & Zhang, K. (2019). Integrated GHG emissions and emission relationships analysis through a disaggregated ecologically-extended input-output model; A case study for Saskatchewan, Canada. *Renewable and Sustainable Energy Reviews*, 106, 97-109.

Liu, Y., & Harris, D. J. (2008). Effects of shelterbelt trees on reducing heating-energy consumption of office buildings in Scotland. *Applied Energy*, 85(2–3), 115–127.

Liu, Y., Zhang, Y., & Liu, S. (2012). Aboveground carbon stock evaluation with different restoration approaches using tree ring chronosequences in Southwest China. *Forest Ecology and Management*, 263, 39–46.

Lowe, W. J., Greene, T. A. (1990). Geographic variation in specific gravity and fiber length of green ash (*Fraxinus pennsylvanic*a Marsh.) in East Texas. *Silvae Genet*, 39, 194-198.

Lupi, C., Rossi, S., Vieira, J., Morin, H., & Deslauriers, A. (2014). Assessment of xylem phenology: a first attempt to verify its accuracy and precision. *Tree Physiol.* 34, 87–93.

Lupi, C, Rossi, S., Vieira, J., Morin, H., & Deslauriers, A. (2014). Technical note Assessment of xylem phenology : a first attempt to verify its accuracy and precision. *Tree Physiology*, 34 (1), 87–93.

Lyles, L., J. Tatarko, & J. D. Dickerson. (1984). Windbreak Effects on Soil Water and Wheat Yield. Transactions of the ASAE, 27(1), 069–072.

Maillet, J., Laroque, C., & Bonsal, B. (2017). A dendroclimatological assessment of shelterbelt trees in a moisture limited environment. *Agricultural and Forest Meteorology*, *237–238,*

30–38.

Makumba, W., Akinnifesi, F. K., Janssen, B., & Oenema, O. (2007). Long-term impact of a gliricidia-maize intercropping system on carbon sequestration in southern Malawi. *Agriculture, Ecosystems and Environment,* 118(1–4), 237–243.

Marchildon, G., (2014). The Prairie Farm Rehabilitation Administration : The Prairie Farm Rehabilitation Administration : Climate Crisis and Federal – Provincial Relations during the Great Depression. *Can. Hist. Rev*, 90(2), 275-301

Mayrinck, R. C., Laroque, C. P., Amichev, B. Y., & van Rees, K. (2019). Above- and below-ground carbon sequestration in shelterbelt trees in Canada: A review. *Forests, 10*(10),1-9.

Metsaranta, J.M., & Lieffers, V.J. (2009). Using dendrochronology to obtain annual data for modelling stand development: A supplement to permanent sample plots. *Forestry* 82, 163–173.

Meyer, T., Sagun, V., & Auer, C. (2017). Reducing Pollen Dispersal using Forest Windbreaks. bioRxiv, 204263.

Mize, C. W., Brandle, J. R., Schoeneberger, M. M., & Bentrup, G. (2008). Ecological Development and function of Shelterbelts in Temperate North America. *Toward Agroforestry Design*, 27–54.

Montagnini, F., & Nair, P. K. R. (2004). Carbon sequestration: An underexploited environmental benefit of agroforestry systems. *Agroforestry Systems*, 61-62(1), 281-295

Motta, R., & Nola, P. (2001). Growth trends and dynamics in sub-alpine forest stands in the Varaita Valley (Piedmont, Italy) and their relationships with human activities and global change. *J. Veg. Sci.* 12, 219–230.

Nair, P. K. R., Kumar, B. M., & Nair, V. D. (2009). Agroforestry as a strategy for carbon sequestration. *Journal of Plant Nutrition and Soil Science*, 172(1), 10 - 23.

Nair, P. K., Nair, V. D., Mohan Kumar, B., & Showalter, J. M. (2010). Carbon sequestration in agroforestry systems. *Advances in Agronomy*, 108, 237-307

Nehrbass-ahles, C., Babst, F., & Klesse, S. (2014). The influence of sampling design on tree-ring-based quantification of forest growth. *Global Change Biology*, 20 (9), 2867–2885.

Nelson, G., Bogard, J., Lividini, K., Arsenault, J., Riley, M., Sulser, T. B., Rosegrant, M. (2018). Income growth and climate change effects on global nutrition security to mid-century. *Nature Sustainability*, *1*(12), 773–781.

Neuman, A. D., & Belcher, K. W. (2011). The contribution of carbon-based payments to wetland conservation compensation on agricultural landscapes. *Agricultural Systems*, *104*(1), 75–81.

Nicoll, B.C., & Ray, D. (1996). Adaptive growth of tree root systems in response to wind action and site conditions. *Tree Physiol.* 16, 891–898.

Nkonya, E., Mirzabaev, A., & Braun, J. Von. (2015). Economics of Land Assessment for Improvement – A Global Degradation and Sustainable Development. Springer, Switzerland.

Norton, D.A., Palmer, G.H., & Ogden, J. (1987). Dendroecological studies in New Zealand. An evaluation of tree age estimates based on increment cores. *New Zeal. J. Bot.* 25, 373–383.

Nuberg, I. K., Mylius, S. J., Edwards, J. M., & Davey, C. (2002). Windbreak research in a South Australian cropping system. *Australian Journal of Experimental Agriculture*, 42(6), 781–795.

Ogbuehi, S. N., & Brandle, J. R. (1982). Influence of Windbreak-Shelter on Soybean Growth, Canopy Structure, and Light Relations. *Crop Science*, 22(2), 269–273.

Olive, A. (2019). In a province defined by a resource-based economy, a carbon tax feels perennially unfair and ineffective, even as emissions skyrocket, retrieved December 12, 2020, from Https://policyoptions.irpp.org/fr/magazines/july-2019/saskatchewans-long-history-of-rejecting-carbon-pricing/

O'Mara, F. P. (2011). The significance of livestock as a contributor to global greenhouse gas emissions today and in the near future. *Animal Feed Science and Technology*, *166–167*, 7–15.

Onyewotu, L. O. Z., Ogigirigi, M. A., & Stigter, C. J. (1994). A study of competitive effects

between a *Eucalyptus camaldulensis* shelterbelt and an adjacent millet (*Pennisetum typhoides*) crop. *Agriculture, Ecosystems and Environment*, 51(3), 281–286.

Palm, C. A., Woomer, P. L., of Nairobi, U., Alegre, J., Arevalo, L., Castilla, C., … van Noordwijk, M. (1999). Carbon Sequestration and Trace Gas Emissions In Slash-And-Burn And Alternative Land Uses In The Humid Tropics. Instituto Nacional de Innovación Agraria. 1 - 39.

Pape, R. (1999). Influence of Thinning and Tree Diameter Class on the Development of Basic Density and Annual Ring Width in Picea abies. *Scand. J. For. Res.* 14, 27–37.

Patil, R. H., Laegdsmand, M., Olesen, J. E., & Porter, J. R. (2012). Sensitivity of crop yield and N losses in winter wheat to changes in mean and variability of temperature and precipitation in Denmark using the FASSET model. *Acta Agriculturae Scandinavica Section B: Soil and Plant Science*, *62*(4), 335–351.

Peichl, M., Thevathasan, N. V., Gordon, A. M., Huss, J., & Abohassan, R. A. (2006). Carbon sequestration potentials in temperate tree-based intercropping systems, southern Ontario, Canada. *Agroforestry Systems*, 66(3), 243–257.

Peri, P. L., & Bloomberg, M. (2002). Windbreaks in southern Patagonia, Argentina: A review of research on growth models, windspeed reduction, and effects on crops. *Agroforestry Systems*, 56(2), 129–144.

Perry, C. H., Woodall, C. W., Liknes, G. C., & Schoeneberger, M. M. (2009). Filling the gap: improving estimates of working tree resources in agricultural landscapes. *Agroforestry Systems*, *75*(1), 91–101.

Pirie, M.R., Fowler, A.M., & Triggs, C.M. (2015). Assessing the accuracy of three commonly used pith offset methods applied to Agathis australis (Kauri) incremental cores. *Dendrochronologia*, 36, 60–68.

Piwowar, J. M., Amichev, B. Y., & Rees, K. C. J. Van. (2017). The Saskatchewan shelterbelt inventory. *Can. J. Soil Sci*,. 438, 433–438.

Possu, W. B., Brandle, J. R., Domke, G. M., Schoeneberger, M., & Blankenship, E. (2016).

Estimating carbon storage in windbreak trees on U.S. agricultural lands. *Agroforestry Systems*, 90(5), 889–904.

Price, L. W. (1993). Hedges and Shelterbelts on the Canterbury Plains, New Zealand: Transformation of an Antipodean landscape. *Annals of the Association of American Geographers*, 83(1), 119–140.

Puri, S., Singh, S., & Khara, A. (1992). Effect of windbreak on the yield of cotton crop in semiarid regions of Haryana. *Agroforestry Systems*, 18(3), 183–195.

Qi, X., Mize, C. W., Batchelor, W. D., Takle, E. S., & Litvina, I. V. (2001). SBELTS: A model of soybean production under tree shelter. *Agroforestry Systems*, 52(1), 53–61.

Qian, B., Zhang, X., Smith, W., Grant, B., Jing, Q., Cannon, A. J., … Zhao, J. (2019). Climate change impacts on Canadian yields of spring wheat, canola and maize for global warming levels of 1.5 °c, 2.0 °c, 2.5 °c and 3.0 °c. *Environmental Research Letters*, *14*(7), 1-13.

R core Team. (2020). R: A language and environment for statistical computing

Raintree, J. B. (1987). The state of the art of agroforestry diagnosis and design. *Agroforestry systems*, 5(3), 219-250.

Rempel, J., Kulshreshtha, S., Van Rees, K., & Amichev, B., (2014). Factors that Influence Shelterbelt Retention and Removal in Prairie Agriculture as Identified by Saskatchewan Producers. Soil Science Workshop, University of Saskatchewan.

Rempel, J.C., Kulshreshtha, Suren, N., Amichev, B.Y., & van Rees, K.C.J. (2017). Costs and benefits of shelterbelts: A review of producers' perception and min map analysis for Saskatchewan, Canada. *Can. J. Soil Sci*. 97, CJSS-2016-0100.

Rennolls, K., & Wang, M. (2005). Distribution With Application To Fitting Forest Tree Diameter Data. *Canadian Journal of Forest Research*, 35(3), 575–579.

Richardson, J., Cooke, J.E.K., Isebrands, J.G., Thomas, B.R., & Van Rees, K.C.J., (2007). Poplar research in Canada — a historical perspective with a view to the future. *Can. J. Bot.* 85, 1136–1146.

Rocha, A. V., Goulden, M.L., Dunn, A.L., & Wofsy, S.C. (2006). On linking interannual tree ring variability with observations of whole-forest CO2 flux. *Glob. Chang. Biol.* 12, 1378–1389.

Rogelj, J., Den Elzen, M., Höhne, N., Fransen, T., Fekete, H., Winkler, H., … Meinshausen, M. (2016). Paris Agreement climate proposals need a boost to keep warming well below 2 °c. *Nature*. 534(7609), 631-639.

Rosenberg, N. J. (1966). Microclimate, air mixing and physiological regulation of transpiration as influenced by wind shelter in an irrigated bean field. *Agricultural Meteorology*, 3(3–4), 197–224.

Rozas, V. (2003). Tree age estimates in Fagus sylvatica and Quercus robur: testing previous and improved methods. *Plant Ecol.* 167, 193–212.

Rudd, L. (2020). *Carbon Life Cycle Assessment of Shelterbelts in Saskatchewan*. M. S. thesis, School of Environment and Sustainability University of Saskatchewan Saskatoon.

Salminen, H., & Varmola, M. (1993). Influence of initial spacing and planting design on the development of young Scots pine (*Pinus sylvestris* L.) stands. *Silva Fenn.*, 27(1), 21-28

Salzer, M.W., Hughes, M.K., Bunn, A.G., & Kipfmueller, K.F. (2009). Recent unprecedented tree-ring growth in bristlecone pine at the highest elevations and possible causes. *Proc. Natl. Acad. Sci. U.S.A.* 106, 20348–20353.

Sands, P. (2010). 3PGPJS User Manual. Retrieved in April 16 2021 from https://3pg.forestry.ubc.ca/documentation/

Saskpower (2019). Federal Carbon Tax set to increase, retrieved December 3 2020, from https://www.saskpower.com/about-us/media-information/news-releases/Federal-Carbon-Tax-set-to-increase-Jan1

Sauer, T. J., Cambardella, C. A., & Brandle, J. R. (2007). Soil carbon and tree litter dynamics in a red cedar-scotch pine shelterbelt. *Agroforestry Systems*, *71*(3), 163–174.

Schindler, D. W., & Donahue, W. F. (2006). An impending water crisis in Canada's western

prairie provinces. *PNAS*, 103(19)7210-7216

Schnitter, R., & Berry, P. (2019). The Climate Change, Food Security and Human Health Nexus in Canada: A Framework to Protect Population Health. *Environmental Research and Public Health*, 16, 1-16.

Schoeneberger, M. M. (2009). Agroforestry: working trees for sequestering carbon on agricultural lands.*Agroforestry Systems*, 75, 27-37.

Shi, P.-J., Huang, J.-G., Hui, C., Grissino-Mayer, H.D., Tardif, J.C., Zhai, L.-H., Wang, F.-S., & Li, B.-L. (2015). Capturing spiral radial growth of conifers using the superellipse to model tree-ring geometric shape. *Front. Plant Sc*i. 6.

Silva, L.C.R., Anand, M., & Leithead, M.D. (2010). Recent widespread tree growth decline despite increasing atmospheric CO_2. *PLoS One* 5(7), 1-7.

Singh, D., & Kohli, R. K. (1992). Impact of *Eucalyptus tereticornis* Sm. shelterbelts on crops. *Agroforestry Systems*, 20(3), 253–266.

Skatter, S., & Kucera, B. (1998). The cause of the prevalent directions of the spiral grain patterns in conifers. *Trees*, 12, 265–273

Smith, F. W., & Long, J. N. (2001). Age-related decline in forest growth: an emergent property. *Forest Ecology and Management*, 144(1-3), 175–181.

Sobool, D. J., Sobool, C. D. J., & All, S. (2004). An economic analysis of afforestation on agricultural land in east central Saskatchewan. M. S. thesis, Agricultural Economics, University of Saskatchewan.,

Stahle, D.W., Mushove, P.T., Cleaveland, M.K., Roig, F., & Haynes, G.A. (1999). Management implications of annual growth rings in Pterocarpus angolensis from Zimbabwe. *For. Ecol. Manage*. 124, 217–229.

Stape, J.L., Ryan, M. G., & Binkley, D. (2004). Testing the utility of the 3-PG model for growth of *Eucalyptus grandis* x *urophylla* with natural and manipulated supplies of water and nutrients. *For. Ecol. Manage*. 193(1–2), 219–234.

Stokes, A., & Berthier, S. (2000). Irregular heartwood formation in Pinus pinaster Ait. is related to eccentric, radial, stem growth. *For. Ecol. Manage*. 135, 115–121.

Strange, C., & Brandle, J. R. (2006). Windbreak Management. University of Nebraska - Lincoln EC1768.

Sun, D., & Dickinson, G. R. (1994). A case study of shelterbelt effect on potato (Solanum tuberosum) yield on the Atherton Tablelands in tropical north Australia. *Agroforestry Systems*, 25(2), 141–151.

Tack, J. D., Quamen, F. R., Kelsey, K., & Naugle, D. E. (2017). Doing more with less: Removing trees in a prairie system improves value of grasslands for obligate bird species. Journal of Environemtal Management, 198(1), 163 – 169.

Tatarinov, F., Bochkarev, Y., Oltchev, A., Nadezhdina, N., & Cermak, J. (2007). Effect of contrasting water supply on the diameter growth of Norway spruce and aspen in mixed stands: a case study from the southern Russian taiga Fyodor. *Ann. For. Sci.* 64, 219–228.

Teets, A., Fraver, S., Hollinger, D.Y., Weiskittel, A.R., Seymour, R.S., & Richardson, A.D., (2018). Linking annual tree growth with eddy-flux measures of net ecosystem productivity across twenty years of observation in a mixed conifer forest. *Agric. For. Meteorol.* 249, 479–487.

Tenzin, J., Tenzin, K., & Hasenauer, H. (2017). Individual tree basal area increment models for broadleaved forests in Bhutan. *For. Int. J. For. Res. For.* 90, 367–380.

Thevs, N., Strenge, E., Aliev, K., Eraaliev, M., Lang, P., Baibagysov, A., & Xu, J. (2017). Tree Shelterbelts as an Element to Improve Water Resource Management in Central Asia. Water, 9(11), 842.

Tickle, P.K., Coops, N. S., Hafner, S. D., Bago, T. & Team. S. (2001). Assessing forest productivity at local scales across a native eucalypt forest using a process model, 3PG-SPATIAL. *For. Ecol. Manage*. (152), 275–291.

Tubiello, F. N., Salvatore, M., Rossi, S., Ferrara, A., Fitton, N., & Smith, P. (2013). The FAOSTAT database of greenhouse gas emissions from agriculture. *Environmental*

Research Letters, *8*(1), 1-11.

Tvinnereim, E., & Mehling, M. (2018). Carbon pricing and deep decarbonisation. *Energy Policy*, *121*, 185–189.

Tyndall, J., & Colletti, J. (2007). Mitigating swine odor with strategically designed shelterbelt systems: a review. *Agroforestry systems*, 69(1), 45-65.

Udawatta, R. P., & Jose, S. (2011). Carbon Sequestration Potential of Agroforestry Practices in Temperate North America (pp. 17–42). Springer, Dordrecht.

United Nations (UN) (2019). World Population Prospects, retrieved January 17, 2020 from https://population.un.org/wpp/

Valentine, H.T., Tritton, L. M., & Furnival., G. M. (1984). Subsampling trees for biomass, volume, or mineral content. *For. Sci.* 30(3), 673–681.

Véronique, R. (1998). Changes in radial tree growth for *Picea abies* , *Larix decidua* , *Pinus cembra* and *Pinus uncinata* near the alpine timberline since 1750. *Trees*, 13, 40–53.

Villalba, R., & Veblen, T.T. (1997). Improving estimates of total tree ages based on increment core samples. *Ecoscienc*e 4, 534–542.

Wang, Y., Hogg, E. H., Price, D. T., Edwards, J., & Williamson, T. (2014). Past and projected future changes in moisture conditions in the Canadian boreal forest. *The Forestry Chronicle*, 90(5), 678–691.

Wang, X., & Feng, Z. (1995). Atmospheric carbon sequestration through agroforestry in China. Energy, 20(2), 117–121.

Wight, B. (1988). 15. Farmstead windbreaks. Agriculture, Ecosystems and Environment, 22–23(C), 261–280.

Wiseman, G., Kort, J., & Walker, D. (2009). Quantification of shelterbelt characteristics using high-resolution imagery. *Agriculture, Ecosystems and Environment*, 131, 111–117

Worbes, M., Staschel, R., Roloff, A., & Junk, W.. (2003). Tree ring analysis reveals age

structure, dynamics and wood production of a natural forest stand in Cameroon. *For. Ecol. Manage*. 173, 105–123

Wright, J. W. (1959). Silvical characteristics of green ash (*Fraxinus pennsylvanica*). Station Paper NE126. Upper Darby, PA: US Department of Agriculture, Forest Service, Northeastern Forest Experiment Station. 18, 126.

Wu, L., He, D., Ji, Z., You, W., Tan, Y., Zhen, X., & Yang, J. (2017). Protection efficiency assessment and quality of coastal shelterbelt for Dongshan Island at the coastal section scale. *Journal of Forestry Research*, 28(3), 577–584.

Xiao, Q., & Huang, M. (2016). Fine root distributions of shelterbelt trees and their water sources in an oasis of arid northwestern China. *Journal of Arid Environments*, 130, 30–39.

Yang, Y., Huang, S., Meng, S.X., Trincado, G., & VanderSchaaf, C.L. (2009). A multilevel individual tree basal area increment model for aspen in boreal mixedwood stands. *Can. J. For. Res.* 39, 2203–2214.

Yoder, B. J., Ryan, M. G., Waring, R. H., Schoettle, A. W., & Kaufmann, M. R. (1994). Evidence of reduced photosynthetic rates in old trees. *Forest Science*, 40(3), 513-527.

Zheng, X., Zhu, J., & Xing, Z. (2016). Assessment of the effects of shelterbelts on crop yields at the regional scale in Northeast China. *Agricultural Systems*, 143, 49–60.

Zhou, X., Brandle, J. R., Schoeneberger, M., & Awada, T. (2007). Developing above-ground woody biomass equations for open-grown, multiple-stemmed tree species: Shelterbelt-grown Russian-olive. *Ecological Modelling*, 202(3–4), 311–323.

Zhou, X. H., Brandle, J. R., Mize, C. W., & Takle, E. S. (2005). Three-dimensional aerodynamic structure of a tree shelterbelt: Definition, characterization and working models. *Agroforestry Systems*, 63(2), 133–147.

Zhu, J.-J. (2008). Wind Shelterbelts. In Encyclopedia of Ecology (pp. 3803–3812). Elsevier

Zweifel, R., Eugster, W., Etzold, S., Dobbertin, M., Buchmann, N., & Häsler, R., (2010). Link between continuous stem radius changes and net ecosystem productivity of a subalpine

Norway spruce forest in the Swiss Alps. *New Phytol.* 187, 819–830.

APPENDIX A

DETAILS OF THE METHODOLOGY TO RETRIEVE TREE GROWTH

Chapter 4 was a complex analysis encompassing many variables, equations, and measurements. Appendix A helps to clarify many facets of this part of the study. Table A1 illustrates how orientation, approach and modes were combined, along with the number of increment cores for each of the 56 modes tested. Figure A1 illustrates the number of rings used to to build Figure 4.2 stressing that the number of rings decreased from the bark to the pith in the B to P orientation and from the pith to the bark in the P to B orientation.

Table A1 - A key to how the 56 modes were constructed for all possiblilities tested. Direction (P to B (pith to the bark) or B to P (bark to the pith)), approach (center or pith), mode, the number of increment cores (IC) of J kind (reaching the center of the pith), the number of increment cores (IC) of the K kind (off-pith or off-center core), total of increment cores used on the mode (J +K) are listed.

Direction	Approach	Mode	# of IC j	# of IC k	J+K
P to B	Center	c_1oc_0	1	0	1
		c_1oc_1	1	1	2
		c_1oc_2	1	2	3
		c_1oc_3	1	3	4
		c_2oc_0	2	0	2
		c_2oc_1	2	1	3
		c_2oc_2	2	2	4
		c_3oc_0	3	0	3
		c_3oc_1	3	1	4
		c_4oc_0	4	0	4
		c_0oc_1	0	1	1
		c_0oc_2	0	2	2
		c_0oc_3	0	3	3
		c_0oc_4	0	4	4
	Pith	P_0oP_1	0	1	1
		P_0oP_2	0	2	2
		P_0oP_3	0	3	3
		P_0oP_4	0	4	4
		P_1oP_0	1	0	1
		P_1oP_1	1	1	2
		P_1oP_2	1	2	3
		P_1oP_3	1	3	4
		P_2oP_0	2	0	2
		P_2oP_1	2	1	3
		P_2oP_2	2	2	4
		P_3oP_0	3	0	3
		P_3oP_1	3	1	4
		P_4oP_0	4	0	4
B to P	Center	c_1oc_0	1	0	1

	c_1oc_1	1	1	2
	c_1oc_2	1	2	3
	c_1oc_3	1	3	4
	c_2oc_0	2	0	2
	c_2oc_1	2	1	3
	c_2oc_2	2	2	4
	c_3oc_0	3	0	3
	c_3oc_1	3	1	4
	c_4oc_0	4	0	4
	c_0oc_1	0	1	1
	c_0oc_2	0	2	2
	c_0oc_3	0	3	3
	c_0oc_4	0	4	4
Pith	P_0oP_1	0	1	1
	P_0oP_2	0	2	2
	P_0oP_3	0	3	3
	P_0oP_4	0	4	4
	P_1oP_0	1	0	1
	P_1oP_1	1	1	2
	P_1oP_2	1	2	3
	P_1oP_3	1	3	4
	P_2oP_0	2	0	2
	P_2oP_1	2	1	3
	P_2oP_2	2	2	4
	P_3oP_0	3	0	3
	P_3oP_1	3	1	4
	P_4oP_0	4	0	4

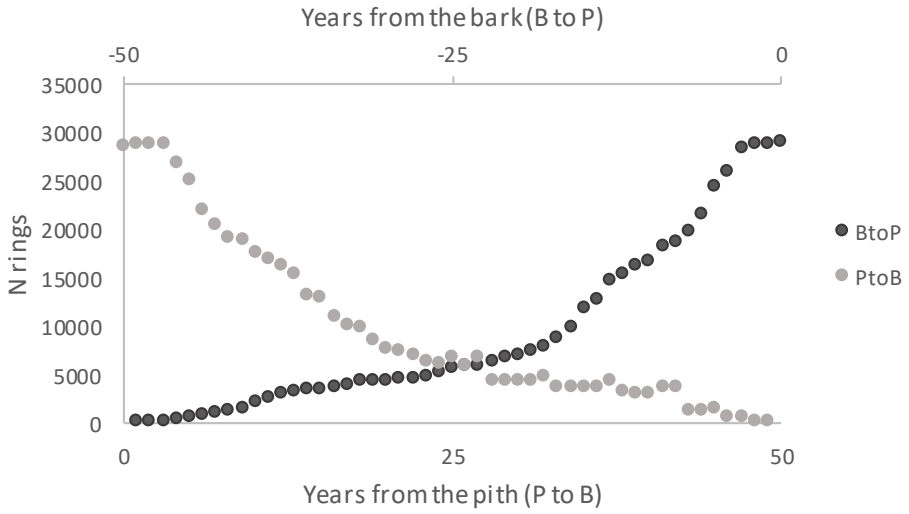

Figure A1 - Number of rings considered for each year for a ring-to-ring analysis.

To assess the significance of the species, mode, and their interactions on the mean absolute error for DBH, a mixed model was fit using the software package R. This mixed model

considered as the fixed part mode, species and its interaction, and the randon part mode was tree. Table A2 shows that mode, species and its interactions significantly affected the error. Figure A2 presents the randon part of the model. The dots are homogeneously distributed, which indicates a good fit.

Table A2 - Analisys of variance of the model listing the factors tested, numerator DF, demoninator DF, F-ratio and p-value. Note: DF = degrees of freedom.

Factors	Numerator DF	Denominator DF	F-ratio	p-value
Intercept	1	966485	37.16030	<.0001
Mode	30	966485	309.89264	<.0001
Species	9	966485	274.63253	<.0001
Mode*Species	270	966485	28.46561	<.0001

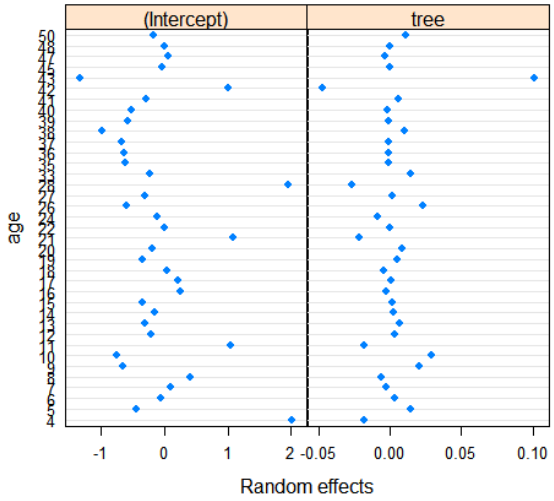

Figure A2 - Random effects on the mixed model tested.

Table A3 ranks the modes according to MAE for DBH and BA. Most species presented the same best (P4, P3, and P3OP1) and worst modes (C1, OC1 and OP1), except for chokecherry, Colorado spruce, and acute willow.

Table A3 - Modes ranked based on MAE and MAE (% Last ring) for DBH and BA. The best three methods are highlighted in red, while the worst three methods are highlighted in blue for each species.

Species	Mode	DBH						BA						Total	
		MAE BtoP	MAE PtoB	Scaled BtoP	Scaled PtoB	SUM	RANK	MAE BtoP	MAE PtoB	Scaled BtoP	Scaled PtoB	SUM	RANK	Sum	Rank
Chokecherry	C1	0.1	0.1	0.6	0.9	1.5	18	0.1	0.2	0.7	0.9	1.6	21	3.1	20
Chokecherry	c1oc1	0.1	0.1	0.7	0.8	1.4	13	0.1	0.2	0.8	0.8	1.5	18	3.0	15
Chokecherry	C1OC2	0.1	0.1	0.7	0.7	1.4	12	0.1	0.2	0.8	0.7	1.5	17	3.0	14
Chokecherry	C1OC3	0.1	0.1	0.7	0.7	1.4	11	0.1	0.2	0.8	0.7	1.5	15	2.9	13
Chokecherry	c2	0.1	0.1	0.6	0.6	1.2	3	0.1	0.1	0.6	0.6	1.2	4	2.4	3
Chokecherry	C2OC1	0.1	0.1	0.6	0.7	1.3	6	0.1	0.1	0.7	0.7	1.3	8	2.6	6
Chokecherry	C2OC2	0.1	0.1	0.7	0.7	1.4	9	0.1	0.2	0.7	0.7	1.4	12	2.8	10

Chokecherry	C3	0.1	0.1	0.6	0.6	1.1	2	0.1	0.1	0.6	0.6	1.1	2	2.3	2
Chokecherry	C3OC1	0.1	0.1	0.6	0.7	1.3	7	0.1	0.1	0.7	0.7	1.3	7	2.6	7
Chokecherry	C4	0.1	0.1	0.6	0.6	1.1	1	0.1	0.1	0.6	0.6	1.1	1	2.3	1
Chokecherry	OC1	0.1	0.2	0.9	0.9	1.8	28	0.1	0.2	1.0	1.0	2.0	28	3.8	28
Chokecherry	OC2	0.1	0.1	0.8	0.8	1.6	23	0.1	0.2	0.9	0.8	1.7	26	3.3	26
Chokecherry	OC3	0.1	0.1	0.7	0.8	1.5	21	0.1	0.2	0.8	0.8	1.6	22	3.1	21
Chokecherry	OC4	0.1	0.1	0.7	0.8	1.4	15	0.1	0.2	0.8	0.7	1.6	19	3.0	18
Chokecherry	OP1	0.1	0.2	0.5	1.0	1.5	20	0.1	0.2	0.7	1.0	1.7	25	3.2	22
Chokecherry	OP2	0.1	0.1	0.5	0.8	1.3	8	0.1	0.2	0.6	0.8	1.4	9	2.7	9
Chokecherry	OP3	0.1	0.1	0.5	0.8	1.3	5	0.1	0.2	0.5	0.7	1.3	5	2.6	5
Chokecherry	OP4	0.1	0.1	0.5	0.7	1.2	4	0.1	0.2	0.5	0.7	1.2	3	2.4	4
Chokecherry	P1	0.1	0.1	1.0	0.7	1.6	26	0.1	0.2	1.0	0.7	1.7	27	3.3	27
Chokecherry	P1OP1	0.1	0.1	0.7	0.8	1.5	17	0.1	0.2	0.7	0.7	1.5	13	3.0	16
Chokecherry	P1OP2	0.1	0.1	0.7	0.8	1.4	14	0.1	0.2	0.7	0.7	1.4	10	2.8	11
Chokecherry	P1OP3	0.1	0.1	0.6	0.8	1.4	10	0.1	0.2	0.6	0.7	1.3	6	2.7	8
Chokecherry	P2	0.1	0.1	0.9	0.7	1.6	24	0.1	0.2	0.9	0.7	1.6	24	3.3	25
Chokecherry	P2OP1	0.1	0.1	0.8	0.7	1.5	19	0.1	0.2	0.8	0.7	1.5	14	3.0	17
Chokecherry	P2OP2	0.1	0.1	0.7	0.7	1.4	16	0.1	0.2	0.7	0.7	1.4	11	2.8	12
Chokecherry	P3	0.1	0.1	1.0	0.7	1.6	25	0.1	0.2	0.9	0.7	1.6	23	3.3	24
Chokecherry	P3OP1	0.1	0.1	0.8	0.7	1.6	22	0.1	0.2	0.8	0.7	1.5	16	3.1	19
Chokecherry	P4	0.1	0.1	1.0	0.7	1.7	27	0.1	0.1	0.9	0.7	1.6	20	3.3	23
Colorado spruce	C1	1.4	0.7	0.4	1.0	1.4	15	14.2	9.4	0.5	0.8	1.3	14	2.7	14
Colorado spruce	c1oc1	1.4	0.6	0.4	0.8	1.2	10	14.3	7.5	0.5	0.6	1.1	10	2.4	10
Colorado spruce	C1OC2	1.5	0.5	0.4	0.7	1.2	6	14.4	6.7	0.5	0.6	1.1	6	2.2	7
Colorado spruce	C1OC3	1.4	0.5	0.4	0.7	1.1	3	14.0	6.3	0.5	0.5	1.0	3	2.1	3
Colorado spruce	c2	1.4	0.7	0.4	0.9	1.4	13	13.9	8.5	0.5	0.7	1.2	13	2.5	13
Colorado spruce	C2OC1	1.4	0.6	0.4	0.8	1.2	8	13.4	7.6	0.4	0.6	1.1	9	2.3	9
Colorado spruce	C2OC2	1.4	0.5	0.4	0.7	1.2	7	13.9	6.8	0.5	0.6	1.0	4	2.2	6
Colorado spruce	C3	1.4	0.6	0.4	0.9	1.3	12	13.7	8.3	0.5	0.7	1.2	12	2.5	12
Colorado spruce	C3OC1	1.4	0.6	0.4	0.8	1.2	9	13.6	7.4	0.5	0.6	1.1	8	2.3	8
Colorado spruce	C4	1.4	0.6	0.4	0.9	1.3	11	13.7	8.3	0.5	0.7	1.2	11	2.5	11
Colorado spruce	OC1	1.4	0.5	0.4	0.7	1.2	5	14.5	6.6	0.5	0.6	1.0	5	2.2	5
Colorado spruce	OC2	1.4	0.5	0.4	0.7	1.1	4	14.2	6.9	0.5	0.6	1.1	7	2.2	4
Colorado spruce	OC3	1.4	0.4	0.4	0.6	1.0	2	14.1	6.0	0.5	0.5	1.0	2	2.0	2
Colorado spruce	OC4	1.4	0.4	0.4	0.6	1.0	1	14.0	5.7	0.5	0.5	1.0	1	2.0	1
Colorado spruce	OP1	2.6	0.6	0.8	0.9	1.6	22	28.9	9.5	1.0	0.8	1.8	28	3.4	27
Colorado spruce	OP2	3.3	0.5	1.0	0.7	1.7	28	29.9	8.2	1.0	0.7	1.7	27	3.4	28
Colorado spruce	OP3	3.3	0.5	1.0	0.7	1.7	26	28.8	7.9	1.0	0.7	1.6	25	3.3	26
Colorado spruce	OP4	2.9	0.5	0.9	0.7	1.6	20	20.0	7.7	0.7	0.7	1.3	15	2.9	18
Colorado spruce	P1	1.7	0.7	0.5	1.0	1.5	18	19.0	11.8	0.6	1.0	1.6	26	3.1	21
Colorado spruce	P1OP1	2.9	0.6	0.9	0.8	1.7	25	24.5	8.8	0.8	0.7	1.6	23	3.2	24
Colorado spruce	P1OP2	3.1	0.5	0.9	0.7	1.6	23	26.9	7.7	0.9	0.7	1.5	22	3.2	23
Colorado spruce	P1OP3	3.3	0.5	1.0	0.7	1.7	27	27.2	8.0	0.9	0.7	1.6	24	3.3	25
Colorado spruce	P2	2.2	0.5	0.7	0.8	1.4	14	19.1	8.6	0.6	0.7	1.4	17	2.8	16
Colorado spruce	P2OP1	2.9	0.5	0.9	0.7	1.6	21	24.5	8.0	0.8	0.7	1.5	20	3.1	20
Colorado spruce	P2OP2	3.1	0.5	0.9	0.7	1.6	24	25.9	7.8	0.9	0.7	1.5	21	3.2	22
Colorado spruce	P3	2.6	0.5	0.8	0.7	1.5	17	22.6	7.4	0.8	0.6	1.4	18	2.8	17
Colorado spruce	P3OP1	2.9	0.5	0.9	0.7	1.5	19	24.5	7.4	0.8	0.6	1.4	19	3.0	19
Colorado spruce	P4	2.6	0.5	0.8	0.6	1.4	16	22.7	6.9	0.8	0.6	1.3	16	2.8	15
Siberian elm	C1	1.1	1.1	1.0	0.8	1.8	27	9.0	13.5	0.9	0.8	1.7	27	3.5	27
Siberian elm	c1oc1	1.0	1.0	0.9	0.7	1.6	24	8.4	11.6	0.9	0.7	1.6	24	3.2	24
Siberian elm	C1OC2	1.0	0.9	0.9	0.6	1.5	19	7.8	11.0	0.8	0.7	1.5	21	3.0	20
Siberian elm	C1OC3	0.9	0.9	0.9	0.6	1.5	15	7.6	10.6	0.8	0.6	1.4	13	2.9	15
Siberian elm	c2	1.0	1.0	0.9	0.7	1.6	25	7.8	12.3	0.8	0.7	1.5	23	3.2	23
Siberian elm	C2OC1	1.0	0.9	0.9	0.7	1.5	21	7.6	11.5	0.8	0.7	1.5	22	3.0	22
Siberian elm	C2OC2	0.9	0.9	0.9	0.6	1.5	16	7.5	11.1	0.8	0.7	1.4	17	2.9	16
Siberian elm	C3	0.9	1.0	0.8	0.7	1.5	22	7.3	11.9	0.8	0.7	1.5	19	3.0	21
Siberian elm	C3OC1	0.9	0.9	0.8	0.7	1.5	17	7.3	11.4	0.8	0.7	1.4	15	2.9	17
Siberian elm	C4	0.9	1.0	0.8	0.7	1.5	20	7.1	11.7	0.7	0.7	1.4	16	3.0	18
Siberian elm	OC1	1.1	1.0	1.0	0.7	1.7	26	9.4	11.7	1.0	0.7	1.7	26	3.4	26
Siberian elm	OC2	1.0	0.9	0.9	0.6	1.5	18	8.1	10.5	0.8	0.6	1.5	20	3.0	19
Siberian elm	OC3	0.9	0.8	0.9	0.6	1.5	14	7.7	10.2	0.8	0.6	1.4	12	2.9	13
Siberian elm	OC4	0.9	0.8	0.8	0.6	1.4	11	7.5	10.1	0.8	0.6	1.4	10	2.8	10
Siberian elm	OP1	1.1	1.4	1.0	1.0	2.0	28	9.6	16.7	1.0	1.0	2.0	28	4.0	28
Siberian elm	OP2	0.9	1.1	0.8	0.8	1.6	23	7.8	13.4	0.8	0.8	1.6	25	3.2	25
Siberian elm	OP3	0.8	1.0	0.7	0.7	1.4	13	7.0	12.0	0.7	0.7	1.4	18	2.9	14
Siberian elm	OP4	0.7	0.9	0.7	0.7	1.3	8	6.4	11.7	0.7	0.7	1.4	9	2.7	8
Siberian elm	P1	0.9	0.8	0.8	0.6	1.4	12	7.7	10.6	0.8	0.6	1.4	14	2.9	12
Siberian elm	P1OP1	0.9	0.9	0.8	0.6	1.4	10	7.1	11.2	0.7	0.7	1.4	11	2.8	11
Siberian elm	P1OP2	0.8	0.9	0.7	0.6	1.4	9	6.8	10.8	0.7	0.6	1.4	8	2.7	9
Siberian elm	P1OP3	0.8	0.8	0.7	0.6	1.3	7	6.5	10.5	0.7	0.6	1.3	7	2.6	7
Siberian elm	P2	0.8	0.6	0.8	0.5	1.2	4	6.5	8.2	0.7	0.5	1.2	4	2.4	4
Siberian elm	P2OP1	0.8	0.7	0.7	0.5	1.3	6	6.5	9.4	0.7	0.6	1.2	6	2.5	6
Siberian elm	P2OP2	0.8	0.7	0.7	0.5	1.3	5	6.4	9.7	0.7	0.6	1.2	5	2.5	5
Siberian elm	P3	0.8	0.6	0.7	0.4	1.1	2	6.2	7.6	0.6	0.5	1.1	2	2.2	2

Siberian elm	P3OP1	0.8	0.7	0.7	0.5	1.2	3	6.2	8.6	0.6	0.5	1.2	3	2.3	3
Siberian elm	P4	0.7	0.5	0.7	0.4	1.0	1	5.8	6.9	0.6	0.4	1.0	1	2.1	1
Green ash	C1	0.4	0.6	0.8	1.0	1.8	27	1.6	3.4	0.8	1.0	1.8	26	3.6	26
Green ash	c1oc1	0.4	0.6	0.8	0.9	1.7	24	1.5	3.1	0.7	0.9	1.6	23	3.3	24
Green ash	C1OC2	0.4	0.5	0.8	0.9	1.7	20	1.4	3.0	0.7	0.9	1.6	21	3.2	21
Green ash	C1OC3	0.4	0.5	0.7	0.9	1.6	16	1.3	3.0	0.6	0.9	1.5	16	3.2	15
Green ash	c2	0.4	0.6	0.7	1.0	1.7	23	1.3	3.2	0.6	0.9	1.6	22	3.3	22
Green ash	C2OC1	0.4	0.6	0.7	0.9	1.7	22	1.3	3.1	0.6	0.9	1.5	20	3.2	20
Green ash	C2OC2	0.4	0.6	0.7	0.9	1.7	19	1.3	3.1	0.6	0.9	1.5	19	3.2	18
Green ash	C3	0.4	0.6	0.7	0.9	1.7	17	1.2	3.1	0.6	0.9	1.5	15	3.2	17
Green ash	C3OC1	0.4	0.6	0.7	0.9	1.7	21	1.3	3.1	0.6	0.9	1.5	18	3.2	19
Green ash	C4	0.4	0.6	0.7	0.9	1.7	18	1.2	3.1	0.6	0.9	1.5	14	3.2	16
Green ash	OC1	0.5	0.5	1.0	0.9	1.9	28	2.0	3.0	0.9	0.9	1.8	27	3.7	28
Green ash	OC2	0.4	0.6	0.8	0.9	1.7	25	1.5	3.1	0.7	0.9	1.6	24	3.4	25
Green ash	OC3	0.4	0.5	0.7	0.9	1.6	15	1.4	2.9	0.6	0.9	1.5	17	3.1	14
Green ash	OC4	0.3	0.5	0.7	0.9	1.6	13	1.3	2.9	0.6	0.9	1.5	13	3.1	13
Green ash	OP1	0.5	0.5	1.0	0.8	1.8	26	2.1	3.1	1.0	0.9	1.9	28	3.7	27
Green ash	OP2	0.4	0.4	0.8	0.6	1.4	11	1.5	2.2	0.7	0.7	1.4	11	2.8	11
Green ash	OP3	0.4	0.3	0.7	0.6	1.3	7	1.3	1.9	0.6	0.6	1.2	7	2.5	7
Green ash	OP4	0.3	0.3	0.7	0.5	1.2	4	1.2	1.7	0.6	0.5	1.1	2	2.3	2
Green ash	P1	0.5	0.4	1.0	0.6	1.6	14	2.1	2.3	1.0	0.7	1.7	25	3.3	23
Green ash	P1OP1	0.4	0.3	0.9	0.6	1.4	12	1.7	2.1	0.8	0.6	1.4	12	2.9	12
Green ash	P1OP2	0.4	0.3	0.8	0.5	1.3	10	1.5	1.9	0.7	0.6	1.3	10	2.6	10
Green ash	P1OP3	0.4	0.3	0.8	0.5	1.2	5	1.3	1.7	0.6	0.5	1.1	5	2.4	5
Green ash	P2	0.4	0.3	0.9	0.4	1.3	9	1.6	1.7	0.8	0.5	1.3	9	2.6	9
Green ash	P2OP1	0.4	0.3	0.8	0.5	1.3	8	1.5	1.7	0.7	0.5	1.2	8	2.5	8
Green ash	P2OP2	0.4	0.3	0.8	0.5	1.2	6	1.4	1.7	0.7	0.5	1.2	6	2.4	6
Green ash	P3	0.4	0.2	0.8	0.4	1.2	2	1.5	1.5	0.7	0.4	1.1	3	2.3	3
Green ash	P3OP1	0.4	0.2	0.8	0.4	1.2	3	1.4	1.6	0.7	0.5	1.1	4	2.3	4
Green ash	P4	0.4	0.2	0.7	0.3	1.1	1	1.3	1.3	0.6	0.4	1.0	1	2.1	1
Manitoba maple	C1	1.3	1.1	0.7	1.0	1.7	26	8.3	8.8	1.0	0.9	1.9	26	3.7	26
Manitoba maple	c1oc1	1.2	0.9	0.7	0.9	1.6	21	7.8	8.0	0.9	0.8	1.8	19	3.4	21
Manitoba maple	C1OC2	1.2	0.9	0.7	0.8	1.5	15	7.6	7.7	0.9	0.8	1.7	16	3.2	16
Manitoba maple	C1OC3	1.2	0.8	0.7	0.8	1.5	10	7.4	7.4	0.9	0.8	1.7	11	3.1	11
Manitoba maple	c2	1.3	0.9	0.7	0.9	1.6	23	8.0	8.2	0.9	0.9	1.8	23	3.4	22
Manitoba maple	C2OC1	1.2	0.9	0.7	0.8	1.6	17	7.7	7.9	0.9	0.8	1.7	18	3.3	17
Manitoba maple	C2OC2	1.2	0.8	0.7	0.8	1.5	14	7.5	7.5	0.9	0.8	1.7	13	3.2	12
Manitoba maple	C3	1.2	0.9	0.7	0.8	1.6	18	7.9	8.0	0.9	0.8	1.8	20	3.3	20
Manitoba maple	C3OC1	1.2	0.8	0.7	0.8	1.5	12	7.6	7.6	0.9	0.8	1.7	14	3.2	13
Manitoba maple	C4	1.2	0.9	0.7	0.8	1.5	16	7.9	8.0	0.9	0.8	1.8	21	3.3	19
Manitoba maple	OC1	1.2	1.0	0.7	1.0	1.7	24	7.7	8.5	0.9	0.9	1.8	22	3.5	24
Manitoba maple	OC2	1.2	0.8	0.7	0.8	1.5	11	7.4	7.3	0.9	0.8	1.6	10	3.1	10
Manitoba maple	OC3	1.2	0.8	0.7	0.8	1.4	9	7.3	7.3	0.9	0.8	1.6	9	3.1	9
Manitoba maple	OC4	1.2	0.8	0.7	0.7	1.4	7	7.2	7.2	0.8	0.8	1.6	8	3.0	8
Manitoba maple	OP1	1.2	1.0	0.7	0.9	1.6	20	8.1	8.6	1.0	0.9	1.9	25	3.4	23
Manitoba maple	OP2	1.5	0.9	0.9	0.8	1.7	25	8.1	8.1	1.0	0.9	1.8	24	3.5	25
Manitoba maple	OP3	1.6	1.0	0.9	0.9	1.9	27	8.3	9.5	1.0	1.0	2.0	28	3.8	27
Manitoba maple	OP4	1.7	1.0	1.0	0.9	1.9	28	8.5	9.3	1.0	1.0	2.0	27	3.9	28
Manitoba maple	P1	1.2	0.8	0.7	0.8	1.5	13	8.0	7.4	0.9	0.8	1.7	17	3.2	14
Manitoba maple	P1OP1	1.2	0.7	0.7	0.7	1.4	6	6.8	6.3	0.8	0.7	1.5	6	2.8	6
Manitoba maple	P1OP2	1.3	0.8	0.8	0.8	1.6	19	7.0	8.0	0.8	0.8	1.7	12	3.2	15
Manitoba maple	P1OP3	1.4	0.8	0.8	0.8	1.6	22	7.3	8.1	0.9	0.9	1.7	15	3.3	18
Manitoba maple	P2	1.1	0.6	0.6	0.6	1.2	3	6.1	5.2	0.7	0.5	1.3	3	2.4	3
Manitoba maple	P2OP1	1.1	0.7	0.7	0.6	1.3	5	6.0	6.4	0.7	0.7	1.4	5	2.7	5
Manitoba maple	P2OP2	1.3	0.7	0.7	0.7	1.4	8	6.4	7.1	0.8	0.8	1.5	7	2.9	7
Manitoba maple	P3	0.9	0.5	0.5	0.5	1.0	2	5.1	4.8	0.6	0.5	1.1	2	2.1	2
Manitoba maple	P3OP1	1.1	0.6	0.6	0.6	1.2	4	5.6	6.0	0.7	0.6	1.3	4	2.5	4
Manitoba maple	P4	0.9	0.5	0.5	0.5	1.0	1	4.8	4.6	0.6	0.5	1.1	1	2.0	1
Hybrid poplar	C1	1.1	0.7	1.0	1.0	1.9	27	7.7	5.9	1.0	0.9	1.9	26	3.8	27
Hybrid poplar	c1oc1	1.1	0.6	0.9	0.9	1.8	24	7.6	5.5	0.9	0.9	1.8	24	3.6	24
Hybrid poplar	C1OC2	1.1	0.6	1.0	0.8	1.8	22	7.6	5.2	0.9	0.8	1.8	22	3.5	22
Hybrid poplar	C1OC3	1.1	0.5	0.9	0.8	1.7	18	7.6	5.0	0.9	0.8	1.7	19	3.5	18
Hybrid poplar	c2	1.1	0.6	0.9	0.8	1.8	23	7.6	5.3	0.9	0.8	1.8	23	3.6	23
Hybrid poplar	C2OC1	1.1	0.6	0.9	0.8	1.7	19	7.5	5.2	0.9	0.8	1.8	20	3.5	20
Hybrid poplar	C2OC2	1.1	0.5	0.9	0.8	1.7	16	7.5	5.0	0.9	0.8	1.7	17	3.5	17
Hybrid poplar	C3	1.1	0.5	0.9	0.8	1.7	17	7.5	5.0	0.9	0.8	1.7	16	3.4	16
Hybrid poplar	C3OC1	1.1	0.5	0.9	0.8	1.7	14	7.5	4.9	0.9	0.8	1.7	14	3.4	14
Hybrid poplar	C4	1.1	0.5	0.9	0.8	1.7	13	7.4	4.9	0.9	0.8	1.7	13	3.4	13
Hybrid poplar	OC1	1.1	0.7	1.0	0.9	1.9	28	8.1	5.9	1.0	0.9	1.9	28	3.9	28
Hybrid poplar	OC2	1.1	0.6	1.0	0.8	1.8	25	7.8	5.5	1.0	0.9	1.8	25	3.6	25
Hybrid poplar	OC3	1.1	0.6	0.9	0.8	1.7	21	7.7	5.1	1.0	0.8	1.8	21	3.5	21
Hybrid poplar	OC4	1.1	0.5	0.9	0.8	1.7	15	7.6	5.0	0.9	0.8	1.7	18	3.4	15
Hybrid poplar	OP1	1.0	0.7	0.9	1.0	1.9	26	7.3	6.3	0.9	1.0	1.9	27	3.8	26
Hybrid poplar	OP2	1.0	0.6	0.9	0.9	1.7	20	7.1	5.3	0.9	0.8	1.7	15	3.5	19
Hybrid poplar	OP3	1.0	0.6	0.9	0.8	1.7	12	7.0	4.9	0.9	0.8	1.6	11	3.3	12

Hybrid poplar	OP4	1.0	0.5	0.9	0.8	1.6	11	7.0	4.6	0.9	0.7	1.6	9	3.3	11
Hybrid poplar	P1	1.0	0.5	0.9	0.7	1.6	7	7.3	4.9	0.9	0.8	1.7	12	3.3	10
Hybrid poplar	P1OP1	1.0	0.5	0.9	0.7	1.6	10	7.1	4.7	0.9	0.7	1.6	10	3.2	9
Hybrid poplar	P1OP2	1.0	0.5	0.9	0.7	1.6	9	7.0	4.5	0.9	0.7	1.6	8	3.2	8
Hybrid poplar	P1OP3	1.0	0.5	0.9	0.7	1.6	8	7.0	4.3	0.9	0.7	1.6	7	3.1	7
Hybrid poplar	P2	1.0	0.4	0.9	0.6	1.5	4	7.1	3.9	0.9	0.6	1.5	6	3.0	4
Hybrid poplar	P2OP1	1.0	0.4	0.9	0.6	1.5	5	7.0	4.0	0.9	0.6	1.5	5	3.0	5
Hybrid poplar	P2OP2	1.0	0.4	0.9	0.6	1.5	6	7.0	4.0	0.9	0.6	1.5	4	3.0	6
Hybrid poplar	P3	1.0	0.4	0.9	0.5	1.4	2	7.0	3.4	0.9	0.5	1.4	2	2.8	2
Hybrid poplar	P3OP1	1.0	0.4	0.9	0.6	1.4	3	7.0	3.6	0.9	0.6	1.4	3	2.9	3
Hybrid poplar	P4	1.0	0.3	0.9	0.5	1.3	1	6.9	3.0	0.9	0.5	1.3	1	2.7	1
Scots pine	C1	0.7	0.4	1.0	0.7	1.7	27	3.6	2.7	1.0	0.7	1.7	27	3.4	27
Scots pine	c1oc1	0.6	0.4	0.9	0.7	1.5	25	3.0	2.6	0.8	0.7	1.5	25	3.1	25
Scots pine	C1OC2	0.5	0.4	0.8	0.7	1.5	23	2.7	2.7	0.7	0.7	1.5	22	2.9	23
Scots pine	C1OC3	0.5	0.4	0.7	0.7	1.4	19	2.6	2.6	0.7	0.7	1.4	18	2.8	19
Scots pine	c2	0.6	0.3	0.9	0.5	1.4	22	3.1	2.1	0.9	0.6	1.4	19	2.9	21
Scots pine	C2OC1	0.6	0.3	0.8	0.6	1.4	18	2.8	2.3	0.8	0.6	1.4	15	2.8	17
Scots pine	C2OC2	0.6	0.4	0.8	0.6	1.4	20	2.7	2.4	0.8	0.6	1.4	16	2.8	18
Scots pine	C3	0.6	0.3	0.9	0.5	1.4	13	2.9	1.9	0.8	0.5	1.3	10	2.7	12
Scots pine	C3OC1	0.6	0.3	0.8	0.5	1.4	14	2.8	2.1	0.8	0.6	1.3	11	2.7	13
Scots pine	C4	0.6	0.3	0.9	0.5	1.3	11	2.8	1.8	0.8	0.5	1.3	7	2.6	8
Scots pine	OC1	0.5	0.5	0.7	0.9	1.6	26	2.7	3.5	0.8	1.0	1.7	26	3.3	26
Scots pine	OC2	0.5	0.4	0.7	0.8	1.4	21	2.5	3.0	0.7	0.8	1.5	24	2.9	22
Scots pine	OC3	0.4	0.4	0.6	0.8	1.4	15	2.4	3.0	0.7	0.8	1.5	21	2.8	20
Scots pine	OC4	0.4	0.4	0.6	0.8	1.3	12	2.3	2.9	0.6	0.8	1.4	17	2.8	15
Scots pine	OP1	0.5	0.6	0.7	1.0	1.7	28	2.8	3.7	0.8	1.0	1.8	28	3.5	28
Scots pine	OP2	0.5	0.5	0.7	0.8	1.5	24	2.6	2.9	0.7	0.8	1.5	23	3.0	24
Scots pine	OP3	0.4	0.4	0.6	0.8	1.4	17	2.4	2.7	0.7	0.7	1.4	14	2.8	16
Scots pine	OP4	0.5	0.4	0.7	0.7	1.4	16	2.4	2.6	0.7	0.7	1.3	12	2.7	14
Scots pine	P1	0.5	0.3	0.7	0.5	1.3	7	2.8	2.5	0.8	0.7	1.4	20	2.7	11
Scots pine	P1OP1	0.5	0.4	0.7	0.6	1.3	10	2.6	2.5	0.7	0.7	1.4	13	2.7	10
Scots pine	P1OP2	0.5	0.4	0.7	0.6	1.3	9	2.5	2.4	0.7	0.6	1.3	9	2.6	9
Scots pine	P1OP3	0.4	0.4	0.6	0.6	1.3	8	2.4	2.3	0.7	0.6	1.3	8	2.6	7
Scots pine	P2	0.5	0.2	0.7	0.4	1.1	3	2.6	2.0	0.7	0.5	1.2	5	2.3	4
Scots pine	P2OP1	0.5	0.3	0.7	0.5	1.2	5	2.5	2.1	0.7	0.6	1.2	6	2.4	5
Scots pine	P2OP2	0.5	0.3	0.6	0.5	1.2	6	2.4	2.1	0.7	0.6	1.2	4	2.4	6
Scots pine	P3	0.4	0.2	0.6	0.4	1.0	2	2.5	1.7	0.7	0.5	1.1	2	2.1	2
Scots pine	P3OP1	0.5	0.3	0.7	0.4	1.1	4	2.4	1.9	0.7	0.5	1.2	3	2.3	3
Scots pine	P4	0.4	0.2	0.6	0.3	0.9	1	2.4	1.5	0.7	0.4	1.1	1	2.0	1
Eastern larch	C1	0.7	0.5	0.9	0.7	1.6	20	4.0	3.6	0.9	0.8	1.6	20	3.3	20
Eastern larch	c1oc1	0.7	0.5	0.9	0.7	1.7	21	4.1	3.5	0.9	0.8	1.6	22	3.3	21
Eastern larch	C1OC2	0.7	0.5	0.9	0.8	1.7	22	4.1	3.5	0.9	0.7	1.6	21	3.3	22
Eastern larch	C1OC3	0.7	0.5	0.9	0.8	1.7	23	4.2	3.5	0.9	0.7	1.6	23	3.3	23
Eastern larch	c2	0.6	0.4	0.8	0.6	1.4	13	3.8	3.1	0.8	0.7	1.5	13	2.9	13
Eastern larch	C2OC1	0.6	0.4	0.9	0.7	1.5	16	4.0	3.2	0.9	0.7	1.5	15	3.1	15
Eastern larch	C2OC2	0.6	0.4	0.9	0.7	1.6	18	4.0	3.2	0.9	0.7	1.6	17	3.1	18
Eastern larch	C3	0.6	0.4	0.8	0.6	1.4	8	3.7	2.9	0.8	0.6	1.4	9	2.8	9
Eastern larch	C3OC1	0.6	0.4	0.8	0.6	1.4	12	3.9	3.0	0.8	0.6	1.5	12	2.9	12
Eastern larch	C4	0.6	0.4	0.8	0.6	1.4	7	3.7	2.8	0.8	0.6	1.4	7	2.8	7
Eastern larch	OC1	0.7	0.6	1.0	1.0	2.0	28	4.6	4.7	1.0	1.0	2.0	28	4.0	28
Eastern larch	OC2	0.7	0.6	1.0	0.9	1.9	27	4.5	4.2	1.0	0.9	1.9	27	3.8	27
Eastern larch	OC3	0.7	0.6	1.0	0.9	1.9	26	4.4	3.9	1.0	0.8	1.8	26	3.6	26
Eastern larch	OC4	0.7	0.5	1.0	0.8	1.8	25	4.4	3.8	0.9	0.8	1.8	25	3.6	25
Eastern larch	OP1	0.6	0.5	0.9	0.8	1.7	24	4.3	3.9	0.9	0.8	1.8	24	3.5	24
Eastern larch	OP2	0.6	0.5	0.8	0.7	1.6	19	4.0	3.5	0.9	0.7	1.6	19	3.2	19
Eastern larch	OP3	0.6	0.4	0.8	0.7	1.5	17	3.9	3.3	0.8	0.7	1.5	16	3.1	16
Eastern larch	OP4	0.6	0.4	0.8	0.7	1.5	14	3.8	3.2	0.8	0.7	1.5	14	3.0	14
Eastern larch	P1	0.7	0.4	0.9	0.6	1.5	15	4.2	3.1	0.9	0.7	1.6	18	3.1	17
Eastern larch	P1OP1	0.6	0.4	0.8	0.6	1.4	11	3.9	2.8	0.8	0.6	1.5	11	2.9	11
Eastern larch	P1OP2	0.6	0.4	0.8	0.6	1.4	10	3.9	2.8	0.8	0.6	1.4	10	2.8	10
Eastern larch	P1OP3	0.6	0.4	0.8	0.6	1.4	9	3.8	2.8	0.8	0.6	1.4	8	2.8	8
Eastern larch	P2	0.6	0.3	0.8	0.5	1.3	6	3.8	2.6	0.8	0.6	1.4	6	2.7	6
Eastern larch	P2OP1	0.6	0.3	0.8	0.5	1.3	4	3.8	2.5	0.8	0.5	1.4	5	2.7	5
Eastern larch	P2OP2	0.6	0.3	0.8	0.5	1.3	5	3.8	2.5	0.8	0.5	1.4	4	2.7	4
Eastern larch	P3	0.6	0.3	0.8	0.5	1.3	3	3.8	2.5	0.8	0.5	1.3	3	2.6	3
Eastern larch	P3OP1	0.6	0.3	0.8	0.5	1.3	2	3.8	2.4	0.8	0.5	1.3	2	2.6	2
Eastern larch	P4	0.6	0.3	0.8	0.4	1.2	1	3.8	2.3	0.8	0.5	1.3	1	2.6	1
Acute willow	C1	0.5	0.1	0.8	0.8	1.5	22	1.2	0.4	0.8	0.8	1.6	22	3.2	22
Acute willow	c1oc1	0.5	0.1	0.8	0.7	1.4	20	1.2	0.4	0.8	0.7	1.5	20	2.9	20
Acute willow	C1OC2	0.5	0.1	0.8	0.6	1.4	14	1.2	0.3	0.8	0.6	1.4	14	2.8	14
Acute willow	C1OC3	0.5	0.1	0.8	0.5	1.3	11	1.2	0.3	0.8	0.5	1.3	11	2.6	11
Acute willow	c2	0.5	0.1	0.8	0.6	1.4	16	1.2	0.3	0.8	0.7	1.5	17	2.9	17
Acute willow	C2OC1	0.5	0.1	0.8	0.5	1.3	12	1.2	0.3	0.8	0.6	1.3	12	2.7	12
Acute willow	C2OC2	0.5	0.1	0.8	0.5	1.3	10	1.2	0.3	0.8	0.5	1.3	10	2.6	10
Acute willow	C3	0.5	0.1	0.8	0.5	1.3	9	1.2	0.3	0.7	0.5	1.3	9	2.6	9

Acute willow	C3OC1	0.5	0.1	0.8	0.5	1.3	8	1.2	0.3	0.8	0.5	1.3	7	2.6	7
Acute willow	C4	0.5	0.1	0.8	0.5	1.2	4	1.2	0.2	0.8	0.5	1.2	4	2.5	4
Acute willow	OC1	0.5	0.1	0.8	0.8	1.6	27	1.3	0.4	0.9	0.8	1.7	25	3.3	26
Acute willow	OC2	0.5	0.1	0.8	0.7	1.5	21	1.3	0.4	0.8	0.7	1.5	21	3.0	21
Acute willow	OC3	0.5	0.1	0.8	0.6	1.4	17	1.3	0.3	0.8	0.6	1.4	15	2.8	15
Acute willow	OC4	0.5	0.1	0.8	0.5	1.4	13	1.3	0.3	0.8	0.6	1.4	13	2.7	13
Acute willow	OP1	0.4	0.2	0.6	1.0	1.6	26	1.0	0.5	0.7	1.0	1.7	23	3.3	25
Acute willow	OP2	0.4	0.1	0.6	0.7	1.3	5	1.0	0.3	0.6	0.6	1.3	5	2.5	5
Acute willow	OP3	0.4	0.1	0.6	0.5	1.1	2	1.0	0.2	0.6	0.4	1.0	2	2.1	2
Acute willow	OP4	0.4	0.1	0.6	0.3	0.9	1	1.0	0.1	0.6	0.3	0.9	1	1.8	1
Acute willow	P1	0.6	0.1	1.0	0.7	1.7	28	1.6	0.4	1.0	0.9	1.9	28	3.6	28
Acute willow	P1OP1	0.5	0.1	0.8	0.6	1.4	15	1.2	0.3	0.8	0.7	1.5	16	2.9	16
Acute willow	P1OP2	0.5	0.1	0.7	0.5	1.3	6	1.1	0.3	0.7	0.5	1.3	6	2.5	6
Acute willow	P1OP3	0.5	0.1	0.7	0.4	1.1	3	1.1	0.2	0.7	0.4	1.1	3	2.2	3
Acute willow	P2	0.6	0.1	1.0	0.6	1.6	25	1.5	0.4	0.9	0.8	1.7	27	3.3	27
Acute willow	P2OP1	0.6	0.1	0.9	0.6	1.4	18	1.3	0.3	0.8	0.6	1.5	18	2.9	18
Acute willow	P2OP2	0.5	0.1	0.8	0.5	1.3	7	1.2	0.3	0.8	0.5	1.3	8	2.6	8
Acute willow	P3	0.6	0.1	1.0	0.6	1.6	24	1.5	0.4	0.9	0.7	1.7	26	3.3	24
Acute willow	P3OP1	0.6	0.1	0.9	0.5	1.4	19	1.3	0.3	0.9	0.6	1.5	19	2.9	19
Acute willow	P4	0.6	0.1	1.0	0.6	1.5	23	1.5	0.4	0.9	0.7	1.7	24	3.2	23
White spruce	C1	0.6	0.6	0.9	1.0	1.9	27	3.9	3.7	0.9	1.0	1.9	27	3.8	27
White spruce	c1oc1	0.6	0.5	0.9	0.9	1.8	24	3.9	3.3	0.9	0.9	1.8	25	3.6	25
White spruce	C1OC2	0.6	0.5	0.9	0.9	1.8	22	3.9	3.0	0.9	0.8	1.7	21	3.5	22
White spruce	C1OC3	0.6	0.5	0.9	0.8	1.8	21	3.9	2.8	0.9	0.7	1.7	18	3.4	20
White spruce	c2	0.6	0.5	0.9	0.9	1.8	20	3.7	3.2	0.9	0.8	1.7	22	3.5	21
White spruce	C2OC1	0.6	0.5	0.9	0.9	1.8	19	3.8	3.0	0.9	0.8	1.7	19	3.4	19
White spruce	C2OC2	0.6	0.5	0.9	0.8	1.8	18	3.8	2.9	0.9	0.8	1.6	17	3.4	18
White spruce	C3	0.6	0.5	0.8	0.9	1.7	16	3.6	3.0	0.8	0.8	1.6	16	3.4	17
White spruce	C3OC1	0.6	0.5	0.9	0.8	1.7	17	3.7	2.9	0.9	0.8	1.6	15	3.3	16
White spruce	C4	0.6	0.5	0.8	0.9	1.7	15	3.6	2.9	0.8	0.8	1.6	14	3.3	14
White spruce	OC1	0.7	0.6	1.0	1.0	2.0	28	4.3	3.8	1.0	1.0	2.0	28	4.0	28
White spruce	OC2	0.6	0.5	1.0	0.9	1.9	26	4.1	3.4	1.0	0.9	1.8	26	3.7	26
White spruce	OC3	0.6	0.5	1.0	0.9	1.8	25	4.1	2.9	1.0	0.8	1.7	23	3.6	24
White spruce	OC4	0.6	0.5	1.0	0.8	1.8	23	4.1	2.8	1.0	0.7	1.7	20	3.5	23
White spruce	OP1	0.5	0.4	0.8	0.8	1.6	14	3.4	3.6	0.8	0.9	1.7	24	3.3	15
White spruce	OP2	0.5	0.3	0.7	0.6	1.3	12	3.2	2.5	0.7	0.6	1.4	12	2.7	12
White spruce	OP3	0.5	0.3	0.7	0.5	1.2	10	3.1	2.0	0.7	0.5	1.3	10	2.5	10
White spruce	OP4	0.5	0.3	0.7	0.5	1.2	8	3.1	1.7	0.7	0.4	1.2	4	2.3	6
White spruce	P1	0.5	0.3	0.8	0.6	1.3	13	3.5	2.9	0.8	0.8	1.6	13	2.9	13
White spruce	P1OP1	0.5	0.3	0.8	0.5	1.3	11	3.2	2.3	0.8	0.6	1.4	11	2.6	11
White spruce	P1OP2	0.5	0.3	0.7	0.5	1.2	9	3.2	2.0	0.7	0.5	1.3	9	2.5	9
White spruce	P1OP3	0.5	0.2	0.7	0.4	1.2	7	3.2	1.7	0.7	0.5	1.2	6	2.4	7
White spruce	P2	0.5	0.2	0.7	0.4	1.1	6	3.1	2.0	0.7	0.5	1.3	8	2.4	8
White spruce	P2OP1	0.5	0.2	0.7	0.4	1.1	4	3.1	1.8	0.7	0.5	1.2	7	2.3	5
White spruce	P2OP2	0.5	0.2	0.7	0.4	1.1	5	3.1	1.7	0.7	0.4	1.2	5	2.3	4
White spruce	P3	0.5	0.2	0.7	0.3	1.1	3	3.1	1.6	0.7	0.4	1.1	3	2.2	3
White spruce	P3OP1	0.5	0.2	0.7	0.3	1.1	2	3.0	1.5	0.7	0.4	1.1	2	2.2	2
White spruce	P4	0.5	0.2	0.7	0.3	1.0	1	3.0	1.2	0.7	0.3	1.0	1	2.0	1

Table A4 lists the effect of the number of increment cores on MAE for DBH and BA for the B to P and for the P to B orientations. In general, the more increment cores used, the better.

Table A4 - MAE, MAE (% based on the last ring), Bias, Bias (%) and Bias (% Last ring) yielded by using, 1, 2, 3 and 4 increment cores for classes of age ranging from 0–10, 10–20, 20–30, 30–40, 40–50 years for DBH and BA.

	Class	Cores	DBH					BA				
			MAE	MAE (% Last ring)	Bias	Bias (%)	Bias (% last ring)	MAE	MAE (% Last ring)	Bias	Bias (%)	Bias (% last ring)
B to P	0 - 10	1	1.00	15.69	0.84	0.20	0.13	6.27	17.08	5.55	-0.04	0.15
		2	0.97	15.46	0.87	0.27	0.14	5.92	16.24	5.48	-0.01	0.15
		3	0.95	15.18	0.87	0.29	0.14	5.86	16.07	5.53	0.05	0.15
		4	0.94	15.03	0.87	0.29	0.14	5.83	16.02	5.55	0.08	0.15
	10 - 20	1	0.71	11.32	0.63	0.19	0.10	4.47	12.52	3.98	0.18	0.11
		2	0.70	11.11	0.63	0.21	0.10	4.27	12.04	3.93	0.22	0.11
		3	0.69	11.05	0.64	0.22	0.10	4.21	11.90	3.91	0.23	0.11
		4	0.69	11.01	0.63	0.23	0.10	4.17	11.82	3.89	0.23	0.11
	20 - 30	1	0.75	10.49	0.61	0.14	0.08	5.43	10.78	4.73	-0.04	0.08
		2	0.77	10.46	0.68	0.18	0.09	5.28	9.93	4.83	-0.04	0.08
		3	0.77	10.49	0.70	0.20	0.09	5.28	9.78	4.91	-0.01	0.08
		4	0.77	10.43	0.71	0.21	0.09	5.24	9.64	4.92	0.01	0.08
	30 - 40	1	1.05	10.64	0.05	-0.09	0.00	8.50	10.62	1.31	-0.77	0.00
		2	0.97	9.54	0.14	-0.04	0.01	7.51	8.94	1.66	-0.65	0.01
		3	0.92	8.96	0.14	-0.02	0.01	7.12	8.33	1.64	-0.68	0.01
		4	0.89	8.58	0.13	0.00	0.01	6.79	7.92	1.53	-0.76	0.01
	40 - 50	1	0.89	9.62	0.39	0.06	0.05	7.46	10.07	2.82	-0.48	0.06
		2	0.83	9.08	0.41	0.07	0.05	6.64	9.08	2.98	-0.93	0.06
		3	0.81	8.91	0.42	0.08	0.06	6.36	8.75	3.04	-1.22	0.06
		4	0.80	8.81	0.43	0.08	0.06	6.21	8.60	3.13	-1.55	0.06
PtoB	0 - 10	1	0.60	9.82	0.05	-11.38	-0.89	4.65	13.12	0.98	-50.81	-0.36
		2	0.51	8.42	0.05	-11.31	-0.88	3.88	10.99	1.18	-44.13	0.21
		3	0.47	7.90	0.05	-11.31	-0.86	3.60	10.22	1.24	-42.02	0.40
		4	0.45	7.58	0.05	-11.26	-0.87	3.43	9.79	1.28	-40.74	0.50
	10 - 20	1	0.45	7.10	-0.04	-8.12	-1.19	3.20	9.20	0.15	-29.12	-1.11
		2	0.38	6.10	-0.04	-8.09	-1.19	2.74	7.81	0.23	-25.72	-0.87
		3	0.36	5.72	-0.04	-8.04	-1.17	2.56	7.28	0.26	-24.52	-0.78
		4	0.35	5.51	-0.04	-8.01	-1.16	2.46	6.98	0.28	-23.89	-0.72
	20 - 30	1	0.59	9.27	-0.37	-16.87	-5.91	5.34	12.54	-3.53	-49.39	-7.96
		2	0.52	8.05	-0.38	-16.93	-5.96	4.64	10.60	-3.52	-45.62	-7.62
		3	0.50	7.80	-0.40	-17.16	-6.20	4.44	10.41	-3.61	-44.94	-8.08
		4	0.47	7.44	-0.39	-16.87	-6.08	4.15	9.85	-3.49	-43.48	-7.83
	30 - 40	1	0.81	8.58	0.12	-0.66	1.23	8.28	11.39	0.94	-8.24	1.41
		2	0.67	7.04	0.12	-0.66	1.23	6.98	9.49	1.22	-5.56	1.82
		3	0.62	6.53	0.12	-0.63	1.26	6.57	8.88	1.34	-4.66	1.99
		4	0.59	6.15	0.12	-0.60	1.25	6.32	8.50	1.38	-4.02	2.07
	40 - 50	1	0.91	9.30	0.02	-8.79	-1.46	10.13	12.38	1.69	-31.13	-1.91
		2	0.77	7.89	0.02	-8.79	-1.46	8.64	10.28	2.02	-28.08	-1.53
		3	0.72	7.40	0.02	-8.86	-1.47	8.10	9.49	2.12	-27.27	-1.44
		4	0.69	7.02	0.02	-8.71	-1.43	7.77	9.00	2.22	-26.35	-1.30

Table A5 shows the correlation between compactness and MAE, MAE (% Last ring), Bias, Bias (%) and Bias (% Last ring) for DBH and BA for each species. Most correlations were negative, meaning that the more circular the cross section, the lower the error.

Table A5 - Correlation between compactness and MAE, MAE (% Last ring), Bias, Bias (%) and Bias (% Last ring) for DBH and BA for each species.

Species	DBH					BA				
	MAE	MAE (%Last ring)	Bias	Bias (%)	Bias (%Last ring)	MAE	MAE (%Last ring)	Bias	Bias (%)	Bias (%Last ring)
Chokecherry	0.57	0.57	0.01	-0.71	-0.37	-0.43	-0.43	-0.24	-0.69	-0.13
Colorado spruce	-0.28	-0.27	-0.04	-0.48	0.10	-0.35	-0.35	-0.65	-0.58	0.19
Siberian elm	-0.31	-0.25	-0.31	-0.67	-0.29	-0.40	-0.51	-0.29	-0.83	-0.24
Green ash	-0.29	-0.21	0.14	-0.76	0.31	-0.69	-0.76	0.23	-0.73	0.50
Manitoba maple	-0.73	-0.62	-0.64	-0.36	-0.48	-0.66	-0.75	-0.59	-0.41	-0.50
Hybrid poplar	-0.58	-0.05	-0.43	-0.72	-0.42	-0.72	-0.74	-0.59	-0.78	-0.33
Scots pine	0.42	0.41	-0.31	-0.53	-0.47	0.00	-0.06	-0.22	-0.47	-0.24
Eastern larch	-0.51	-0.52	-0.81	-0.96	-0.71	-0.81	-0.81	-0.70	-0.92	-0.49
Acute willow	-0.69	-0.69	-0.59	-0.86	-0.33	-0.71	-0.71	-0.59	-0.86	-0.02
White spruce	-0.38	0.18	-0.77	-0.89	-0.35	-0.61	-0.68	-0.61	-0.89	0.06

APPENDIX B

DETAILS OF 3-PG FITTING REGARDING TREE BIOMASS ESTIMATES AND THE YIELDED ERROR

These appendix materials further detail the aspects assessed in Chapter 5. Sampling sites are shown in Figure B1. In almost all cases, more than one tree was sampled at a site. Although the number of trees used in this study is not ideal, and more trees should be incorporated for more robust conclusions, it needs to be pointed out that all sampling was destructive. It was very challenging to find farmers willing to allow their trees to be harvested. Over two summers, and approximately 2500 phone calls, only a few landowners agreed to allow their trees to be cut. In most cases, farmers did not want to allow trees that took years to grow, to be cut. This fact resulted in an overall low number of trees sampled, and an even lower number of individuals sampled within each species.

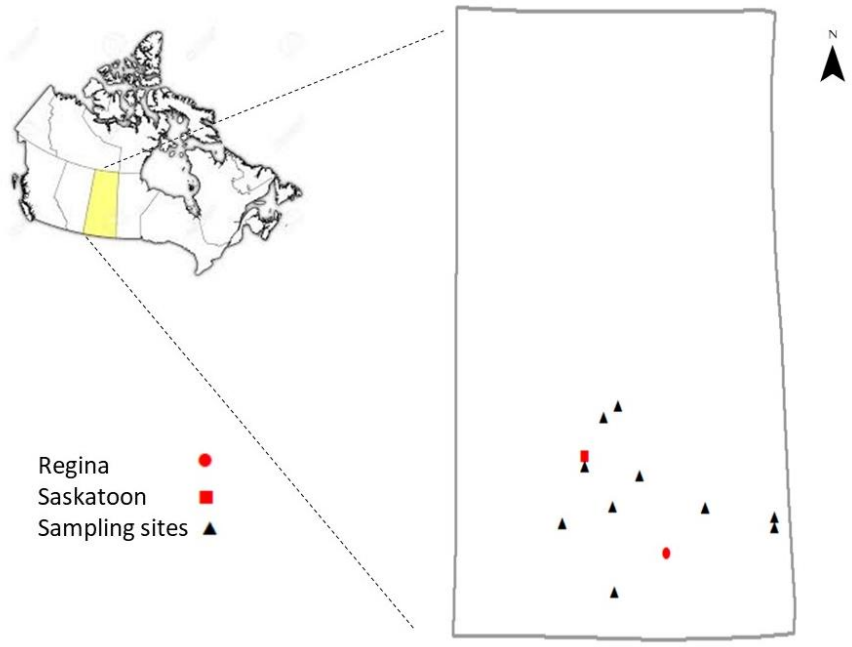

Figure B1 - Sampling sites in Saskatchewan, Canada.

Figures B2 and B3 show the estimated DBH and tree biomass for each tree from the year 1 to 60.

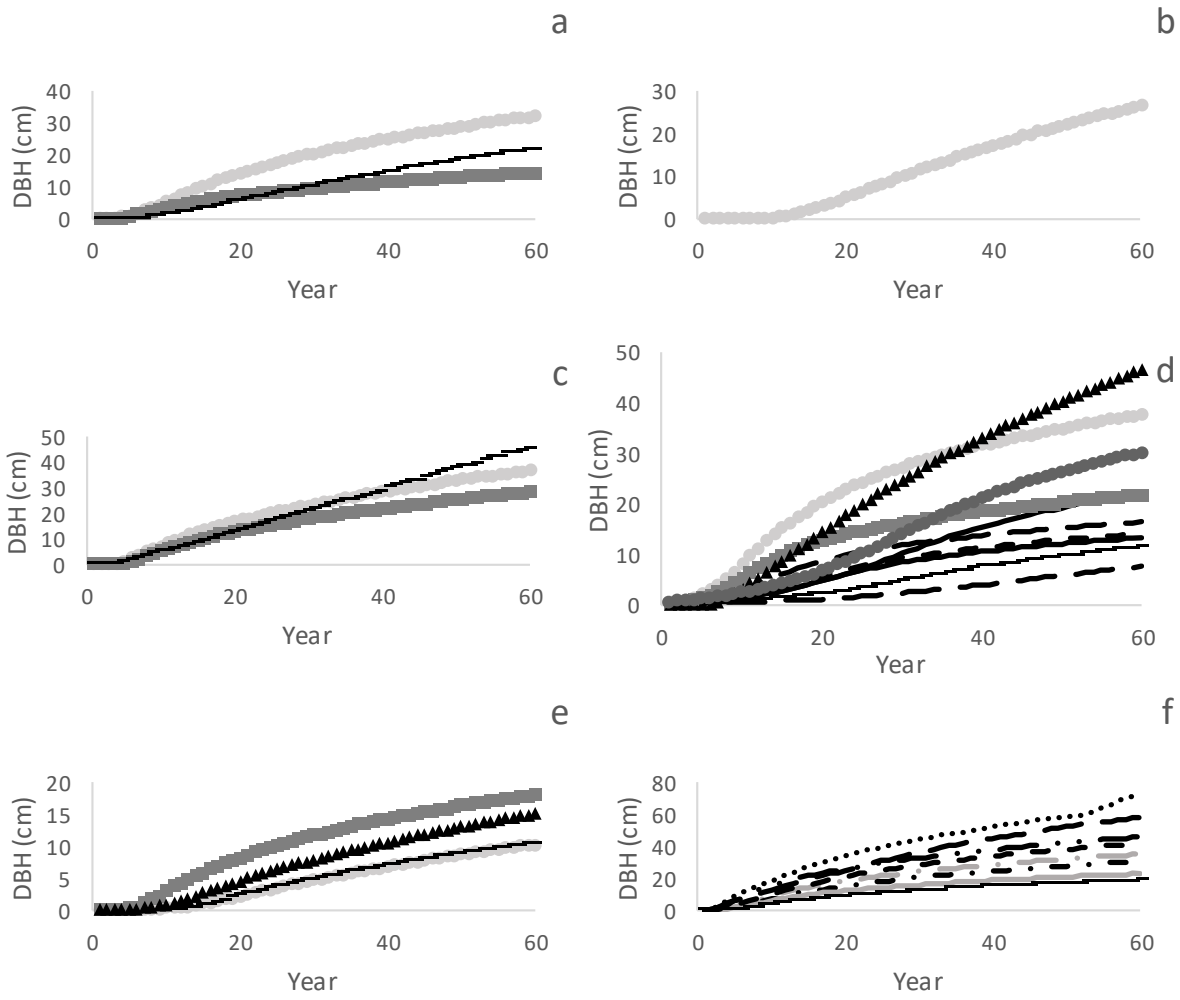

Figure B2 - Predicted DBH through time for each tree by species. Each line represents an individual tree. The trees are, a) Green ash (n=3); b) Scots pine (n=1); c) Manitoba maple (n=3); d) White spruce (n=10); e) Caragana (n=4); f) Hybrid poplar (n=8). Note: n = number of trees for each species.

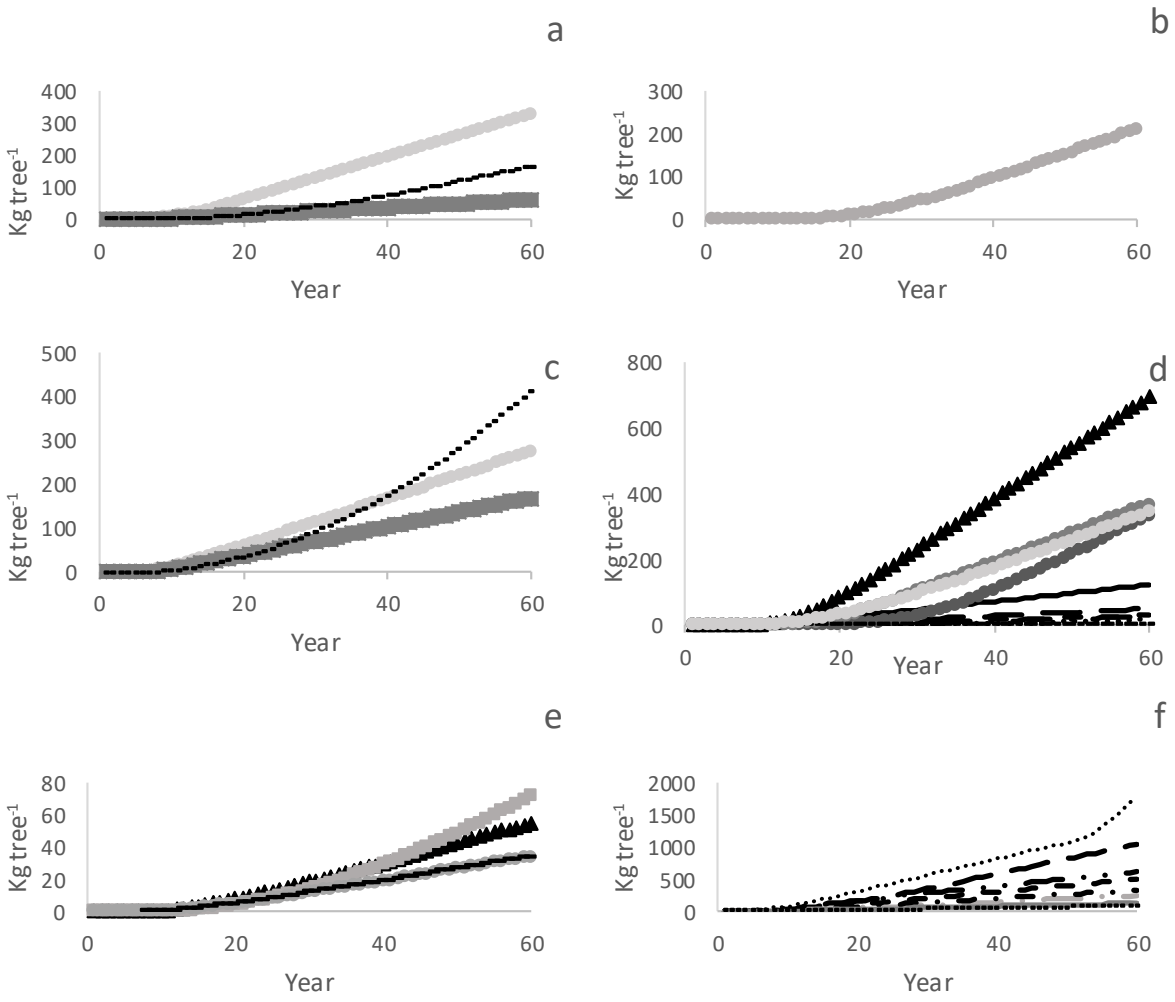

Figure B3 - Predicted tree biomass through time for each tree by species. Each line represents an individual tree. The trees are, a) Green ash (n=3); b) Scots pine (n=1); c) Manitoba Maple (n=3); d) White spruce (n=10); e) Caragana (n=4); f) Hybrid poplar (n=8). Note: n = number of trees for each species.

Figure B4 and B5 illustrates RMSE and bias, respectively, for the fitting of each tree over time. The number in the legends is each tree's age.

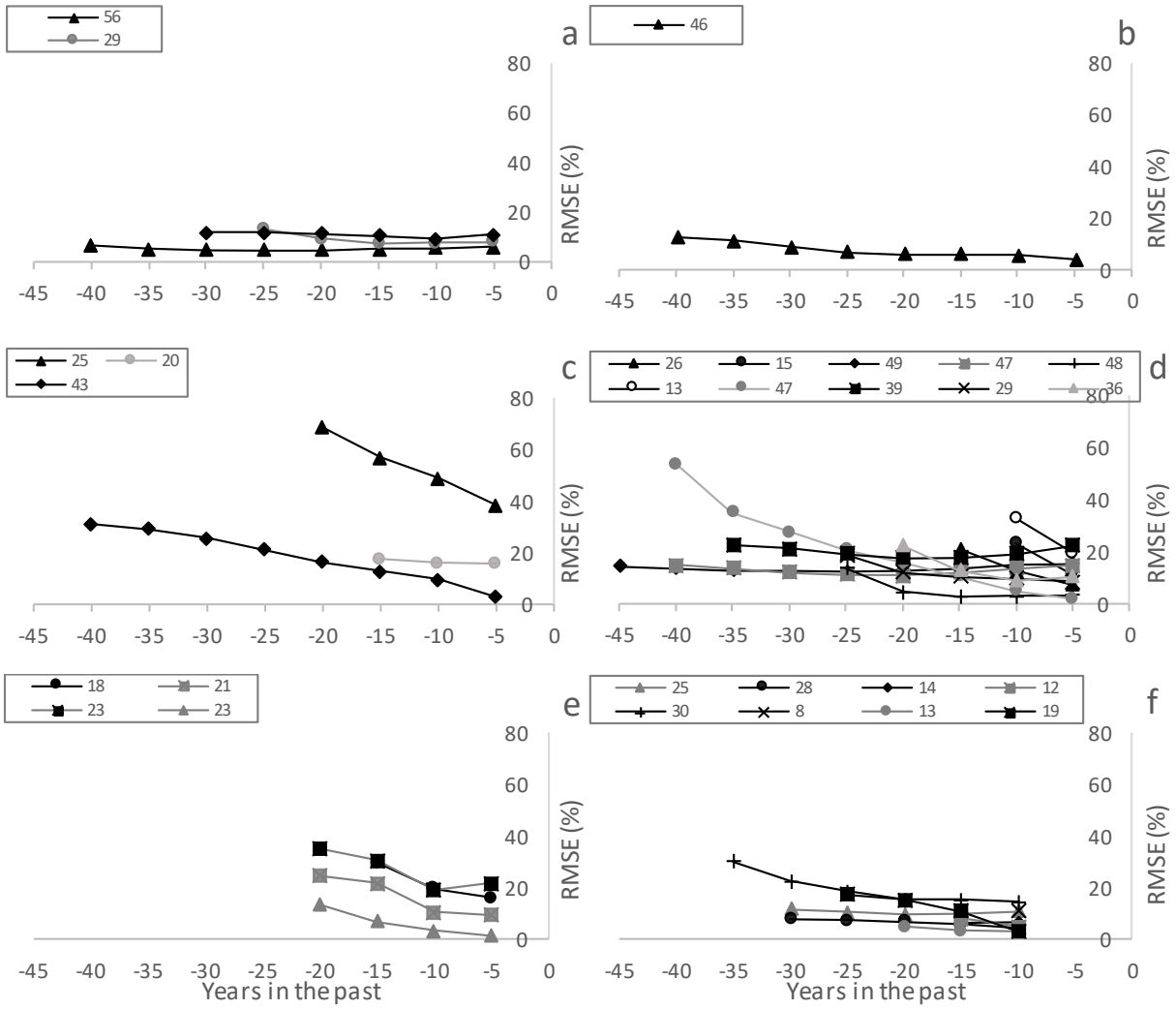

Figure B4 - RMSE through time as fitted for each tree, for each species. The legend box indicates the age of each tree related to each symbol. The trees are, a) Green ash (n=3); b) Scots pine (n=1); c) Manitoba maple (n=3); d) White spruce (n=10); e) Caragana (n=4); f) Hybrid poplar (n=8). Note: n = number of trees for each species.

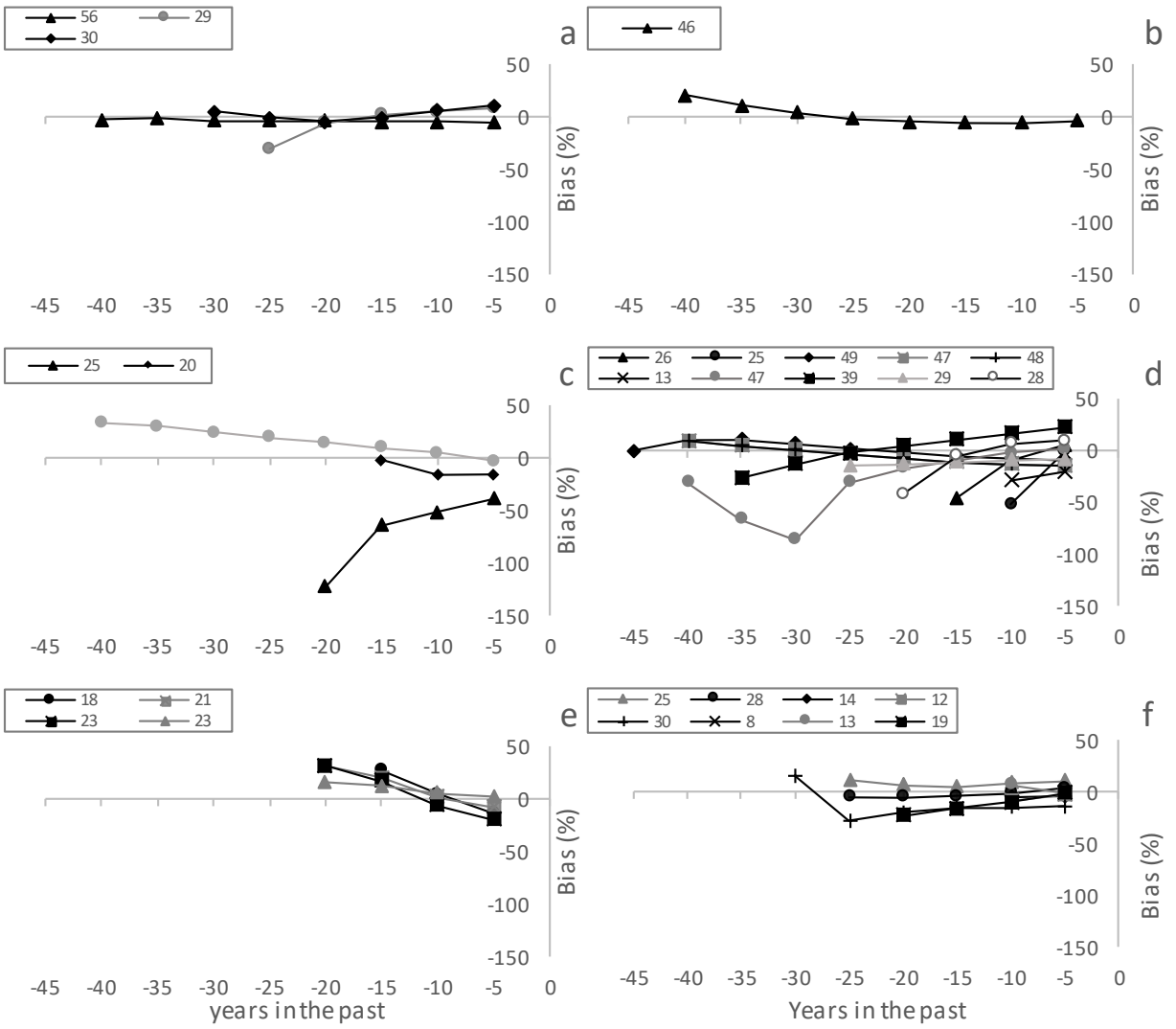

Figure B5 - Bias fitted through time for each tree, for each species. The legend box indicates the age of each tree related to each symbol. The trees are, a) Green ash (n=3); b) Scots pine (n=1); c) Manitoba maple (n=3); d) White spruce (n=10); e) Caragana (n=4); f) Hybrid poplar (n=8). Note: n= number of trees for each species.

APPENDIX C

PRACTICAL STEP-BY-STEP GUIDE OF SOME OF THE PROGRMAS AND PROCEDURTES IN CHAPTER 4 AND 5

This is a step-by-step guide describing some of the methods I used in Chapter 4 and 5, with tips from lessons that I learned when working on this study. By writing this Appendix, I aim to aid those interested in applying similar methodologies in this dissertation and those starting in the related dendrochronology discipline.

Pre-field Checklist

Before sampling trees in the field, it is necessary to plan the field day including the necessary equipment and seeking permission to visit the site/s. At each site, before the visit, I visualize the existing shelterbelts using Google Earth, which helps to better understand the existing shelterbelts configuration at the site. Google Earth also assists in identifying the location you are looking for, and the road network that is needed to get to the location. This step allowed our field crew to avoid knocking on the wrong door.

It is important to bring the following items to the field, preferably in a waterproof Rubbermaid bucket with a lid, which assists in keeping water from the equipment, and helps keep the equipment from being lost.

1. Increment borers
2. GPS
3. Straws
4. Masking tape
5. Measuring tape – caliper and DBH tape
6. Hypsometer
7. Sharpie – permanent marker
8. Field notebook

In the field

In the field, the items to be measured are: tree height with the hypsometer; spacing between trees with the measuring tape; and DBH, with the caliper or the DBH calibrated tape. Tree age can be estimated by asking the landowner or by looking at PFRA records if available

for the location, or a tree can be cored at its base, and its rings can be counted later in the lab. To retrieve DBHs over time, as in Chapter 4, increment cores need to be taken at the DBH height, as instructed in the next paragraphs.

In the field, do not core leaning trees if possible, to avoid increment cores with potential reaction wood. Avoid sampling dead or dying trees, because they often present rotten wood in their centers, and this wood often gets stuck in the increment borer, especially during extraction. In case it does happen, never insert any metal instruments into the cutting end of the increment borer to unblock the borer. Use a soft implement, such as a twig or a golf tee instead, or if needed, try to core another healthy piece of wood, so it will help push the jammed piece of wood out of the borer.

Before coring, tie some flagging tape to the increment borer spoon to avoid losing it in the field. Do not put the spoon on the ground to avoid the risk of stepping on it, or potentially bending it. Core the tree at a 90 ° angle to the main stem. To make sure you have cored the tree deep enough, and thereby increase the chance to reach the pith, place the spoon parallel to the increment borer on the outside of the tree to estimate how far you have cored. By observing where the end of the spoon is in relation to the tree diameter, you can better guesstimate if you have cored far enough, or if you need to core deeper. In most cases, try to go past the center of the tree by a few cm, to better increase the chance of extending past the pith. In case you need to sample a small tree, be sure to go slow and do not core too far, because you can pass right through the entire stem quickly, and this might unnecessarily damage the tree.

Be careful when inserting the spoon into the increment borer to extract the increment core. Insert the spoon inverted on top of the core, otherwise you can jam the increment core with the spoon and sometimes twist the core. After extraction, store the increment core in a straw, close it with a masking tape, and properly label it.

The main species I sampled in my shelterbelt study have their peculiarities that I learned when coring them: hybrid poplar may spill water out of the boring hole when you are coring them; green ash wood was the hardest to core; Manitoba maple commonly had rotten interior wood, so I often had to re-core the same tree to get a good sample; the needles of young spruce may hurt when coring, so I often used gloves and a long sleeve t-shirt when sampling this species.

In the laboratory

In the laboratory, the increment cores are first glued on wooden boards using wood glue. The direction of fibers have to be observed, glued in perpendicular position to the board. Rubber bands can be used to immobilize the increment cores on the board until the glue is dry. Weighting down the drying boards, with items such as heavy books, may help keep the samples in place. Let the samples dry at least overnight and the next day check to make sure that cores are well affixed to the boards, and that there are no gaps between the board and the increment core. If you do find any gaps, fill them with glue again and let the second gluing dry.

After the glue is dry, the boards need to be sanded, so the rings can be more easily seen. The increment cores should be sanded with the lowest grit sandpaper first, moving to progressively finer paper (e.g., 80 to 600 grit). Be sure to follow all safety protocols and personal protective equipment when using mechanized equipment. After the rings are clearly visible, scan the boards, and measure the rings with image J, using the extension Object J. Image J can be downloaded free from the Image J webpage (https://imagej.nih.gov/ij/download.html) and object J can also be downloaded freely (https://sils.fnwi.uva.nl/bcb/objectj/download/). Examples of how to use the Object J on ImageJ to measure the rings are provided here (https://sils.fnwi.uva.nl/bcb/objectj/examples/TreeRings/TreeRings-9.htm). Figure C1a illustrates how to activate Object J, in Image J, and how object J appears in Image J after it is activated (Figure C1b, red box).

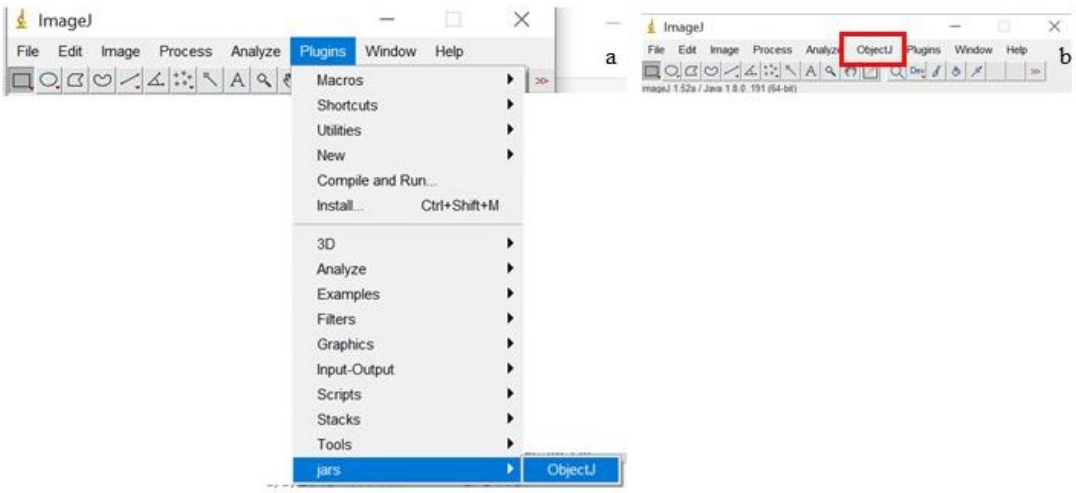

Figure C1 - a) Activating Object J in program Image J; b) Object J ready to operate on Image J.

Figure C2 shows the rings of an increment core measured using ImageJ. The window in the left shows the objects I created to measure the rings. In this case, to measure rings on

increment cores, we have the "Begin", in pink, used to indicate the pith on the core. After marking the pith (the starting point), each ring boundary is automatically marked on the increment core (blue dots). The yellow arrow on the top left allows you to drag and change a dot's position, if you disagree with where it was automatically placed. Another useful feature for this protocol is the black gun in the top left box because it allows you to delete dots if you wish to do so. The window in the middle shows the increment cores measured and how many ring boundaries were found. In the example bellow, the increment core contained 41 ring boundaries.

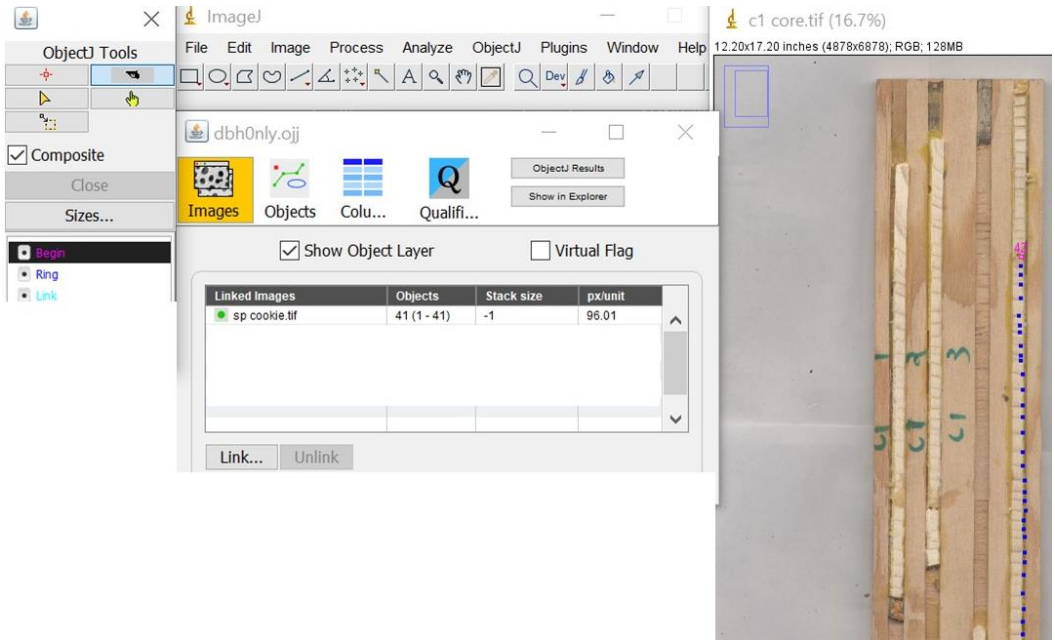

Figure C2 - ObjectJ screenshot showing the features to measure ring widths in an increment core.

After the rings are measured, DBHs over the years are calculated as in Chapter 5. Next, the DBHs are used in the 3-PG model to predict foliage, stem and root biomass, diameter, stand volume, and height, in monthly or yearly steps. The 3-PG model can be freely downloaded from the Forestry department website at the University of British Columbia, at (https://3pg.forestry.ubc.ca/software/), where they provide the software and a manual with detailed instructions on how to use the model.

Figure C3 and Figure C4 illustrates how to fit the alpha parameter, as in Chapter 5. It illustrates the spreadsheet where 3-PG runs, with an inset graph showing the observed (in brown) and estimated DBH data (in black). Observed DBHs need to be pasted in the cells indicated by the arrow in Figure C3 and Figure C4. A user needs to vary the alpha value (red square on Figure

C3 and Figure C4) and press the run button on the top left to run the model so it can estimate the outputs. Fitting can be assessed by i) comparing coincidence between estimated and observed values on the top right chart; ii) by observing if observed versus estimated plots (in the middle of the page in the red circle) follow a straight line with 45º and the R^2 yielded; iii) RMSE and bias (red box right bottom). Figure C3 and Figure C4 illustrates examples of a bad and a good fit. Figure C3 shows the line fitting considering an alpha value of 0.03. As can be seen, the brown and black lines are apart on the chart on the right. Also, observed versus estimated values do not follow a straight line in a 45º (chart at the center). R^2 was 0.9352, and RMSE and bias were 85.83 and -101.34, respectively. Next, on Figure C4, we can see a better fitting with alpha as 0.012 for this run. The brown and black lines now coincide (chart on the right), observed and predicted DBH coincide more, following a line more similar to a straight line and R^2 is 0.944. RMSE and bias were 12.75 and 4.90. By finding the most suitable alpha for each model, 3-PG will estimate the output necessary to calculate biomass growth and carbon stock over the years for that shelterbelt.

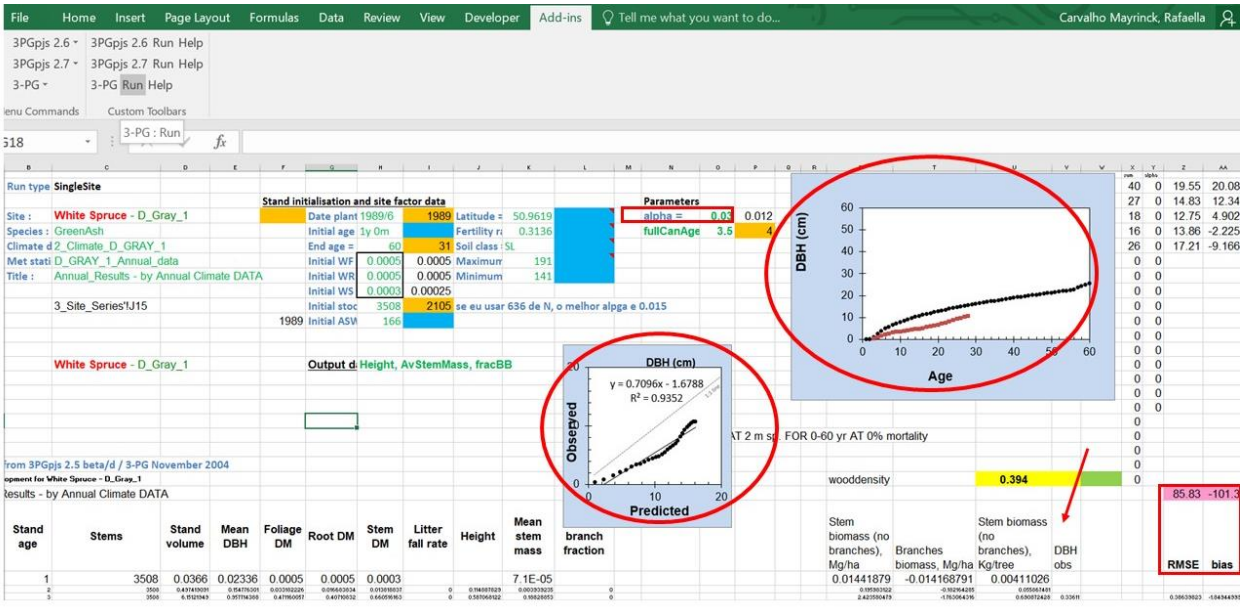

Figure C3 - 3-PG spreadsheet showing a poor fit, using an alpha value of 0.03. The red circle illustrates the divergence between observed (brown) and estimated (black) values.

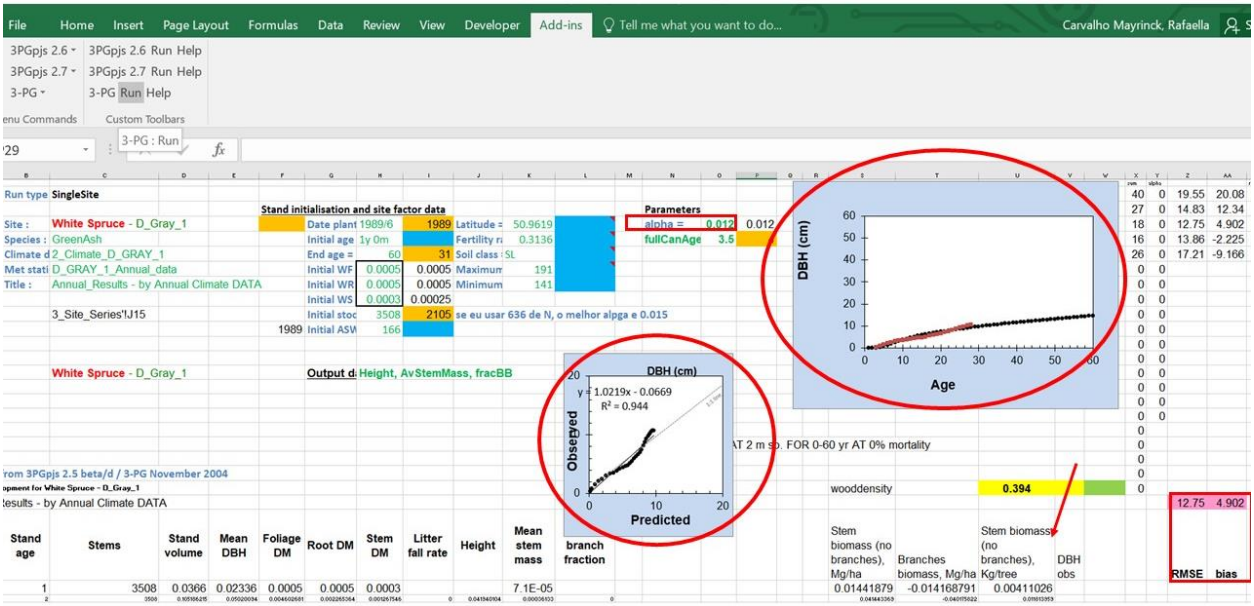

Figure C4 - 3-PG spreadsheet showing a good fit, using an alpha value of 0.012. The red circle illustrates the convergence between observed (brown) and estimated (black) values.